Supporting Information for

Mechanistic Investigation of the Castagnoli-Cushman Multicomponent Reactions Leading to a 3-Component Synthesis of Dihydroisoquinolones

Sara Y. Howard,[†] Michael J. Di Maso,[†] Kristin Shimabukuro,[†] Noah P. Burlow,[†] Darlene Q. Tan,[†] James C. Fettinger,[†] Thomas C. Malig,[‡] Jason E. Hein,[‡] Jared T. Shaw[†,*]

[†]Department of Chemistry, University of California, One Shields Ave, Davis, CA, 95616
[‡]Department of Chemistry University of British Columbia 2036 Main Mall Vancouver, BC Canada V6T 1Z1

Email Jared T. Shaw— jtshaw@ucdavis.edu

Experimental Details and Compound Characterization

Table of Contents

DESICCANT SCREEN FOR THE SYNTHESIS OF DIHYDROISOQUINOLONES S2

MEASUREMENT OF A SECONDARY DEUTERIUM ISOTOPE EFFECT BY A COMPETITION EXPERIMENT S2

REACT IR EXPERIMENTS..... S7

X-RAY CRYSTALLOGRAPHIC DATA S15

LCMS TRACES..... S38

^{1}H AND ^{13}C NMR SPECTRA S59

Desiccant Screen for the synthesis of dihydroisoquinolones

Table S1. Desiccant screen for the 3CR

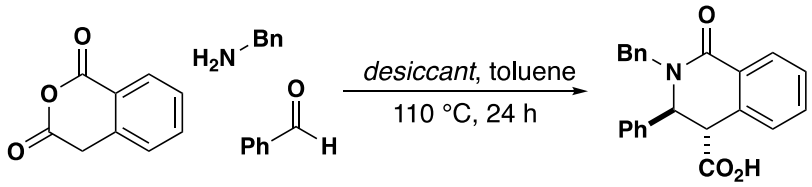

Entry	Desiccant	Yield (%)	dr
1	—	71	>95:5
2	Na_2SO_4	84	>95:5
3	4 Å MS	70	>95:5

Measurement of a Secondary Deuterium Isotope Effect by a Competition Experiment

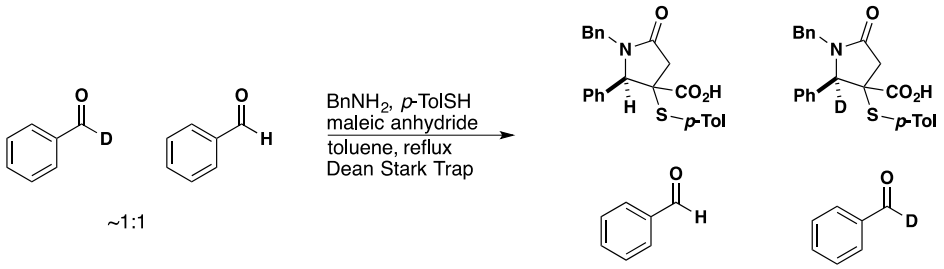

Figure S1. Proposed deuterium exchange reaction.

Summary:

A solution of benzaldehyde-α-d1 (0.10 mL, 1.0 mmol),[1] benzaldehyde (0.10 mL, 1.0 mmol) and 1,3,5-trimethoxybenzene 69 mg, 0.40 mmol) in 30 mL of toluene was divided as follows:
Control: 2 mL of the above solution was concentrated and analyzed by ^{1}H NMR, as detailed below.
4CR Experiment: 15 mL of the above solution taken to 84% conversion, as detailed below.

4CR Experimental

To a dry, 100-mL, round-bottomed flask were added maleic anhydride (100 mg, 1.00 mmol) and *p*-thiocresol (124 mg, 1.00 mmol). The aldehyde solution described above (15 mL) and benzylamine (0.110 mL, 1.00 mmol) were added sequentially by syringe. The flask was fitted with a Dean Stark apparatus and heated to reflux for 8 hours. The resulting solution was allowed to cool to room temperature. The reaction was concentrated *in vacuo*. ^{1}H NMR analysis indicated that 16% of the substrate *p*-tolualdehyde remained (integration against internal standard, 84% conversion).

Collection and integration of ^{1}H NMR and calculation of the Deuterium Isotope Effect

Quantitative ^{1}H NMR data were collected on a 600 MHz Varian spectrometer at 298K. Proton spectra were collected using a 45-degree pulse and a 30 second delay. Two independent spectra were obtained for each of the samples, providing four spectra. Each spectrum was manually integrated three times applying zeroth-order baseline correction. Average integration, relative integration (R/R_0), and calculated deuterium isotope effect are listed in Table S2 and summarized in Figure S2. The deuterium isotope effect was calculated using the equation:[2]

$$KIE = (\ln(1-F))/\ln[(1-F)R/R_0]$$

F: Percent conversion of the substrate during the 4CR.
R/R_0: the proportion of deuterium in the recovered, unreacted substrate compared to the proportion of deuterium in the reserved control.

All standard deviations were calculated according to the reported procedures.[2]

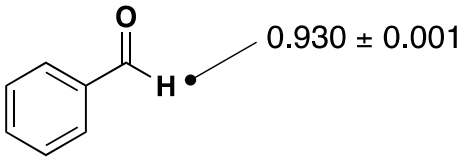

Figure S2. The measured deuterium isotope of benzaldehyde in the 4CR.

Table S2. Average integration, relative integration, and the calculated Deuterium isotope effect.

Average Integrations		
	-CHO (Ref)	*Ortho*-H
^{1}H NMR (600 MHz, $CDCl_3$) δ:	10.00 ppm	7.87 ppm
Control	1000	3989.22
Standard Deviation	–	5.71
Experiment	1000	3470.43
Standard Deviation	–	9.64
Relative Integrations (R/R_0)		
	-CHO (Ref)	*Ortho*-H
^{1}H NMR (600 MHz, $CDCl_3$) δ:	10.00 ppm	7.87 ppm
Experiment/Control	1	0.870
Standard Deviation	–	0.003
Calculated Deuterium Isotope Effect		
	-CHO (Ref)	*Ortho*-H
^{1}H NMR (600 MHz, $CDCl_3$) δ:	10.00 ppm	7.87 ppm
Experiment (84 $\pm$ 0.04% conv)	1	0.930
Standard Deviation	–	0.001

Natural Abundance Isotope experiment

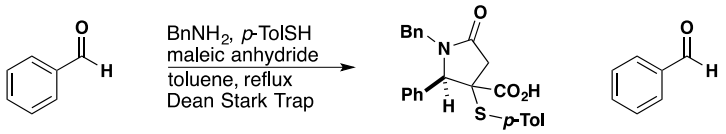

Figure S3. Proposed natural abundance isotope experiment.

Summary:

p-tolualdehyde was purchased from Oakwood Chemicals (lot No.: G03L) and used in all of the experiments.

Control: 50 μL, analyzed by ^{13}C as detailed below.

4CR experiment 1: (1.65 mL, 74% conversion, detailed below)

4CR experiment 2: (1.65 mL, 76% conversion, detailed below)

4CR experimental 1.

To a dry, 500-mL, round-bottomed flask were added maleic anhydride (1.38g, 14.0 mmol), *p*-thiocresol (1.74g, 14.0 mmol), 1,3,5-trimethoxybenzene (474 mg, 2.80 mmol), and 200 mL of toluene. *p*-Tolualdehyde (1.65 mL, 14.0 mmol) and benzylamine (1.55 mL, 14.0 mmol) were added sequentially by syringe. The flask was fitted with a Dean Stark apparatus and heated to reflux for 6.5 hours. The resulting solution was allowed to cool to room termperature. ^{1}H NMR analysis indicated that 26% of the substrate *p*-tolualdehyde remained (integration against internal standard, 74% conversion). The reaction was concentrated *in vacuo* and the unreacted starting material was purified by flash-column chromatography (5:95 EtOAc:hex).

4CR experimental 2.

To a dry, 500-mL, round-bottomed flask were added maleic anhydride (1.38g, 14.0 mmol), *p*-thiocresol (1.74g, 14.0 mmol), 1,3,5-trimethoxybenzene (474 mg, 2.80 mmol), and 200 mL of toluene. *p*-Tolualdehyde (1.65 mL, 14.0 mmol) and benzylamine (1.55 mL, 14.0 mmol) were added sequentially by syringe. The flask was fitted with a Dean Stark apparatus and heated to reflux for 6.5 hours. The resulting solution was allowed to cool to room termperature. ^{1}H NMR analysis indicated that 24% of the substrate *p*-tolualdehyde remained (integration against internal standard, 76% conversion). The reaction was concentrated *in vacuo* and the unreacted starting material was purified by flash-column chromatography (5:95 EtOAc:hex).

Collection and integration of ^{13}C NMR and calculation of $^{12}C/^{13}C$ isotope effects.

Quantitative ^{13}C NMR data were collected on an 800 MHz Bruker Avance III spectrometer equipped with a 5 mm CPTCI H/C/N/D Z-gradient cryogenic probe, with the temperature regulated at 298K. Carbon spectra with inverse-gated decoupling were collected using a zgig30 Bruker pulse program, a 65 second recycle delay, a 1.4 second acquisition time, a 240 ppm spectral width, 128k acquired points, 256 scan averages with 4 dummy scans, and WALTZ proton decoupling applied during acquisition but not during the relaxation delay. The recycle delay was set to 5 times the slowest-relaxing ^{13}C resonance of interest, as measured using the T1 inversion

recovery method. The samples were prepared by diluting 50 μL of *p*-tolualdehyde in 1 mL of $CDCl_3$. Three independent spectra were obtained for each of the samples, providing nine spectra. Each spectrum was manually integrated three times applying zeroth-order baseline correction. Average integration, relative integration (R/R_0), and calculated $^{12}C/^{13}C$ isotope effect are listed in Table S3 and summarized in Figure S4. The $^{12}C/^{13}C$ isotope effects were calculated using the equation:[2]

$$KIE = (\ln(1-F))/\ln[(1-F)R/R_0]$$

F: Percent conversion of the substrate during the 4CR.
R/R_0: the proportion of ^{13}C in the recovered, unreacted substrate compared to the proportion of ^{13}C in the control.

All standard deviations were calculated according to the reported procedures.[2]

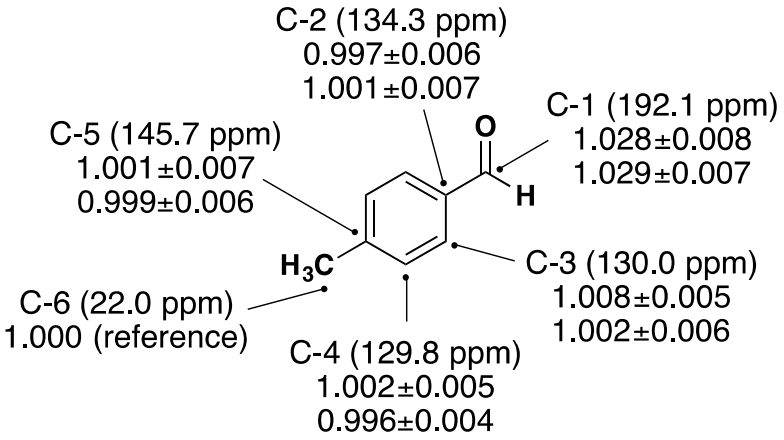

Figure S4. Measured $^{12}C/^{13}C$ isotope effects for AMR and Carbon numbering.

Table S3. Average integrations, relative integrations, and the calculated $^{12}C/^{13}C$ isotope effects for the 4CR depicted above.

Average Integrations						
	C-6 (ref)	C-1	C-5	C-2	C-3	C-4
^{13}C NMR (201 MHz, $CDCl_3$) δ:	22.0	192.1	145.7	134.3	130.0	129.8
Control	1000	972.38	1007.29	1016.51	2006.26	2044.52
Standard Deviation	–	7.73	7.64	7.21	7.15	6.81
Experiment 1	1000	1008.03	1015.55	1012.75	2028.31	2049.34
Standard Deviation	–	5.55	5.87	3.91	10.85	10.21
Experiment 2	1000	1012.58	1006.18	1018.33	2011.84	2033.38
Standard Deviation	–	5.23	5.05	7.85	16.08	11.10
Relative Integrations (R/R_o)						
	C-6 (ref)	C-1	C-5	C-2	C-3	C-4
^{13}C NMR (201 MHz, $CDCl_3$) δ:	22.0	192.1	145.7	134.3	130.0	129.8
Experiment 1 / Control	1	1.037	1.008	0.996	1.011	1.002
Standard Deviation	–	0.010	0.0096	0.008	0.006	0.006
Experiment 2 / Control	1	1.041	0.999	1.002	1.003	0.995
Standard Deviation	–	0.0099	0.0091	0.010	0.0088	0.0064
Calculated $^{12}C/^{13}C$ Isotope Effects						
	C-6 (ref)	C-1	C-5	C-2	C-3	C-4
^{13}C NMR (201 MHz, $CDCl_3$) δ:	22.0	192.1	145.7	134.3	130.0	129.8
Experiment 1 (73.5 $\pm$ 0.1 % conv)	1	1.028	1.001	0.997	1.008	1.002
Standard Deviation	–	0.008	0.007	0.006	0.005	0.005
Experiment 2 (76.0 $\pm$ 0.1% conv.)	1	1.029	0.999	1.001	1.002	0.996
Standard Deviation	–	0.007	0.006	0.007	0.006	0.004

References

1. J. J. Gajewski, W. Bocian, N. J. Harris, L. P. Olson and J. P. Gajewski, *J. Am. Chem. Soc.*, 1999, **121**, 326-334.
2. D. A. Singleton and A. A. Thomas, *J. Am. Chem. Soc.*, 1995, **117**, 9357-9358.

React IR Experiments

ReactIR data was collected using a Mettler-Toledo ReactIR 15 with an MCT detector, and a DSTDiComp probe with a diamond ATR crystal. A spectral window of 3000 to 650 cm^{-1} was used for all experiments. ReactIR data analysis was performed on the second derivative of the IR spectra to allow for better peak deconvolution.

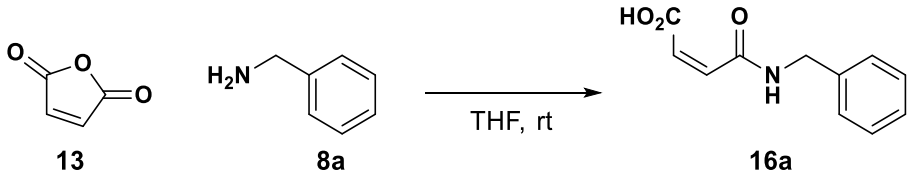

Figure S5. React IR experiment of maleic anhydride and benzylamine

The ReactIR probe was inserted into the reaction vial through a fitted septum and subsequently blanked in air. THF (10 mL) was added to the vial and the probe was blanked again. Next, maleic anhydride (0.147 g, 1.5 mmol) was added to the vial. The solution was monitored for 6 minutes using ReactIR before benzylamine (0.164 ml, 1.5 mmol) was added.

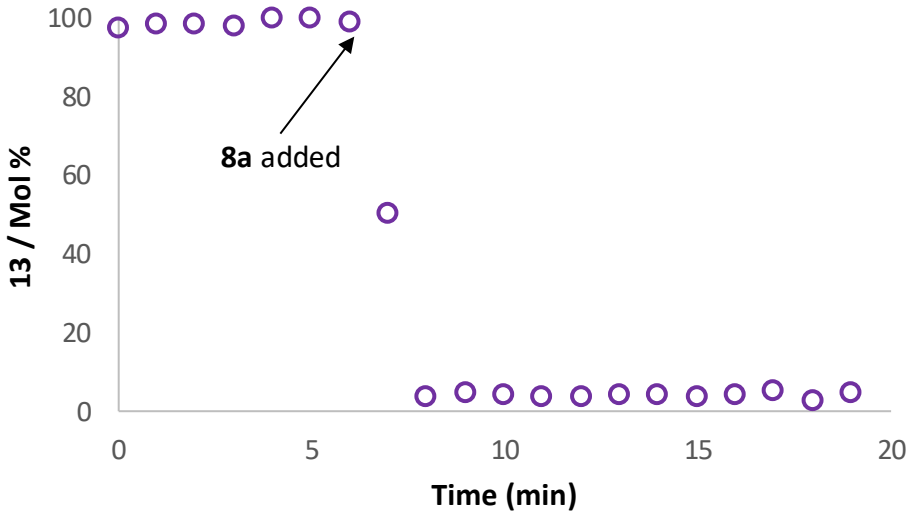

Figure S6. ReactIR data displaying conversion of anhydride **13** when benzylamine (**8a**) is added. Anhydride **13** was trended via measuring the peak height at 1783 cm^{-1}.

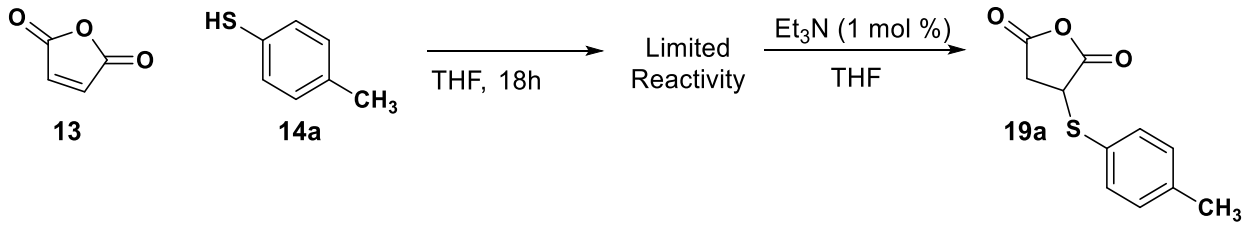

Figure S7. Reaction of maleic anhydride and *p*-tolSH.

The ReactIR probe was inserted into the reaction vial through a fitted septum and subsequently blanked in air. THF (9 mL) was added to the vial and the probe was blanked again. Maleic anhydride **13** (0.147 g, 1.50 mmol), and *p*-tolSH (0.186 g, 1.50 mmol) in THF (1 mL) were added to the reaction vial. After 18 hours had elapsed triethylamine (2 µl, 0.015 mmol) was added.

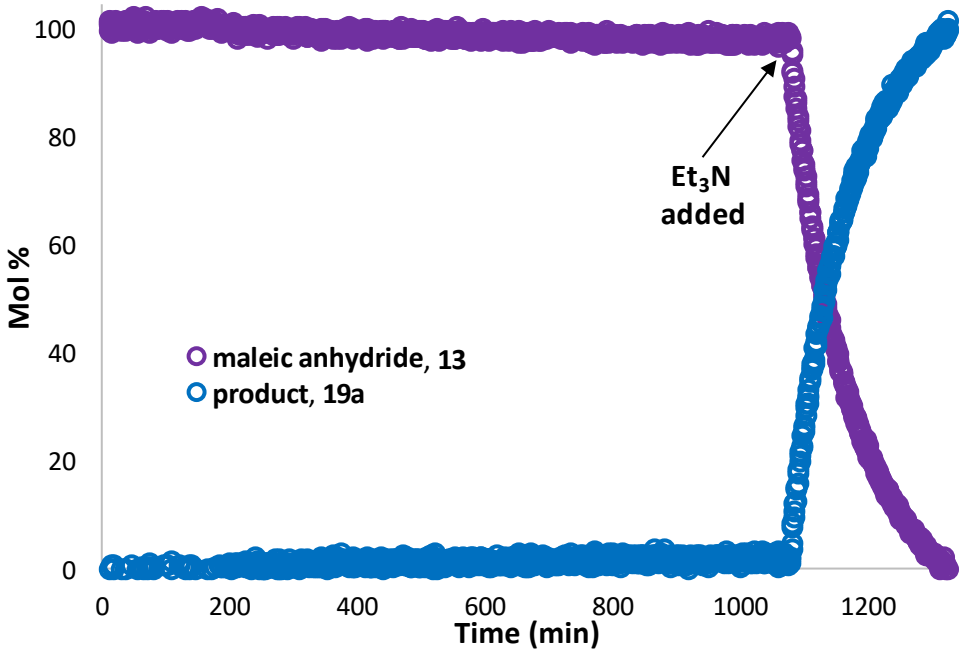

Figure S8. ReactIR data displaying the acceleration of the conversion of maleic anhydride **13** to **19** when trimethylamine is added. Anhydride **13** was trended via measuring the peak height at 1783 cm^{-1}. Product **19** was trended via measuring the peak height at 1794 cm^{-1}.

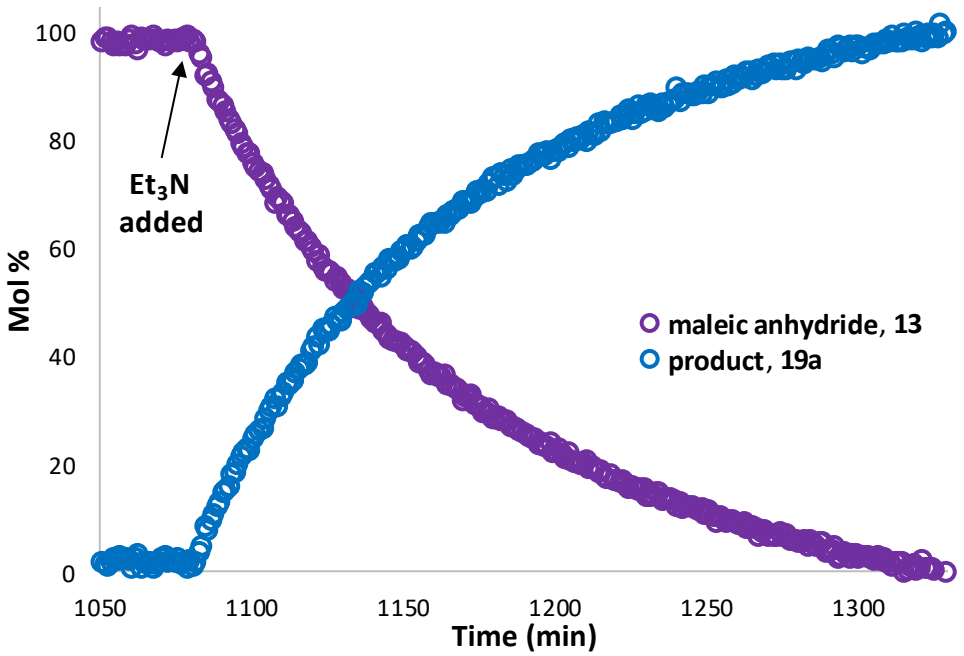

Figure S9. Zoomed in region of ReactIR data highlighting the acceleration of the conversion of maleic anhydride **13** to product **19** when trimethylamine is added. Anhydride **13** was trended via measuring the peak height at 1783 cm^{-1}. Product **19** was trended via measuring the peak height at 1794 cm^{-1}.

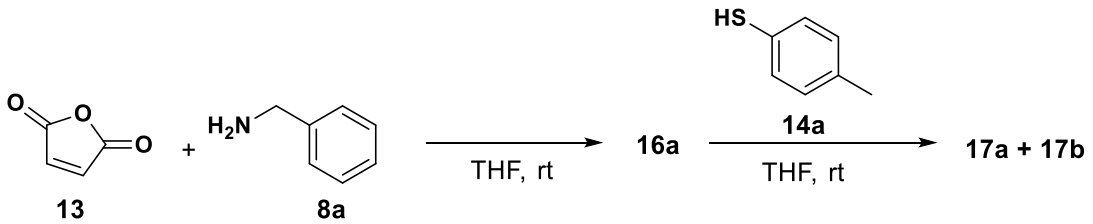

Figure S10. Reaction of maleic anyhdride and benzylamine, followed by addition of *p*-tolSH.

The ReactIR probe was inserted into the reaction vial through a fitted septum and subsequently blanked in air. THF (10 mL) was added to the vial and the probe was blanked again. Maleic anhydride **13** (0.147 g, 1.50 mmol), and benzylamine **8a** (0.164 mL, 1.50 mmol) were added to the reaction vial. After five minutes, *p*-tolSH (0.186 g, 1.50 mmol) was added to the reaction.

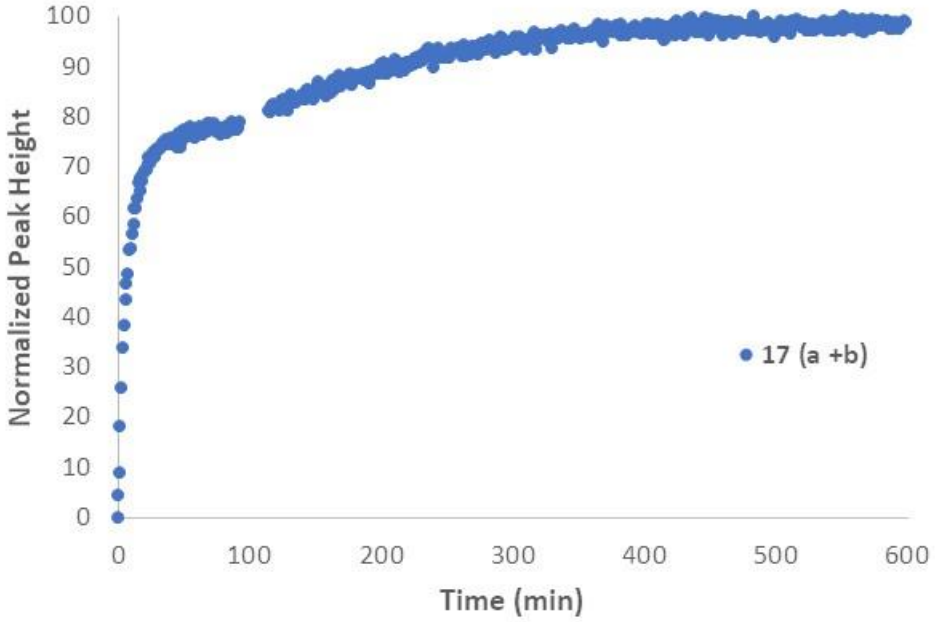

Figure S11. ReactIR data displaying the formation **17a** and **17b** when 4-methylbenzenethiol is added to a solution of **16a**. Products **17a**/**17b** were trended via measuring the peak height at 1737 cm^{-1}.

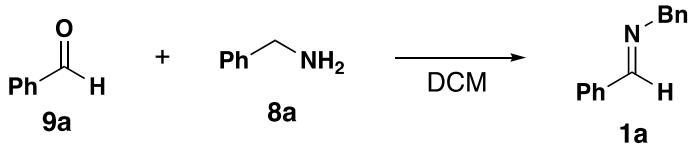

Figure S12. Reaction of benzylamine and benzaldehyde to form *N*-benzylideneaniline.

The ReactIR probe was inserted into the reaction vial through a fitted septum and subsequently blanked in air. DCM (9.8 mL) was added to the vial and the probe was blanked again. Benzaldehyde (106 mg, 1.00 mmol) followed by benzylamine (107 mg, 1.00 mmol) were added to the reaction vial.

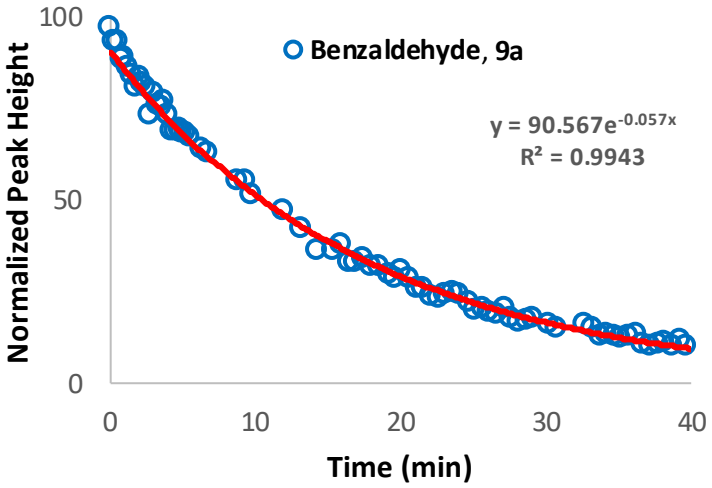

Figure S13. ReactIR data displaying consumption of benzaldehyde (**9a**) when benzylamine (**8a**) is added. Benzaldehyde (**9a**) was trended via measuring the peak height at 1704 cm^{-1}. The consumption profile was fitted to an exponential decay curve, $y = 90.6e^{-0.057x}$, $R^2 = 0.994$.

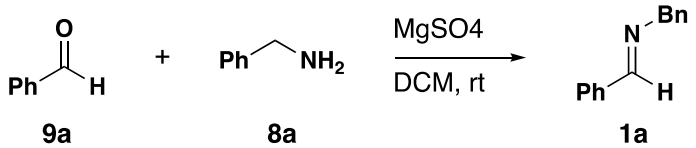

Figure S14. Reaction of benzylamine and benzaldehyde to form *N*-benzylideneaniline in the presence of dessicant.

Benzaldehyde (106 mg, 1.00 mmol) and $MgSO_4$ (241 mg, 2.00 mmol) added to DCM (9.8 mL) at room temperature. Benzylamine (107 mg, 1.00 mmol) added to initiate reaction.

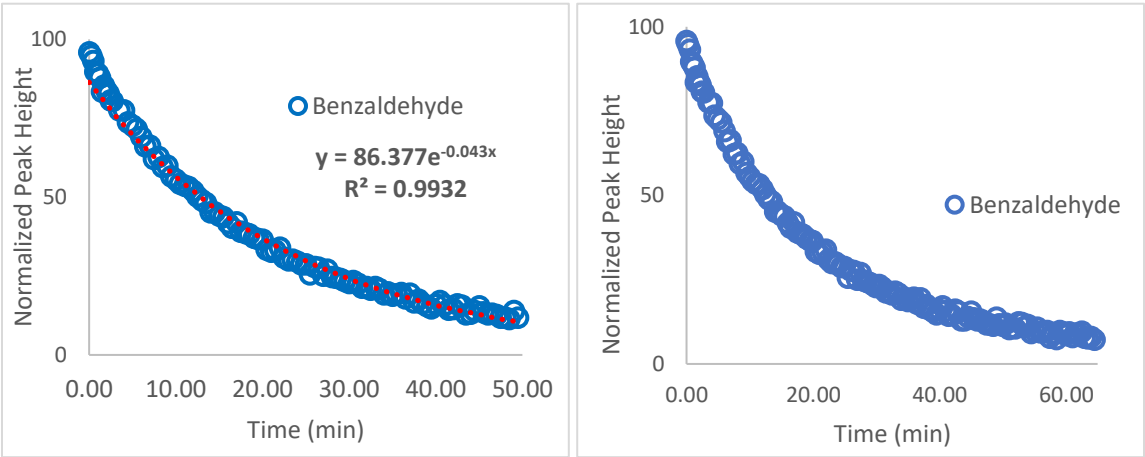

Figure S15. Imine condensation in the presence of $MgSO_4$

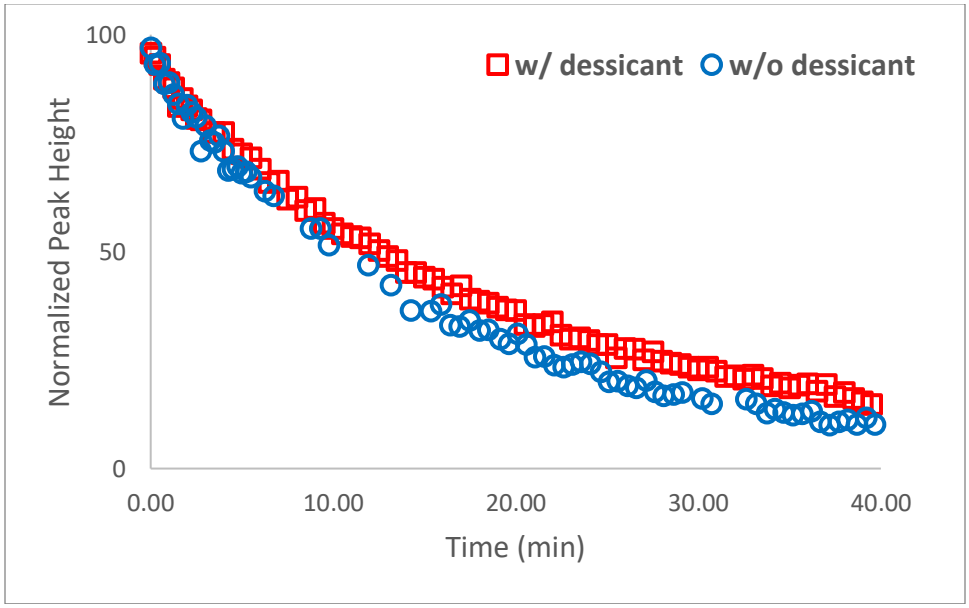

Figure S16. Comparing benzaldehyde consumption profiles during imine formation in the presence and absence of desiccant ($MgSO_4$)

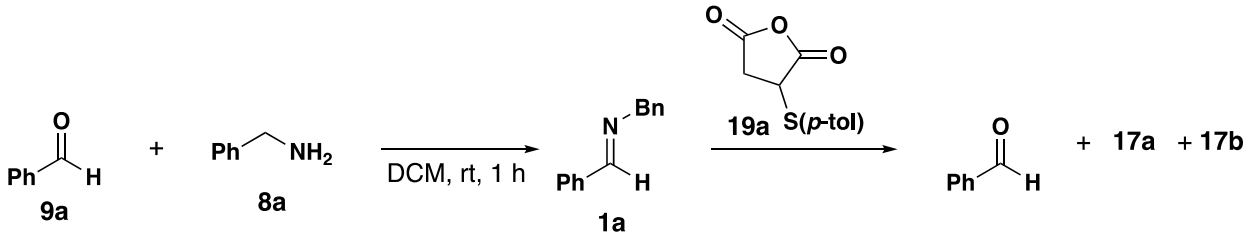

Figure S17. Reaction of benzaldehyde, benzylamine, followed by addition of anhydride.

Benzaldehyde (21 mg, 0.20 mmol) added to DCM (1.96 mL) at room temperature. Benzylamine (21 mg, 0.20 mmol) added to initiate reaction. After complete consumption of benzaldehyde based on IR data (60 minutes) anhydride **19a** (44 mg, 0.20 mmol) was added as a solid. ^{1}H NMR and LCMS of crude mixture confirms reformation of benzaldehyde, although some imine is still present. Ratio benzaldehyde:imine ~5:1 (explains when benzaldehyde did not go back to 100% and why some anhydride still remained). New peak on LCMS with M+1 = 330, matches mass of ring opened-amide product of benzylamine and anhydride.

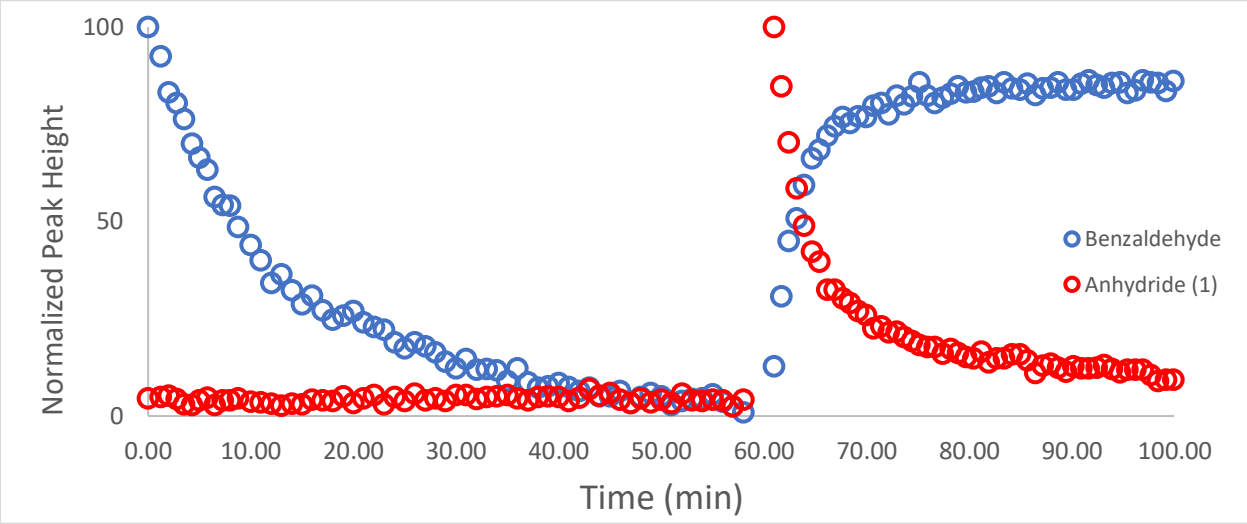

Figure S18. Imine condensation followed by anhydride addition

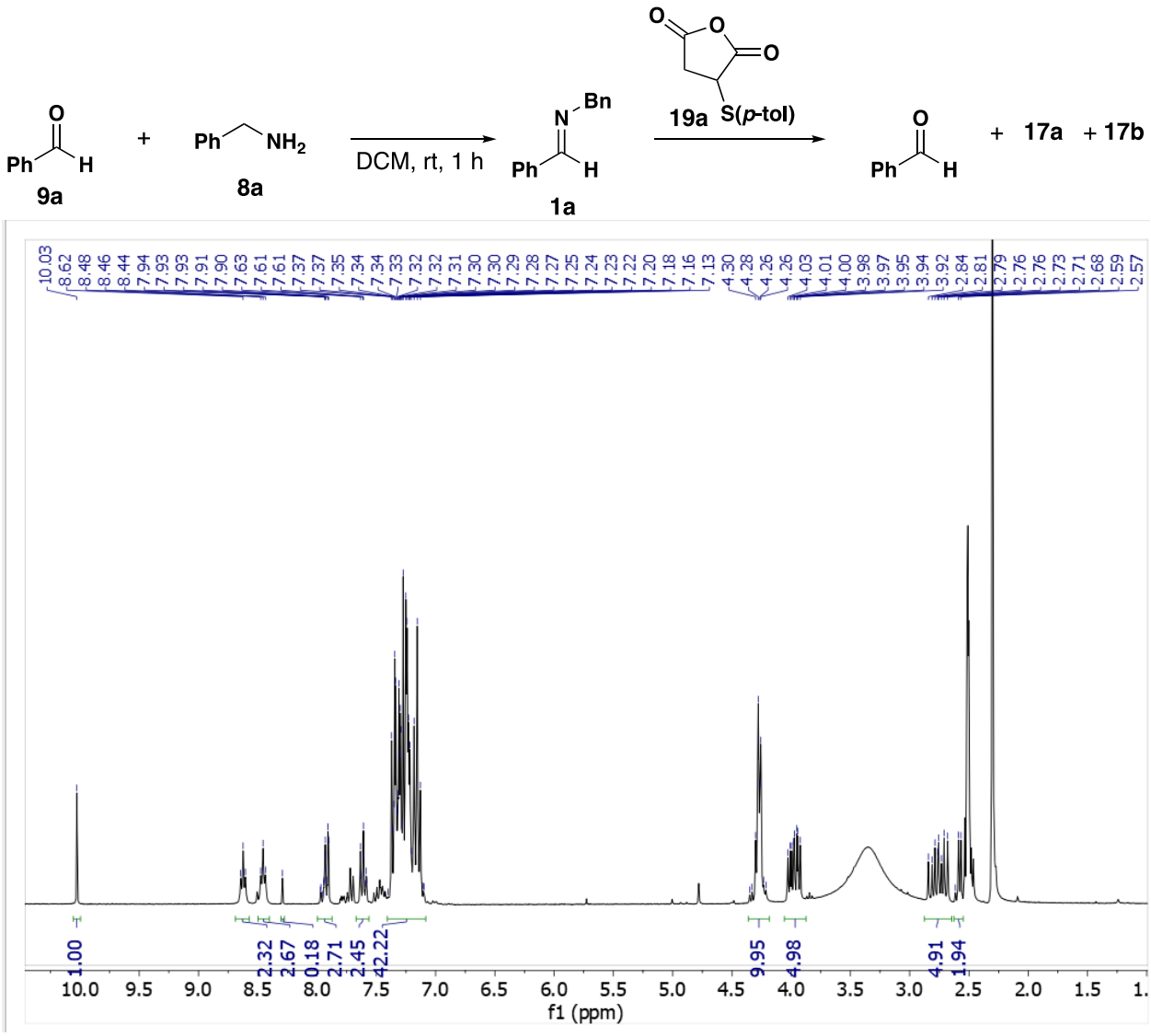

Figure S19. ^{1}H NMR (DMSO d-6) of crude reaction mixture.

X-Ray Crystallographic Data

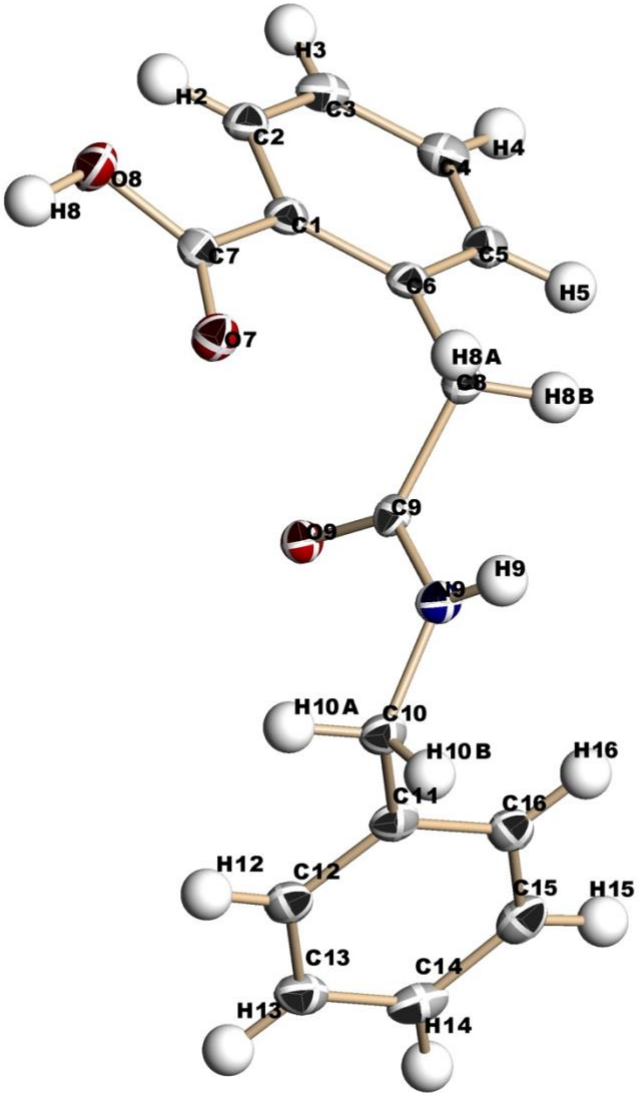

Figure S20: Crystal structure of **26a**. Crystals obtained from slow evaporation in dichloromethane. Thermal ellipsoids are drawn at the 50% probability level.

Table S4. Crystal data and structure refinement for [$C_{16}H_{15}NO_3$].

Identification code	JF2960FMI
Empirical formula	C16 H15 N O3
Formula weight	269.29
Temperature	90(2) K
Wavelength	1.54178 Å

Crystal system	Monoclinic	
Space group	$P2_1/c$	
Unit cell dimensions	a = 11.9787(4) Å	⟨= 90°.
	b = 11.3965(4) Å	®= 97.599(3)°.
	c = 9.5812(3) Å	© = 90°.
Volume	1296.49(8) $Å^3$	
Z	4	
Density (calculated)	1.380 Mg/m^3	
Absorption coefficient	0.782 mm^{-1}	
F(000)	568	
Crystal size	0.325 x 0.047 x 0.036 mm^3	
Crystal color and habit	Colorless Rod	
Diffractometer	Bruker APEX-II CCD	
Theta range for data collection	3.723 to 67.692°.	
Index ranges	-12<=h<=14, -13<=k<=13, -11<=l<=11	
Reflections collected	5179	
Independent reflections	2318 [R(int) = 0.0260]	
Observed reflections (I > 2sigma(I))	1946	
Completeness to theta = 67.679°	98.8 %	
Absorption correction	Semi-empirical from equivalents	
Max. and min. transmission	0.9247 and 0.8204	
Solution method	SHELXT (Sheldrick, 2014)	
Refinement method	SHELXL-2017/1 (Sheldrick, 2017) Full-matrix least-squares on F^2	
Data / restraints / parameters	2318 / 0 / 241	
Goodness-of-fit on F^2	1.013	
Final R indices [I>2sigma(I)]	R1 = 0.0330, wR2 = 0.0847	
R indices (all data)	R1 = 0.0413, wR2 = 0.0899	
Largest diff. peak and hole	0.180 and -0.170 $e.Å^{-3}$	

Table S5. Atomic coordinates (x 10^4) and equivalent isotropic displacement parameters ($Å^2$x 10^3) for JF2960FMI. U(eq) is defined as one third of the trace of the orthogonalized U^{ij} tensor.

	x	y	z	U(eq)
C(1)	6455(1)	7111(1)	4844(2)	19(1)
C(2)	7247(1)	7414(1)	6000(2)	21(1)
C(3)	7441(1)	8574(1)	6379(2)	24(1)
C(4)	6855(1)	9456(1)	5597(2)	25(1)
C(5)	6076(1)	9167(1)	4441(2)	22(1)
C(6)	5850(1)	8006(1)	4056(2)	19(1)
C(7)	6245(1)	5847(1)	4501(2)	20(1)
O(7)	5500(1)	5475(1)	3633(1)	24(1)
C(8)	4980(1)	7780(1)	2792(2)	20(1)
O(8)	6985(1)	5138(1)	5256(1)	29(1)
C(9)	3876(1)	7268(1)	3132(1)	18(1)
N(9)	3138(1)	7043(1)	2000(1)	21(1)
O(9)	3667(1)	7089(1)	4350(1)	20(1)
C(10)	2040(1)	6503(1)	2070(2)	22(1)
C(11)	1254(1)	7224(1)	2841(2)	21(1)
C(12)	602(1)	6665(1)	3746(2)	24(1)
C(13)	-213(1)	7284(1)	4351(2)	26(1)
C(14)	-357(1)	8474(2)	4100(2)	28(1)
C(15)	324(1)	9048(1)	3252(2)	26(1)
C(16)	1119(1)	8426(1)	2615(2)	23(1)

Table S6. Bond lengths [Å] and angles [°] for JF2960FMI.

C(1)-C(2)	1.404(2)
C(1)-C(6)	1.4107(19)
C(1)-C(7)	1.491(2)
C(2)-C(3)	1.382(2)
C(2)-H(2)	0.960(16)
C(3)-C(4)	1.388(2)
C(3)-H(3)	0.956(17)
C(4)-C(5)	1.390(2)
C(4)-H(4)	0.983(18)
C(5)-C(6)	1.391(2)
C(5)-H(5)	0.967(17)
C(6)-C(8)	1.5113(19)
C(7)-O(7)	1.2129(17)
C(7)-O(8)	1.3393(17)
C(8)-C(9)	1.5191(18)
C(8)-H(8A)	0.951(16)
C(8)-H(8B)	0.987(17)
O(8)-H(8)	0.93(3)
C(9)-O(9)	1.2429(17)
C(9)-N(9)	1.3308(18)
N(9)-C(10)	1.4615(18)
N(9)-H(9)	0.866(19)
C(10)-C(11)	1.514(2)
C(10)-H(10A)	1.000(16)
C(10)-H(10B)	0.986(17)
C(11)-C(16)	1.394(2)
C(11)-C(12)	1.395(2)
C(12)-C(13)	1.392(2)
C(12)-H(12)	0.972(17)
C(13)-C(14)	1.383(2)
C(13)-H(13)	0.964(19)
C(14)-C(15)	1.389(2)
C(14)-H(14)	0.982(18)
C(15)-C(16)	1.391(2)

C(15)-H(15)	0.971(18)
C(16)-H(16)	0.982(17)

C(2)-C(1)-C(6)	119.36(13)
C(2)-C(1)-C(7)	119.22(13)
C(6)-C(1)-C(7)	121.40(12)
C(3)-C(2)-C(1)	121.01(14)
C(3)-C(2)-H(2)	120.8(10)
C(1)-C(2)-H(2)	118.2(10)
C(2)-C(3)-C(4)	119.68(14)
C(2)-C(3)-H(3)	118.3(10)
C(4)-C(3)-H(3)	122.0(10)
C(3)-C(4)-C(5)	119.84(14)
C(3)-C(4)-H(4)	120.5(11)
C(5)-C(4)-H(4)	119.7(11)
C(4)-C(5)-C(6)	121.53(14)
C(4)-C(5)-H(5)	118.3(10)
C(6)-C(5)-H(5)	120.2(10)
C(5)-C(6)-C(1)	118.55(13)
C(5)-C(6)-C(8)	117.64(13)
C(1)-C(6)-C(8)	123.79(13)
O(7)-C(7)-O(8)	122.25(13)
O(7)-C(7)-C(1)	125.19(13)
O(8)-C(7)-C(1)	112.56(12)
C(6)-C(8)-C(9)	114.91(11)
C(6)-C(8)-H(8A)	112.3(9)
C(9)-C(8)-H(8A)	105.5(9)
C(6)-C(8)-H(8B)	107.9(10)
C(9)-C(8)-H(8B)	107.9(9)
H(8A)-C(8)-H(8B)	108.1(13)
C(7)-O(8)-H(8)	111.0(14)
O(9)-C(9)-N(9)	122.62(12)
O(9)-C(9)-C(8)	123.61(12)
N(9)-C(9)-C(8)	113.76(12)
C(9)-N(9)-C(10)	123.29(12)
C(9)-N(9)-H(9)	120.1(12)

C(10)-N(9)-H(9)	116.5(12)
N(9)-C(10)-C(11)	114.57(12)
N(9)-C(10)-H(10A)	109.6(8)
C(11)-C(10)-H(10A)	110.6(9)
N(9)-C(10)-H(10B)	106.6(9)
C(11)-C(10)-H(10B)	109.8(9)
H(10A)-C(10)-H(10B)	105.2(12)
C(16)-C(11)-C(12)	118.84(13)
C(16)-C(11)-C(10)	121.64(13)
C(12)-C(11)-C(10)	119.43(13)
C(13)-C(12)-C(11)	120.55(15)
C(13)-C(12)-H(12)	120.8(10)
C(11)-C(12)-H(12)	118.6(10)
C(14)-C(13)-C(12)	120.20(15)
C(14)-C(13)-H(13)	120.0(11)
C(12)-C(13)-H(13)	119.8(11)
C(13)-C(14)-C(15)	119.61(14)
C(13)-C(14)-H(14)	120.8(11)
C(15)-C(14)-H(14)	119.5(11)
C(14)-C(15)-C(16)	120.39(15)
C(14)-C(15)-H(15)	120.6(10)
C(16)-C(15)-H(15)	119.0(10)
C(15)-C(16)-C(11)	120.30(14)
C(15)-C(16)-H(16)	119.8(10)
C(11)-C(16)-H(16)	119.9(10)

Symmetry transformations used to generate equivalent atoms:

Table S7. Anisotropic displacement parameters ($Å^2 x 10^3$) for JF2960FMI. The anisotropic displacement factor exponent takes the form: $-2\pi^2[h^2 a^{*2} U^{11} + ... + 2 h k a^* b^* U^{12}]$

	U^{11}	U^{22}	U^{33}	U^{23}	U^{13}	U^{12}
C(1)	16(1)	24(1)	18(1)	1(1)	5(1)	0(1)
C(2)	15(1)	28(1)	21(1)	2(1)	4(1)	1(1)
C(3)	16(1)	34(1)	23(1)	-3(1)	2(1)	-3(1)
C(4)	21(1)	25(1)	29(1)	-4(1)	6(1)	-3(1)
C(5)	19(1)	22(1)	26(1)	2(1)	6(1)	1(1)
C(6)	15(1)	25(1)	19(1)	1(1)	5(1)	0(1)
C(7)	18(1)	24(1)	20(1)	3(1)	6(1)	1(1)
O(7)	25(1)	23(1)	22(1)	-1(1)	-1(1)	0(1)
C(8)	20(1)	21(1)	19(1)	2(1)	3(1)	1(1)
O(8)	26(1)	22(1)	37(1)	7(1)	-6(1)	1(1)
C(9)	19(1)	17(1)	16(1)	1(1)	2(1)	4(1)
N(9)	20(1)	28(1)	15(1)	0(1)	2(1)	1(1)
O(9)	20(1)	23(1)	17(1)	1(1)	3(1)	1(1)
C(10)	19(1)	26(1)	20(1)	-1(1)	-1(1)	0(1)
C(11)	16(1)	27(1)	18(1)	-3(1)	-4(1)	-2(1)
C(12)	20(1)	27(1)	22(1)	0(1)	-2(1)	-2(1)
C(13)	19(1)	37(1)	23(1)	-1(1)	1(1)	-2(1)
C(14)	18(1)	40(1)	24(1)	-7(1)	-1(1)	5(1)
C(15)	25(1)	26(1)	25(1)	-2(1)	-5(1)	4(1)
C(16)	21(1)	28(1)	19(1)	0(1)	-2(1)	-3(1)

Table S8. Hydrogen coordinates (x 10^4) and isotropic displacement parameters ($Å^2$x 10^{-3}) for JF2960FMI.

	x	y	z	U(eq)
H(2)	7652(12)	6793(14)	6522(17)	18(4)
H(3)	7972(13)	8741(14)	7190(18)	23(4)
H(4)	6992(14)	10284(16)	5848(19)	32(5)
H(5)	5692(13)	9798(15)	3898(18)	23(4)
H(8A)	5243(13)	7248(14)	2143(17)	17(4)
H(8B)	4812(13)	8535(15)	2304(18)	24(4)
H(8)	6734(19)	4360(20)	5210(30)	65(7)
H(9)	3310(14)	7186(15)	1170(20)	29(5)
H(10A)	2147(12)	5702(14)	2493(16)	14(4)
H(10B)	1696(13)	6371(14)	1089(18)	22(4)
H(12)	719(13)	5832(15)	3931(18)	25(4)
H(13)	-666(15)	6886(17)	4960(20)	36(5)
H(14)	-920(14)	8922(16)	4537(19)	33(5)
H(15)	262(13)	9890(16)	3110(18)	28(4)
H(16)	1579(13)	8836(15)	1992(17)	23(4)

Table S9. Torsion angles [°] for JF2960FMI.

C(6)-C(1)-C(2)-C(3)	0.2(2)
C(7)-C(1)-C(2)-C(3)	-177.99(13)
C(1)-C(2)-C(3)-C(4)	-0.8(2)
C(2)-C(3)-C(4)-C(5)	0.2(2)
C(3)-C(4)-C(5)-C(6)	1.1(2)
C(4)-C(5)-C(6)-C(1)	-1.7(2)
C(4)-C(5)-C(6)-C(8)	179.36(12)
C(2)-C(1)-C(6)-C(5)	1.09(19)
C(7)-C(1)-C(6)-C(5)	179.19(12)
C(2)-C(1)-C(6)-C(8)	179.92(12)
C(7)-C(1)-C(6)-C(8)	-2.0(2)
C(2)-C(1)-C(7)-O(7)	171.38(13)
C(6)-C(1)-C(7)-O(7)	-6.7(2)
C(2)-C(1)-C(7)-O(8)	-9.08(18)
C(6)-C(1)-C(7)-O(8)	172.82(12)
C(5)-C(6)-C(8)-C(9)	-108.66(14)
C(1)-C(6)-C(8)-C(9)	72.50(17)
C(6)-C(8)-C(9)-O(9)	3.0(2)
C(6)-C(8)-C(9)-N(9)	-177.97(12)
O(9)-C(9)-N(9)-C(10)	-3.6(2)
C(8)-C(9)-N(9)-C(10)	177.36(12)
C(9)-N(9)-C(10)-C(11)	63.28(18)
N(9)-C(10)-C(11)-C(16)	44.46(18)
N(9)-C(10)-C(11)-C(12)	-139.00(13)
C(16)-C(11)-C(12)-C(13)	3.5(2)
C(10)-C(11)-C(12)-C(13)	-173.14(13)
C(11)-C(12)-C(13)-C(14)	-2.3(2)
C(12)-C(13)-C(14)-C(15)	-0.6(2)
C(13)-C(14)-C(15)-C(16)	2.3(2)
C(14)-C(15)-C(16)-C(11)	-1.1(2)
C(12)-C(11)-C(16)-C(15)	-1.8(2)
C(10)-C(11)-C(16)-C(15)	174.76(12)

Symmetry transformations used to generate equivalent atoms:

6 July, 2020

JF2960 Cu (NYH-IV-061)

A colorless rod with approximate orthogonal dimensions 0.036 x 0.047 x 0.325mm^3 was placed and optically centered on the Bruker Duo[1] APEXII CCD system at –183°C(90K). Indexing of the unit cell used a random set of reflections collected from three series of 0.5° wide ω-scans, 10 seconds per frame, and 30 frames per series that were well distributed in reciprocal space. Data were collected [CuKα] with 0.5° wide scans, variable time per frame dependent upon detector 2θ angle and varying φ and omega angles such that nearly all unique reflections were collected at least once. The crystal to detector distance was 4.96cm, thus providing a nearly complete sphere of data to $2\theta_{max}$=137.20°.

Structural determination and Refinement:

All crystallographic calculations were performed on an Intel Xeon E5-1620v2 at 3.70GHz an eight core processor and 16GB of extended memory. Data collected were corrected for Lorentz and polarization effects with Saint[1] and absorption using Blessing's method and merged as incorporated with the program Sadabs[2,3]. The SHELXTL[4] program package was implemented to determine the probable space group and set up the initial files. System symmetry, systematic absences and intensity statistics indicated the centrosymmetric monoclinic space group $P2_1/c$ (no. 14). The structure was determined by direct methods with the non-hydrogen atoms being located directly for the molecule using the program XT[5]. The structure was refined with XL[6]. The 8861 data collected were merged, based upon identical indices to 5179 data, then for least squares refinement to 2318 unique data [R(int)=0.0260]. All non-hydrogen atoms were refined anisotropically. Hydrogen atoms were idealized initially and then allowed to refine freely throughout the final refinement stage. The final structure was refined to convergence with R(F)=4.13%, wR(F^2)=8.99%, GOF=1.013 for all 2318 unique reflections [R(F)=3.30, wR(F^2)=8.47% for those 1946 data with Fo > 4σ(Fo)]. The final difference-Fourier map was featureless indicating that the structure is both correct and complete.

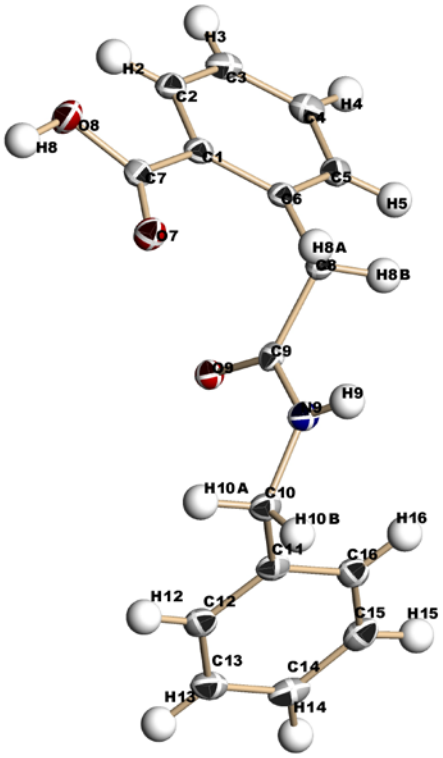

References:

1. Bruker (2019) APEX3 (Version 2019.0) and (2016) SAINT (Version 8.37a). Bruker AXS Inc., Madison, Wisconsin, USA.
2. An Empirical Correction for Absorption Anisotropy, Blessing, R. H. (1995). Acta Cryst., A51, 33-38.

3. Sheldrick, G.M., SADABS (2016) Version 2016/2, 'Siemens Area Detector Absorption Correction' Universität Göttingen: Göttingen, Germany.

4. Sheldrick, G.M., (2002). SHELXTL. Version 6.1. Bruker AXS Inc., Madison, Wisconsin, USA.

5. Sheldrick, G. M., (2014) SHELXT, Universität Göttingen: Göttingen, Germany. Structure determination program. Private communication.

6. Sheldrick, G. M., (2017). SHELXL2017/1. Universität Göttingen: Göttingen, Germany.

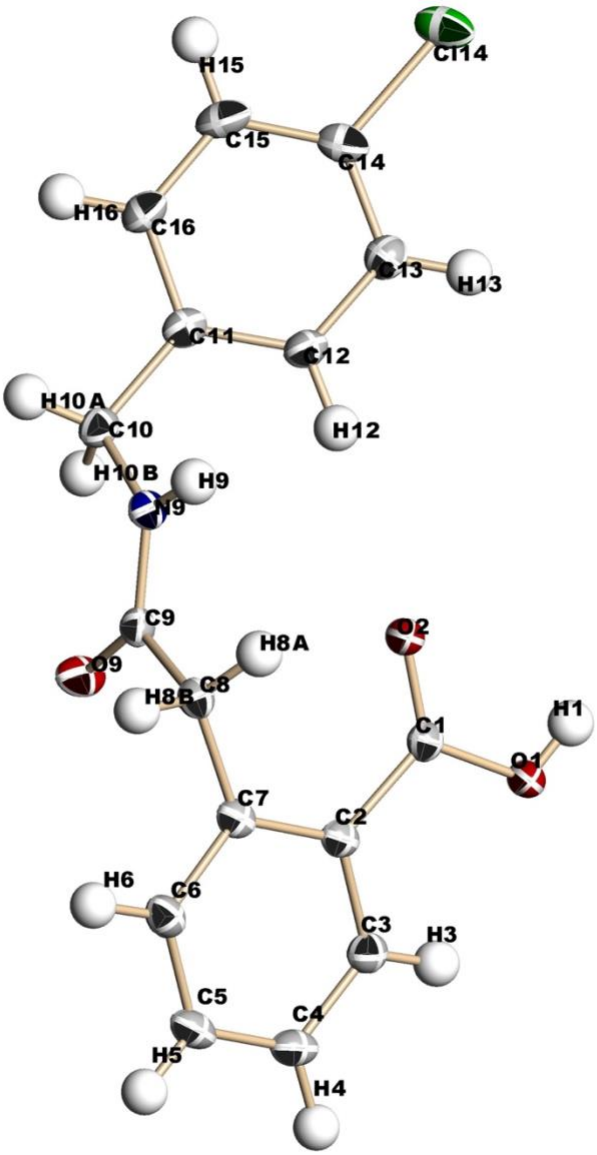

Figure S21. Crystal structure of **26b**. Crystals obtained from slow evaporation in dichloromethane. Thermal ellipsoids are drawn at the 50% probability level.

Table S10. Crystal data and structure refinement for [$C_{16}H_{14}NO_3Cl$].

Identification code	JF3007LMI (NYH-IV-178)
Empirical formula	C16 H14 Cl N O3
Formula weight	303.73
Temperature	100(2) K

Wavelength	0.71073 Å	
Crystal system	Monoclinic	
Space group	$P2_1/n$	
Unit cell dimensions	a = 16.5114(9) Å	⟨= 90°.
	b = 4.8160(3) Å	®= 97.8796(19)°.
	c = 17.8572(10) Å	© = 90°.
Volume	1406.58(14) $Å^3$	
Z	4	
Density (calculated)	1.434 Mg/m^3	
Absorption coefficient	0.281 mm^{-1}	
F(000)	632	
Crystal size	0.204 x 0.059 x 0.058 mm^3	
Crystal color and habit	White Rod	
Diffractometer	Bruker Photon100 CMOS	
Theta range for data collection	2.303 to 27.562°.	
Index ranges	-21<=h<=21, -6<=k<=6, -23<=l<=22	
Reflections collected	11924	
Independent reflections	3248 [R(int) = 0.0351]	
Observed reflections (I > 2sigma(I))	2729	
Completeness to theta = 25.242°	99.9 %	
Absorption correction	Semi-empirical from equivalents	
Max. and min. transmission	0.9766 and 0.8140	
Solution method	SHELXT (Sheldrick, 2014)	
Refinement method	SHELXL-2017/1 (Sheldrick, 2017) Full-matrix least-squares on F^2	
Data / restraints / parameters	3248 / 0 / 247	
Goodness-of-fit on F^2	1.036	
Final R indices [I>2sigma(I)]	R1 = 0.0407, wR2 = 0.1027	
R indices (all data)	R1 = 0.0504, wR2 = 0.1093	
Extinction coefficient	0.0126(16)	
Largest diff. peak and hole	0.500 and -0.432 $e.Å^{-3}$	

Table S11. Atomic coordinates (x 10^4) and equivalent isotropic displacement parameters ($Å^2$x 10^3) for JF3007LMI. U(eq) is defined as one third of the trace of the orthogonalized U^{ij} tensor.

	x	y	z	U(eq)
C(1)	4614(1)	2268(3)	4258(1)	20(1)
O(1)	4244(1)	2279(3)	4869(1)	25(1)
C(2)	4228(1)	371(3)	3656(1)	20(1)
O(2)	5210(1)	3719(2)	4196(1)	24(1)
C(3)	3612(1)	-1423(3)	3827(1)	23(1)
C(4)	3205(1)	-3151(3)	3281(1)	25(1)
C(5)	3405(1)	-3071(4)	2551(1)	25(1)
C(6)	4015(1)	-1306(3)	2378(1)	23(1)
C(7)	4447(1)	421(3)	2921(1)	19(1)
C(8)	5125(1)	2186(3)	2684(1)	20(1)
C(9)	5965(1)	928(3)	2939(1)	20(1)
N(9)	6575(1)	2740(3)	3072(1)	20(1)
O(9)	6060(1)	-1607(2)	2980(1)	28(1)
C(10)	7420(1)	1930(3)	3329(1)	23(1)
C(11)	7812(1)	3898(3)	3928(1)	21(1)
C(12)	7376(1)	4941(3)	4477(1)	24(1)
C(13)	7724(1)	6823(4)	5017(1)	26(1)
C(14)	8522(1)	7648(4)	5000(1)	26(1)
Cl(14)	8945(1)	10125(1)	5657(1)	35(1)
C(15)	8981(1)	6611(4)	4475(1)	30(1)
C(16)	8623(1)	4736(4)	3937(1)	26(1)

Table S12. Bond lengths [Å] and angles [°] for JF3007LMI.

C(1)-O(2)	1.2230(19)
C(1)-O(1)	1.3216(19)
C(1)-C(2)	1.487(2)
O(1)-H(1)	0.81(3)
C(2)-C(3)	1.400(2)
C(2)-C(7)	1.409(2)
C(3)-C(4)	1.384(2)
C(3)-H(3)	0.94(2)
C(4)-C(5)	1.389(3)
C(4)-H(4)	0.98(2)
C(5)-C(6)	1.385(2)
C(5)-H(5)	0.92(2)
C(6)-C(7)	1.396(2)
C(6)-H(6)	0.978(19)
C(7)-C(8)	1.510(2)
C(8)-C(9)	1.525(2)
C(8)-H(8A)	0.96(2)
C(8)-H(8B)	0.970(19)
C(9)-O(9)	1.232(2)
C(9)-N(9)	1.330(2)
N(9)-C(10)	1.460(2)
N(9)-H(9)	0.86(2)
C(10)-C(11)	1.508(2)
C(10)-H(10A)	0.937(19)
C(10)-H(10B)	0.98(2)
C(11)-C(12)	1.388(2)
C(11)-C(16)	1.395(2)
C(12)-C(13)	1.389(2)
C(12)-H(12)	0.96(2)
C(13)-C(14)	1.381(2)
C(13)-H(13)	0.954(19)
C(14)-C(15)	1.377(3)
C(14)-Cl(14)	1.7491(17)
C(15)-C(16)	1.391(3)

C(15)-H(15)	0.96(2)
C(16)-H(16)	0.948(19)

O(2)-C(1)-O(1)	122.69(14)
O(2)-C(1)-C(2)	123.86(14)
O(1)-C(1)-C(2)	113.44(14)
C(1)-O(1)-H(1)	108.6(17)
C(3)-C(2)-C(7)	120.12(15)
C(3)-C(2)-C(1)	118.30(15)
C(7)-C(2)-C(1)	121.54(14)
C(4)-C(3)-C(2)	120.91(16)
C(4)-C(3)-H(3)	120.9(12)
C(2)-C(3)-H(3)	118.2(12)
C(3)-C(4)-C(5)	119.35(16)
C(3)-C(4)-H(4)	119.2(12)
C(5)-C(4)-H(4)	121.4(12)
C(6)-C(5)-C(4)	120.00(16)
C(6)-C(5)-H(5)	119.5(13)
C(4)-C(5)-H(5)	120.5(13)
C(5)-C(6)-C(7)	121.96(16)
C(5)-C(6)-H(6)	118.5(11)
C(7)-C(6)-H(6)	119.5(11)
C(6)-C(7)-C(2)	117.63(15)
C(6)-C(7)-C(8)	117.96(15)
C(2)-C(7)-C(8)	124.41(14)
C(7)-C(8)-C(9)	111.77(13)
C(7)-C(8)-H(8A)	112.1(11)
C(9)-C(8)-H(8A)	110.2(11)
C(7)-C(8)-H(8B)	107.7(11)
C(9)-C(8)-H(8B)	107.7(11)
H(8A)-C(8)-H(8B)	107.1(16)
O(9)-C(9)-N(9)	123.52(15)
O(9)-C(9)-C(8)	121.01(14)
N(9)-C(9)-C(8)	115.38(14)
C(9)-N(9)-C(10)	123.27(14)
C(9)-N(9)-H(9)	118.4(13)

C(10)-N(9)-H(9)	117.7(13)
N(9)-C(10)-C(11)	110.76(13)
N(9)-C(10)-H(10A)	109.9(11)
C(11)-C(10)-H(10A)	110.2(12)
N(9)-C(10)-H(10B)	106.8(12)
C(11)-C(10)-H(10B)	111.3(12)
H(10A)-C(10)-H(10B)	107.8(17)
C(12)-C(11)-C(16)	118.54(16)
C(12)-C(11)-C(10)	120.94(14)
C(16)-C(11)-C(10)	120.52(15)
C(11)-C(12)-C(13)	121.40(15)
C(11)-C(12)-H(12)	120.7(12)
C(13)-C(12)-H(12)	117.9(12)
C(14)-C(13)-C(12)	118.50(16)
C(14)-C(13)-H(13)	120.6(12)
C(12)-C(13)-H(13)	120.9(12)
C(15)-C(14)-C(13)	121.76(16)
C(15)-C(14)-Cl(14)	119.83(13)
C(13)-C(14)-Cl(14)	118.40(14)
C(14)-C(15)-C(16)	119.00(16)
C(14)-C(15)-H(15)	120.4(14)
C(16)-C(15)-H(15)	120.6(14)
C(15)-C(16)-C(11)	120.76(16)
C(15)-C(16)-H(16)	119.9(11)
C(11)-C(16)-H(16)	119.4(11)

Symmetry transformations used to generate equivalent atoms:

Table S13. Anisotropic displacement parameters ($Å^2 x 10^3$) for JF3007LMI. The anisotropic displacement factor exponent takes the form: $-2\pi^2[h^2 a^{*2} U^{11} + ... + 2 h k a^* b^* U^{12}]$

	U^{11}	U^{22}	U^{33}	U^{23}	U^{13}	U^{12}
C(1)	19(1)	20(1)	22(1)	-1(1)	4(1)	2(1)
O(1)	25(1)	27(1)	25(1)	-7(1)	8(1)	-7(1)
C(2)	17(1)	16(1)	25(1)	-2(1)	1(1)	3(1)
O(2)	23(1)	26(1)	24(1)	-6(1)	6(1)	-5(1)
C(3)	20(1)	20(1)	28(1)	0(1)	4(1)	2(1)
C(4)	19(1)	19(1)	36(1)	0(1)	0(1)	-1(1)
C(5)	22(1)	20(1)	32(1)	-5(1)	-4(1)	1(1)
C(6)	23(1)	21(1)	24(1)	-3(1)	-1(1)	3(1)
C(7)	18(1)	16(1)	24(1)	0(1)	-1(1)	4(1)
C(8)	22(1)	17(1)	20(1)	0(1)	3(1)	2(1)
C(9)	22(1)	19(1)	19(1)	0(1)	5(1)	1(1)
N(9)	21(1)	14(1)	25(1)	1(1)	3(1)	2(1)
O(9)	25(1)	14(1)	46(1)	1(1)	4(1)	1(1)
C(10)	21(1)	20(1)	29(1)	1(1)	7(1)	2(1)
C(11)	21(1)	18(1)	25(1)	6(1)	3(1)	1(1)
C(12)	18(1)	24(1)	28(1)	1(1)	4(1)	-1(1)
C(13)	25(1)	26(1)	25(1)	2(1)	4(1)	1(1)
C(14)	28(1)	25(1)	22(1)	5(1)	-4(1)	-6(1)
Cl(14)	40(1)	37(1)	24(1)	4(1)	-4(1)	-15(1)
C(15)	21(1)	39(1)	29(1)	8(1)	2(1)	-8(1)
C(16)	22(1)	31(1)	26(1)	5(1)	7(1)	-1(1)

Table S14. Hydrogen coordinates (x 10^4) and isotropic displacement parameters ($Å^2$x 10^{-3}) for JF3007LMI.

	x	y	z	U(eq)
H(1)	4457(15)	3440(50)	5157(14)	44(7)
H(3)	3486(12)	-1440(40)	4324(12)	27(5)
H(4)	2768(12)	-4360(40)	3414(11)	29(5)
H(5)	3131(13)	-4170(50)	2177(12)	31(5)
H(6)	4150(11)	-1300(40)	1862(11)	20(5)
H(8A)	5105(11)	4060(40)	2862(11)	21(5)
H(8B)	5048(11)	2260(40)	2136(11)	23(5)
H(9)	6458(12)	4490(40)	3071(11)	24(5)
H(10A)	7717(11)	1900(40)	2918(11)	22(5)
H(10B)	7403(12)	30(40)	3525(12)	29(5)
H(12)	6815(13)	4400(40)	4488(11)	28(5)
H(13)	7417(11)	7550(40)	5388(11)	23(5)
H(15)	9543(14)	7150(50)	4488(13)	44(6)
H(16)	8935(11)	3980(40)	3578(11)	20(4)

Table S15. Torsion angles [°] for JF3007LMI.

O(2)-C(1)-C(2)-C(3)	172.49(15)
O(1)-C(1)-C(2)-C(3)	-8.6(2)
O(2)-C(1)-C(2)-C(7)	-9.7(2)
O(1)-C(1)-C(2)-C(7)	169.17(14)
C(7)-C(2)-C(3)-C(4)	-0.6(2)
C(1)-C(2)-C(3)-C(4)	177.21(14)
C(2)-C(3)-C(4)-C(5)	-0.9(2)
C(3)-C(4)-C(5)-C(6)	1.0(2)
C(4)-C(5)-C(6)-C(7)	0.2(2)
C(5)-C(6)-C(7)-C(2)	-1.6(2)
C(5)-C(6)-C(7)-C(8)	177.58(15)
C(3)-C(2)-C(7)-C(6)	1.8(2)
C(1)-C(2)-C(7)-C(6)	-175.93(14)
C(3)-C(2)-C(7)-C(8)	-177.37(14)
C(1)-C(2)-C(7)-C(8)	4.9(2)
C(6)-C(7)-C(8)-C(9)	-100.82(16)
C(2)-C(7)-C(8)-C(9)	78.34(19)
C(7)-C(8)-C(9)-O(9)	32.5(2)
C(7)-C(8)-C(9)-N(9)	-150.87(14)
O(9)-C(9)-N(9)-C(10)	-4.2(3)
C(8)-C(9)-N(9)-C(10)	179.27(14)
C(9)-N(9)-C(10)-C(11)	-138.56(15)
N(9)-C(10)-C(11)-C(12)	38.9(2)
N(9)-C(10)-C(11)-C(16)	-140.24(15)
C(16)-C(11)-C(12)-C(13)	1.3(2)
C(10)-C(11)-C(12)-C(13)	-177.93(15)
C(11)-C(12)-C(13)-C(14)	-0.1(3)
C(12)-C(13)-C(14)-C(15)	-1.4(3)
C(12)-C(13)-C(14)-Cl(14)	177.40(13)
C(13)-C(14)-C(15)-C(16)	1.6(3)
Cl(14)-C(14)-C(15)-C(16)	-177.16(14)
C(14)-C(15)-C(16)-C(11)	-0.4(3)
C(12)-C(11)-C(16)-C(15)	-1.0(3)
C(10)-C(11)-C(16)-C(15)	178.15(16)

Symmetry transformations used to generate equivalent atoms:

Table S16. Hydrogen bonds for JF3007LMI [Å and °].

D-H...A	d(D-H)	d(H...A)	d(D...A)	<(DHA)
O(1)-H(1)...O(2)#1	0.81(3)	1.83(3)	2.6273(17)	172(2)
N(9)-H(9)...O(9)#2	0.86(2)	1.99(2)	2.8503(17)	172.7(19)

Symmetry transformations used to generate equivalent atoms:

#1 -x+1,-y+1,-z+1 #2 x,y+1,z

21 January, 2021

JF3007 NYH-1-178

A white rod with approximate orthogonal dimensions 0.058 x 0.059 x 0.204mm^3 was placed and optically centered on the Bruker[1] Venture Dual source Kappa Photon100 diffractometer at –173°C(100K). Indexing of the unit cell used a random set of reflections collected from three series of 0.5° wide ω-scans, 5 seconds per frame, and 30 frames per series that were well distributed in reciprocal space. Data were collected [MoKα] with 0.3° wide scans, variable time per frame dependent upon detector 2θ angle and varying φ and omega angles such that nearly all unique reflections were collected at least once. The crystal to detector distance was 65.00mm, thus providing a complete sphere of data to $2\theta_{max}$=55.15°.

Structural determination and Refinement:

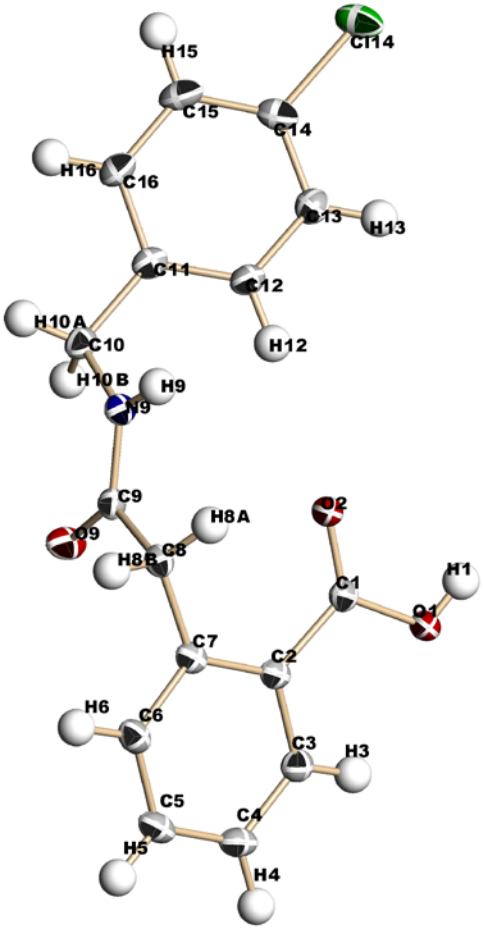

All crystallographic calculations were performed on a Surface Pro7 with Intel i7-1065G7 at 1.30GHz with four cores, eight processors and 16GB of extended memory. Data collected were corrected for Lorentz and polarization effects with Saint[1] and absorption using Blessing's method and merged as incorporated with the program Sadabs[2,3]. The SHELXTL[4] program package was implemented to determine the probable space group and set up the initial files. System symmetry, systematic absences and intensity statistics indicated the centrosymmetric monoclinic space group $P2_1/n$ (no. 14). The structure was determined by direct methods with the location of nearly all of the non-hydrogen atoms for the molecule of using the program XT[5]. The structure was refined with XL[6]. The 30430 data collected were merged for identical indices to 11924 reflections and then for least squares refinement to 3248 unique data [R(int)=0.0351]. Non-hydrogen atoms were refined anisotropically. Hydrogen atoms were idealized initially and then allowed to refine freely throughout the final refinement. The final structure was refined to convergence with R(F)=5.04%, wR(F^2)=10.93%, GOF=1.036 for all 3248 unique reflections [R(F)=4.07, wR(F^2)=10.27% for those 2729 data with Fo > 4σ(Fo)]. The final difference-Fourier map was featureless indicating that the structure is both correct and complete.

References:

1. Bruker (2019) APEX3 (Version 2019.1) and (2016) SAINT (Version 8.37a). Bruker AXS Inc., Madison, Wisconsin, USA.
2. An Empirical Correction for Absorption Anisotropy, Blessing, R. H. (1995). Acta Cryst., A51, 33-38.

3. Sheldrick, G.M., SADABS (2016) Version 2016/2, 'Siemens Area Detector Absorption Correction' Universität Göttingen: Göttingen, Germany.

4. Sheldrick, G.M., (2002). SHELXTL. Version 6.1. Bruker AXS Inc., Madison, Wisconsin, USA.

5. Sheldrick, G. M., (2014) SHELXT, Universität Göttingen: Göttingen, Germany. Structure determination program. Private communication.

6. Sheldrick, G. M., (2017). SHELXL2017/1. Universität Göttingen: Göttingen, Germany.

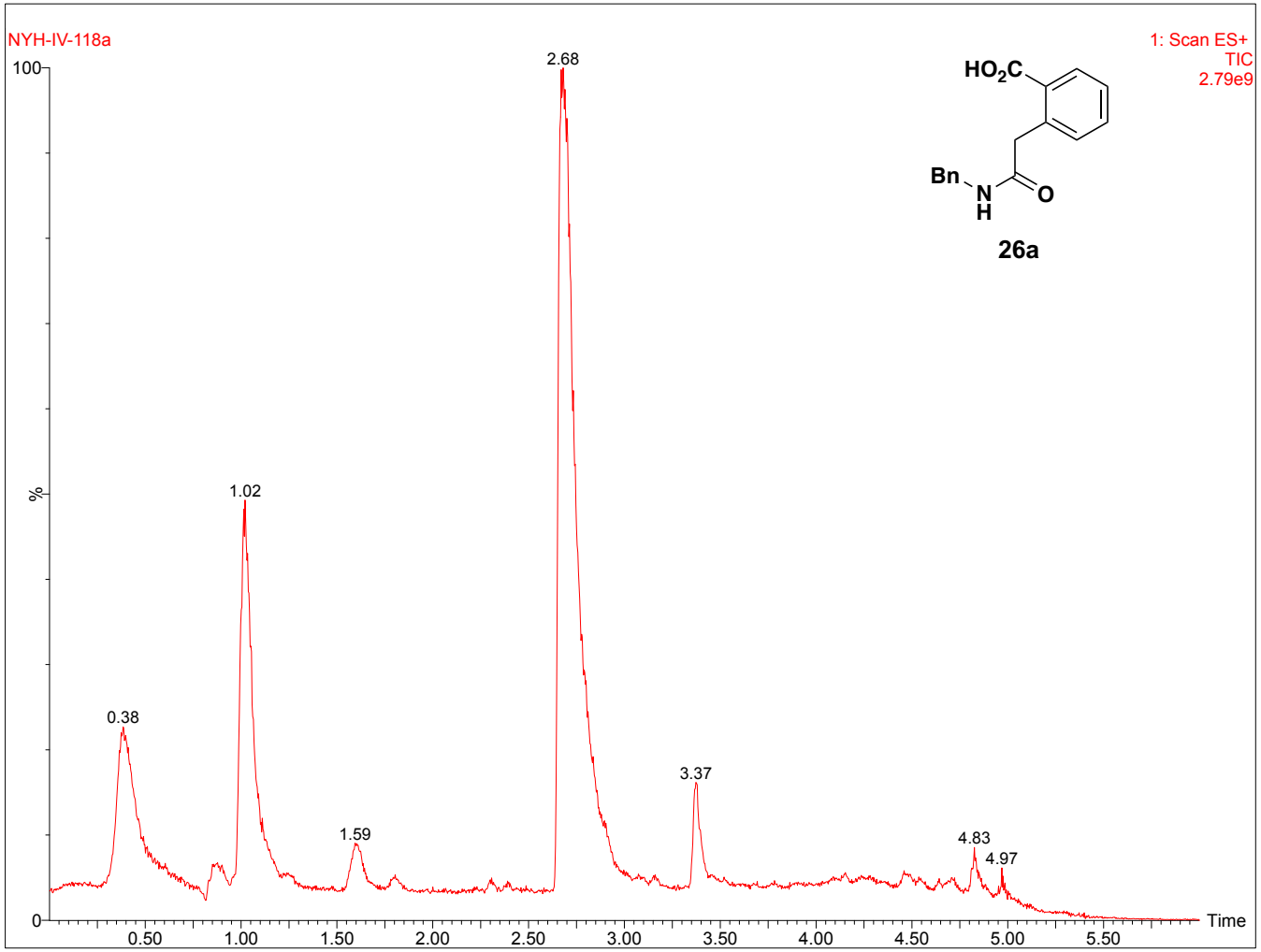
NYH-IV-118a
1: Scan ES+
TIC
2.79e9
100
%
0
2.68
1.02
0.38
1.59
3.37
4.83
4.97
0.50
1.00
1.50
2.00
2.50
3.00
3.50
4.00
4.50
5.00
5.50
Time
HO2C
Bn
N
H
O
26a

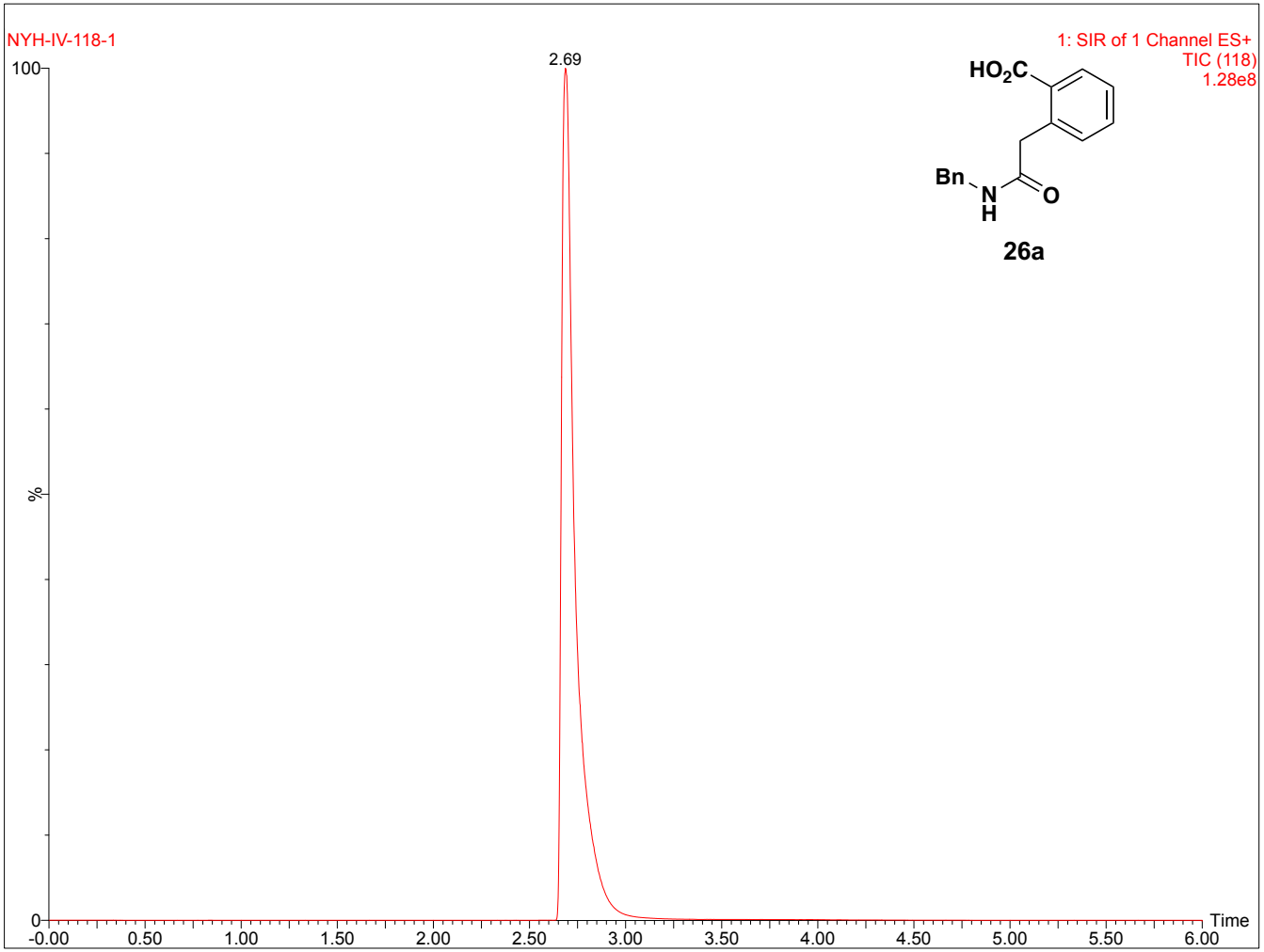
NYH-IV-118-1
1: SIR of 1 Channel ES+
TIC (118)
1.28e8
2.69
100
%
0
Time
-0.00
0.50
1.00
1.50
2.00
2.50
3.00
3.50
4.00
4.50
5.00
5.50
6.00
HO2C
Bn
N
H
O
26a

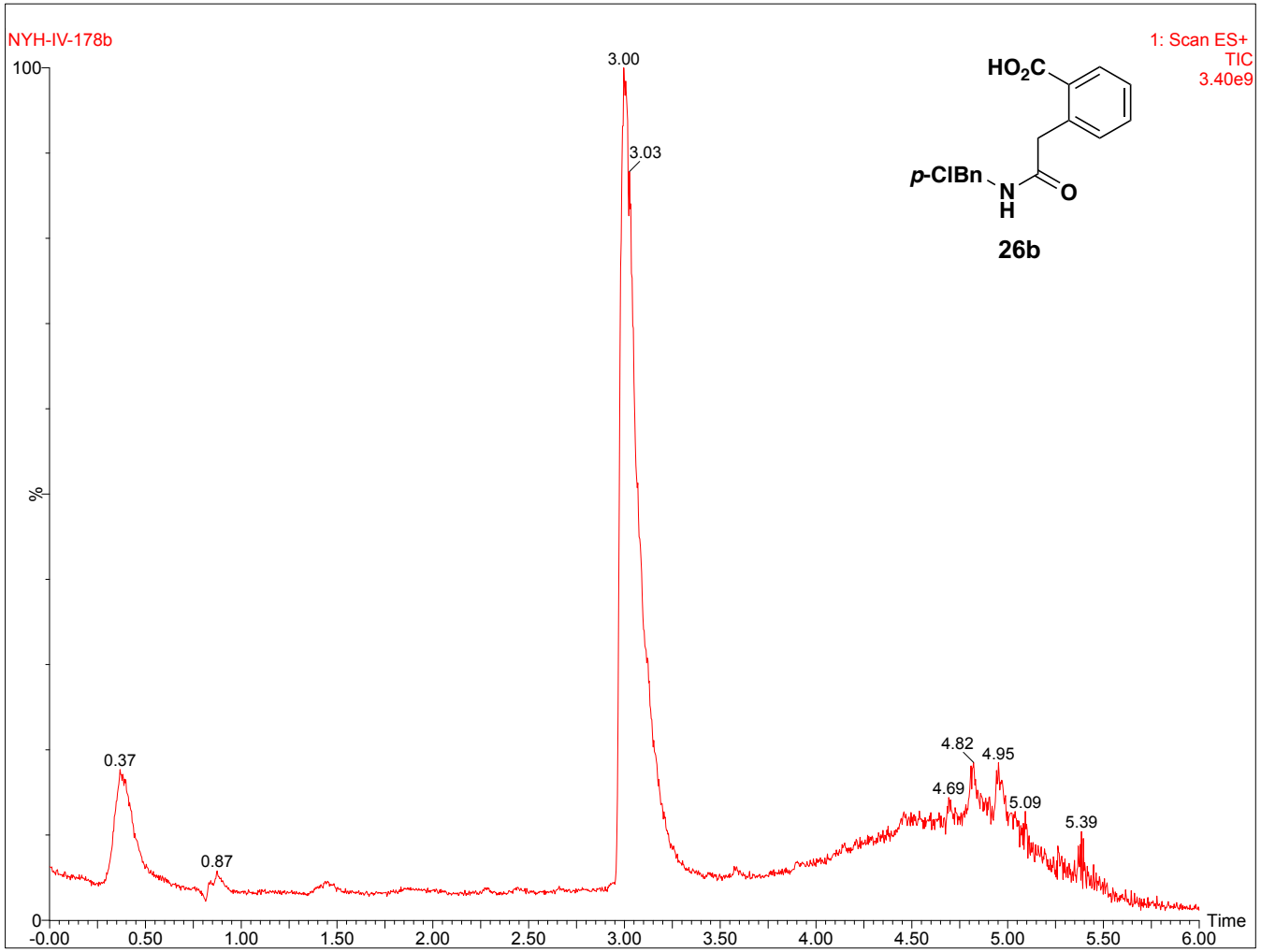
NYH-IV-178b
1: Scan ES+
TIC
3.40e9
100
%
0
3.00
3.03
0.37
0.87
4.69
4.82
4.95
5.09
5.39
Time
-0.00
0.50
1.00
1.50
2.00
2.50
3.00
3.50
4.00
4.50
5.00
5.50
6.00
HO2C
p-ClBn
N
H
O
26b

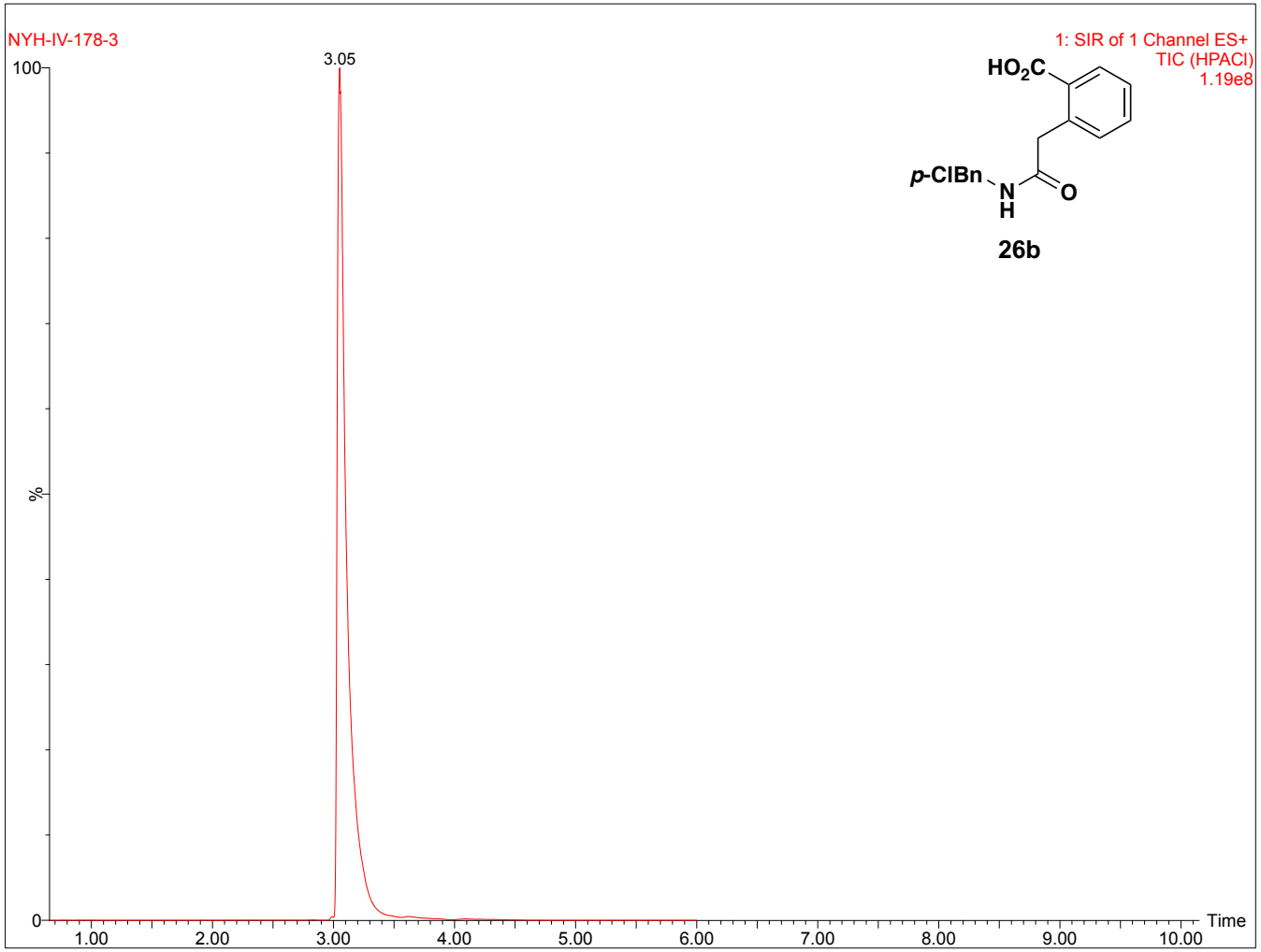
NYH-IV-178-3
1: SIR of 1 Channel ES+
TIC (HPACI)
1.19e8
3.05
100
%
0
1.00
2.00
3.00
4.00
5.00
6.00
7.00
8.00
9.00
10.00
Time
HO2C
p-ClBn
N
H
O
26b

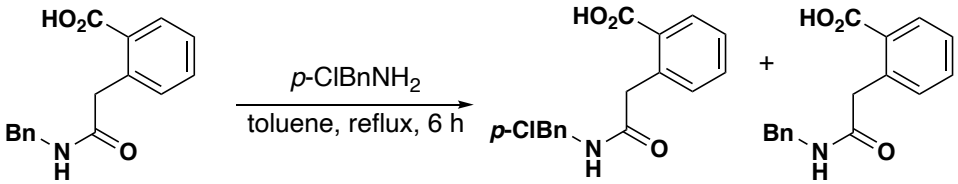
HO2C
Bn
N
H
O
p-ClBnNH2
toluene, reflux, 6 h
p-ClBn
+

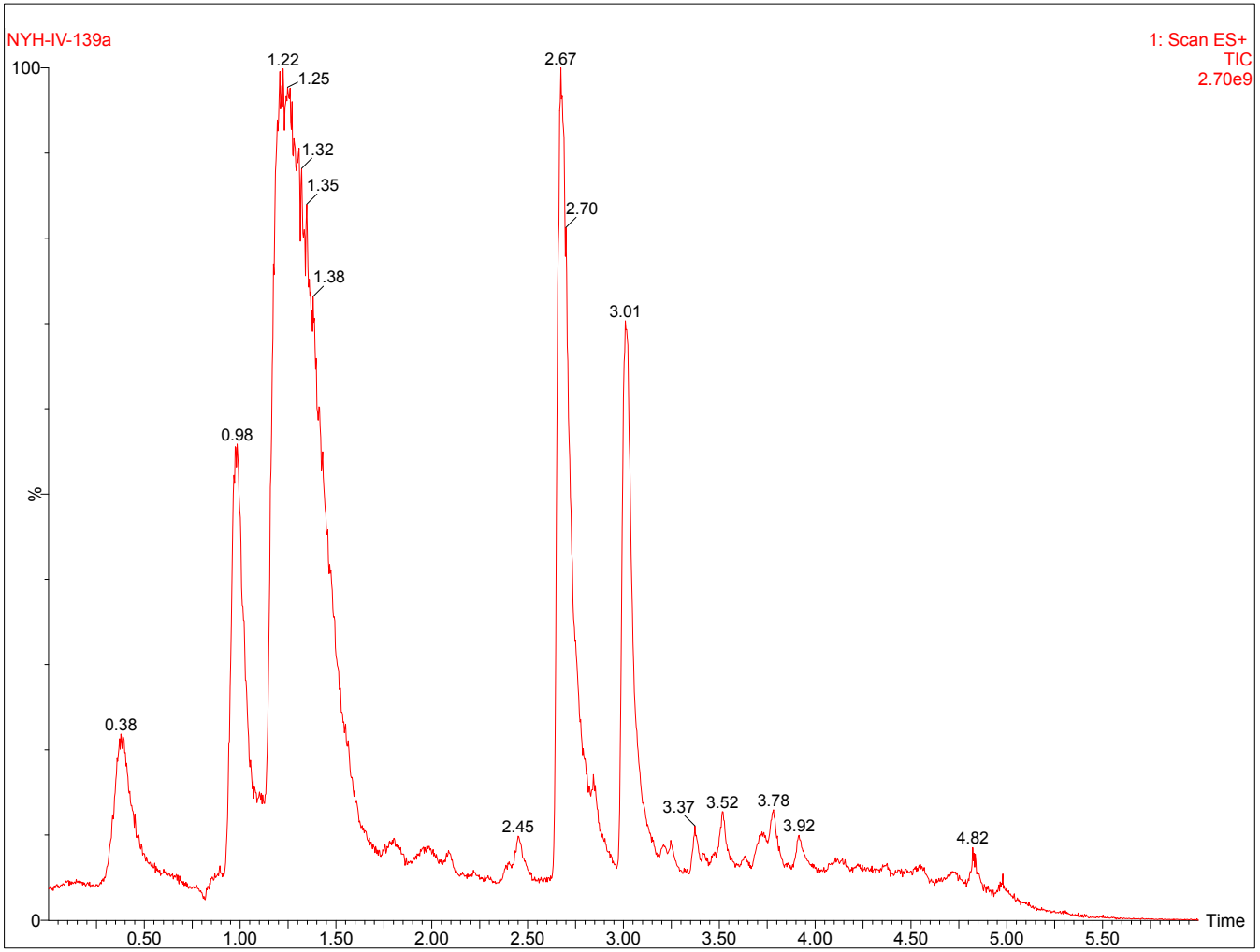
NYH-IV-139a
1: Scan ES+
TIC
2.70e9
100
%
0
1.22
1.25
1.32
1.35
1.38
2.67
2.70
3.01
0.98
0.38
2.45
3.37
3.52
3.78
3.92
4.82
0.50
1.00
1.50
2.00
2.50
3.00
3.50
4.00
4.50
5.00
5.50
Time

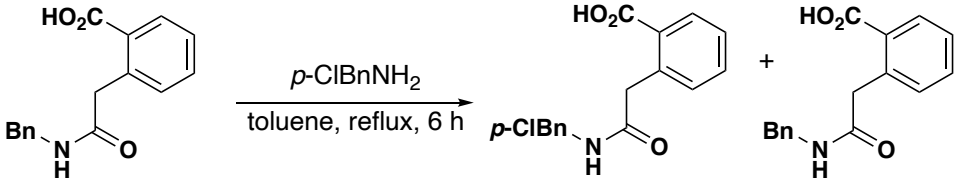
HO2C
Bn
N
H
O
p-ClBnNH2
toluene, reflux, 6 h
HO2C
p-ClBn
N
H
O
+
HO2C
Bn
N
H
O

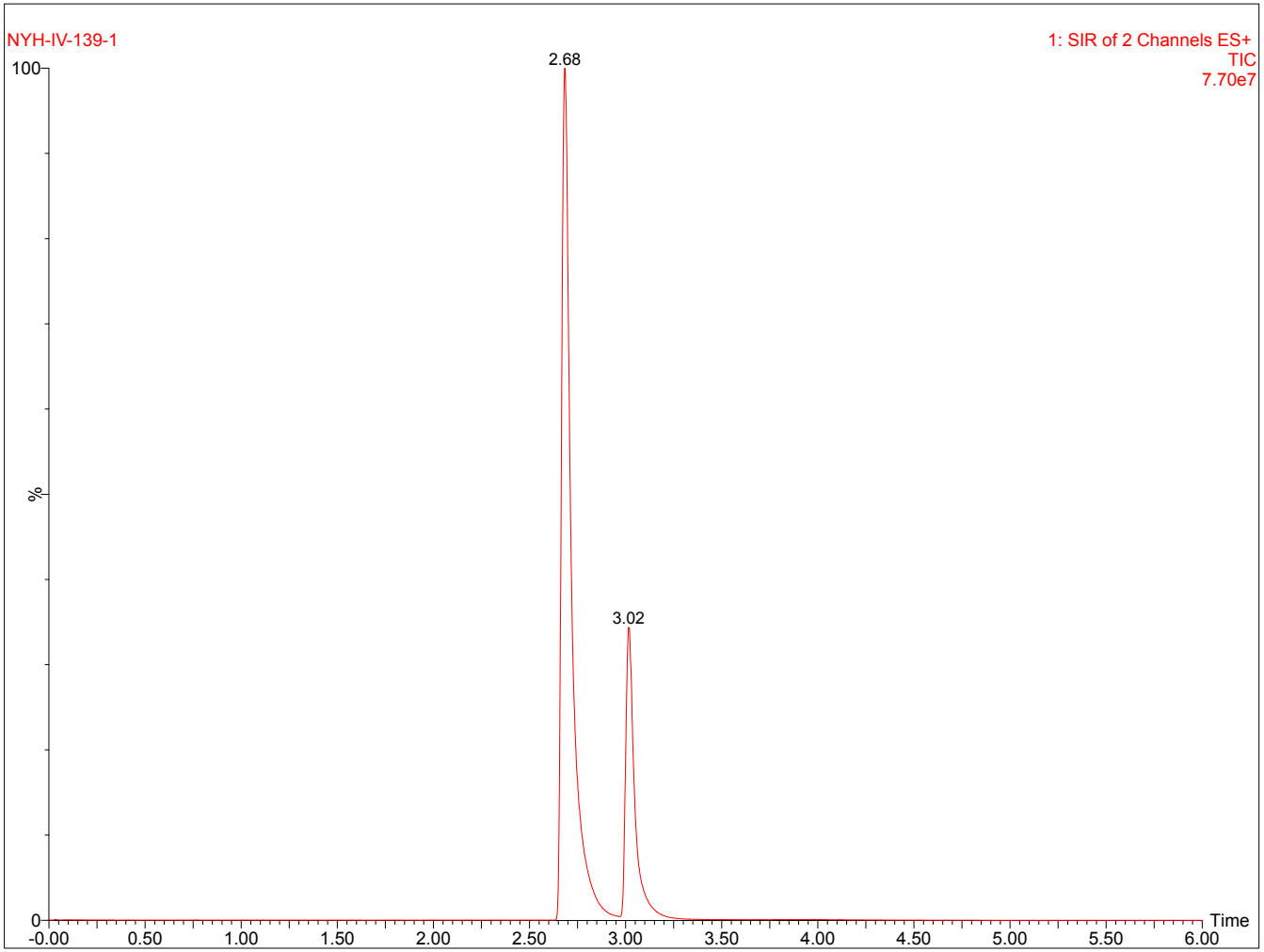
NYH-IV-139-1
1: SIR of 2 Channels ES+
TIC
7.70e7
2.68
3.02
100
%
0
Time
-0.00
0.50
1.00
1.50
2.00
2.50
3.00
3.50
4.00
4.50
5.00
5.50
6.00

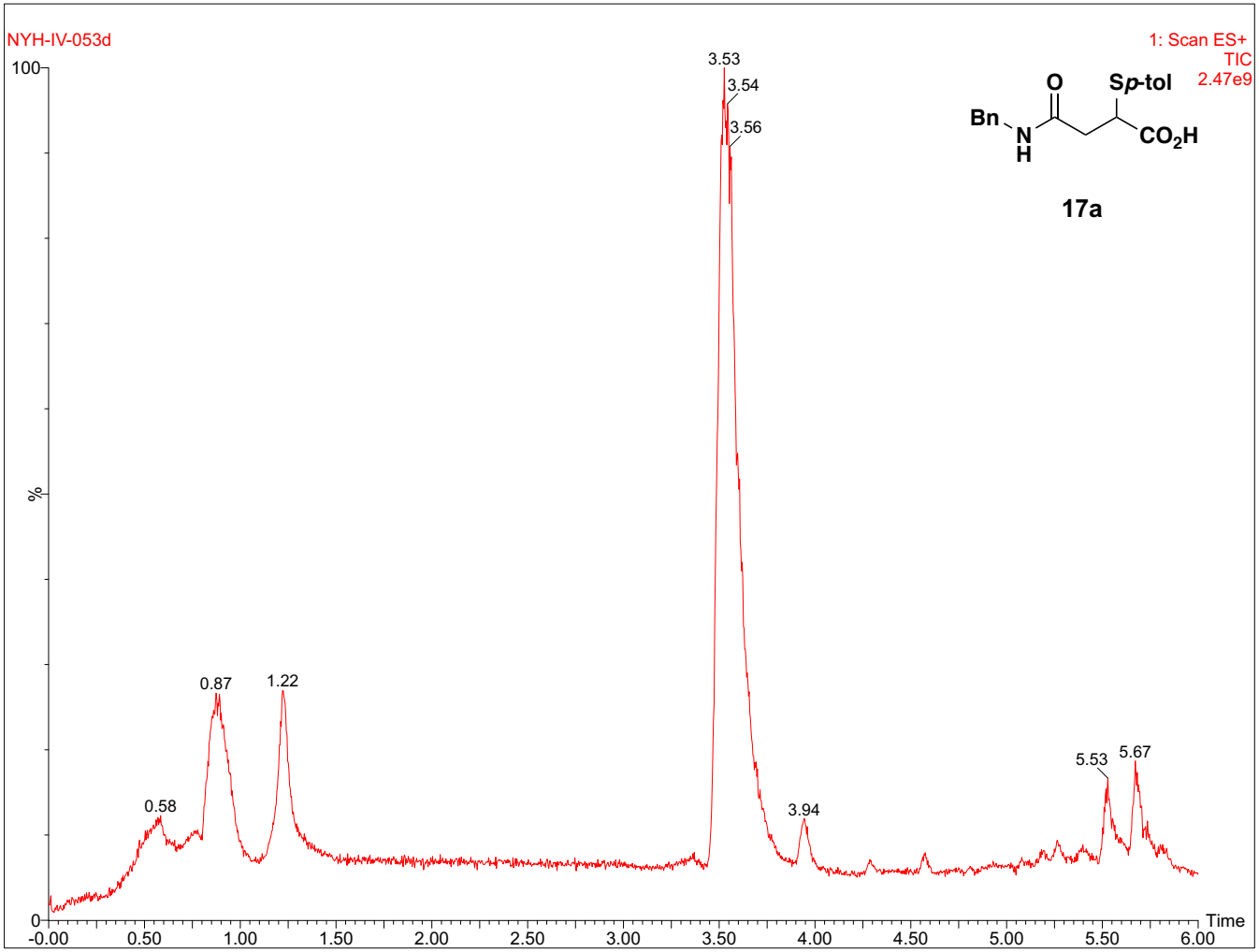
NYH-IV-053d
1: Scan ES+
TIC
2.47e9
100
%
0
3.53
3.54
3.56
0.87
1.22
0.58
3.94
5.53
5.67
Time
-0.00
0.50
1.00
1.50
2.00
2.50
3.00
3.50
4.00
4.50
5.00
5.50
6.00
Bn
N
H
O
Sp-tol
CO2H
17a

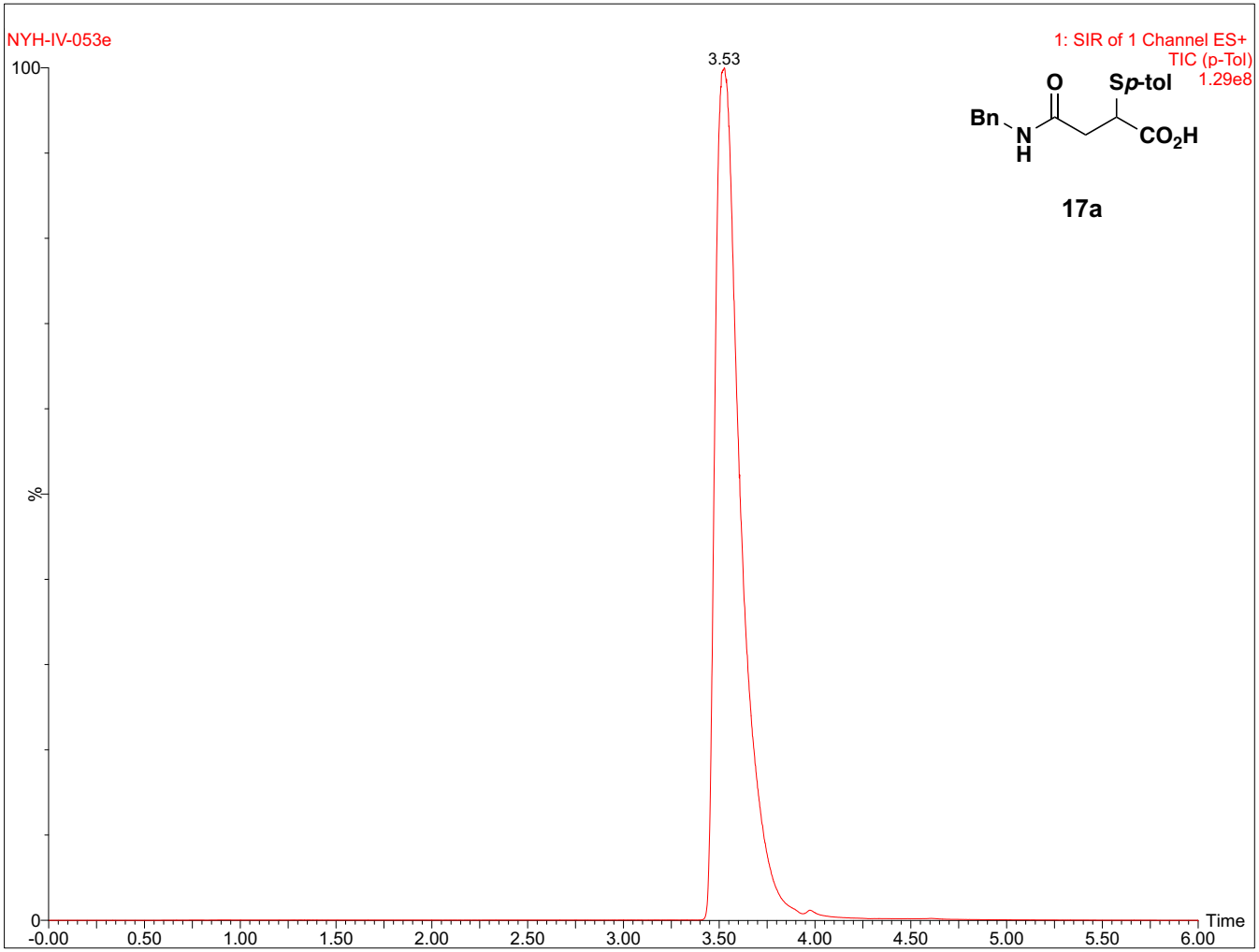
NYH-IV-053e
1: SIR of 1 Channel ES+
TIC (p-Tol)
1.29e8
3.53
100
%
0
Time
-0.00
0.50
1.00
1.50
2.00
2.50
3.00
3.50
4.00
4.50
5.00
5.50
6.00
Bn
N
H
O
Sp-tol
CO2H
17a

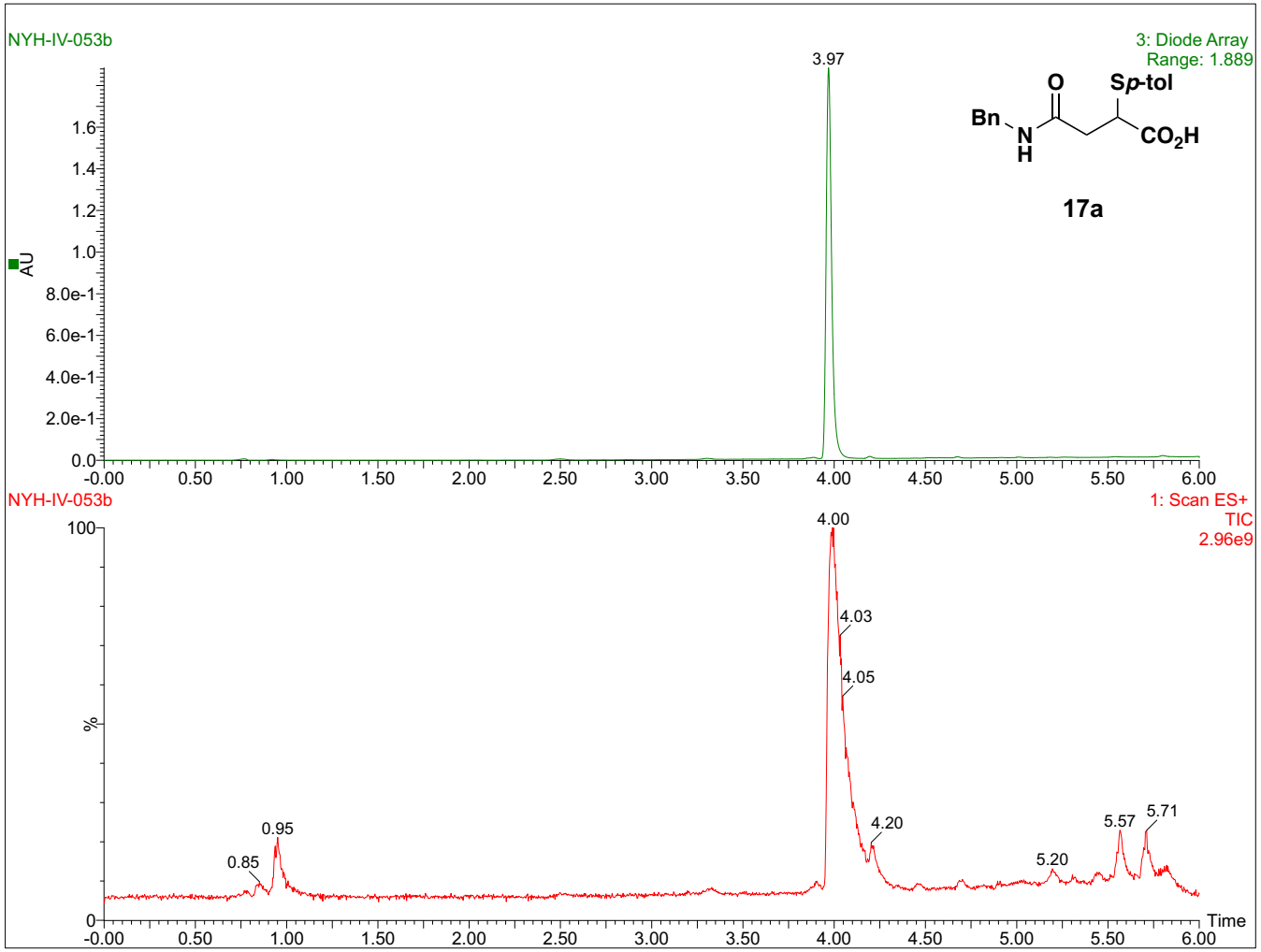

Note: there was a discrepancy in the retention time of 17a in one of the LCMS runs wherein the retention time deviated from 3.53 to 3.97.

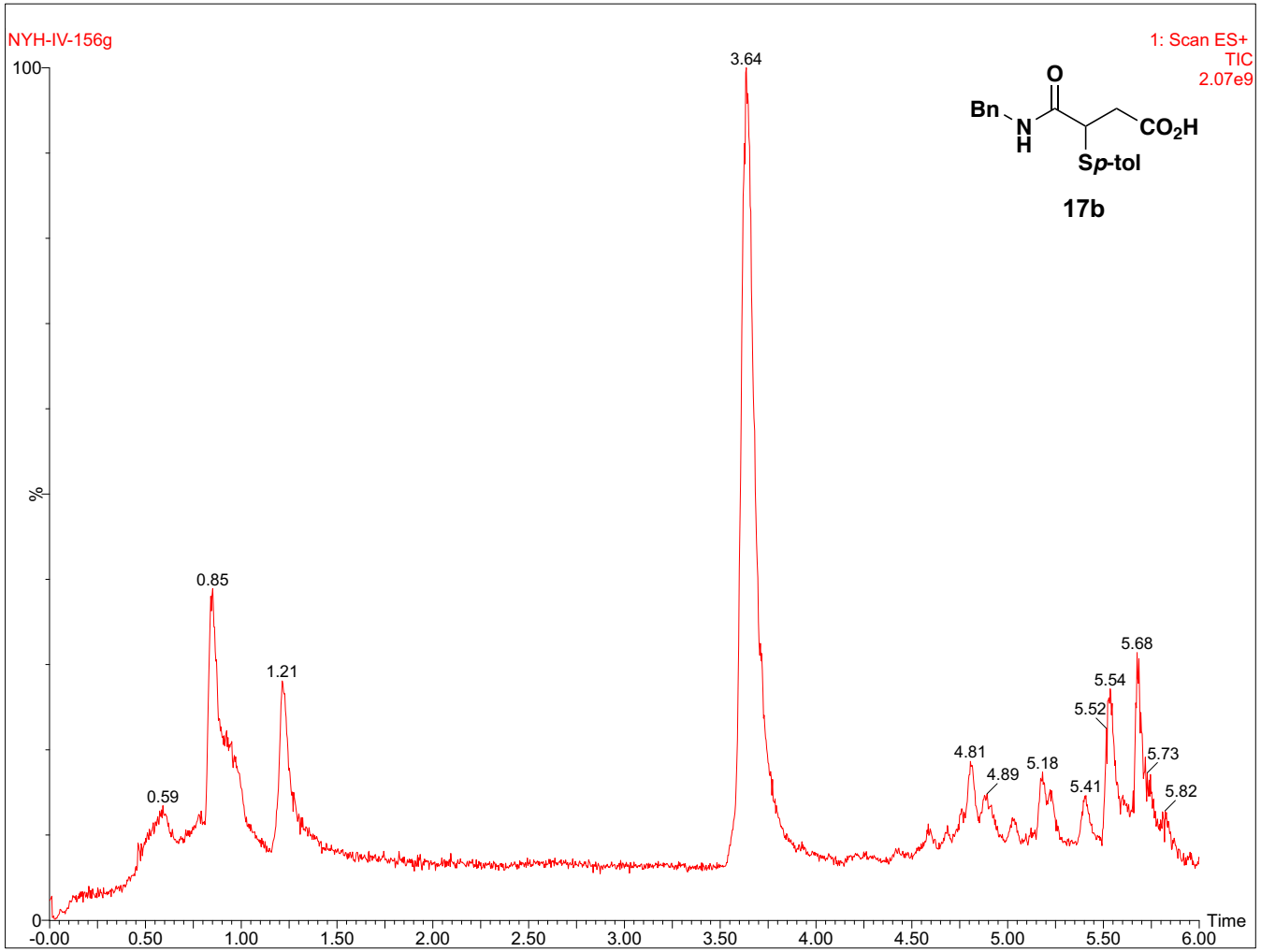
NYH-IV-156g
1: Scan ES+
TIC
2.07e9
100
%
0
3.64
0.85
1.21
0.59
4.81
4.89
5.18
5.41
5.52
5.54
5.68
5.73
5.82
Time
-0.00
0.50
1.00
1.50
2.00
2.50
3.00
3.50
4.00
4.50
5.00
5.50
6.00
Bn
N
H
O
CO2H
Sp-tol
17b

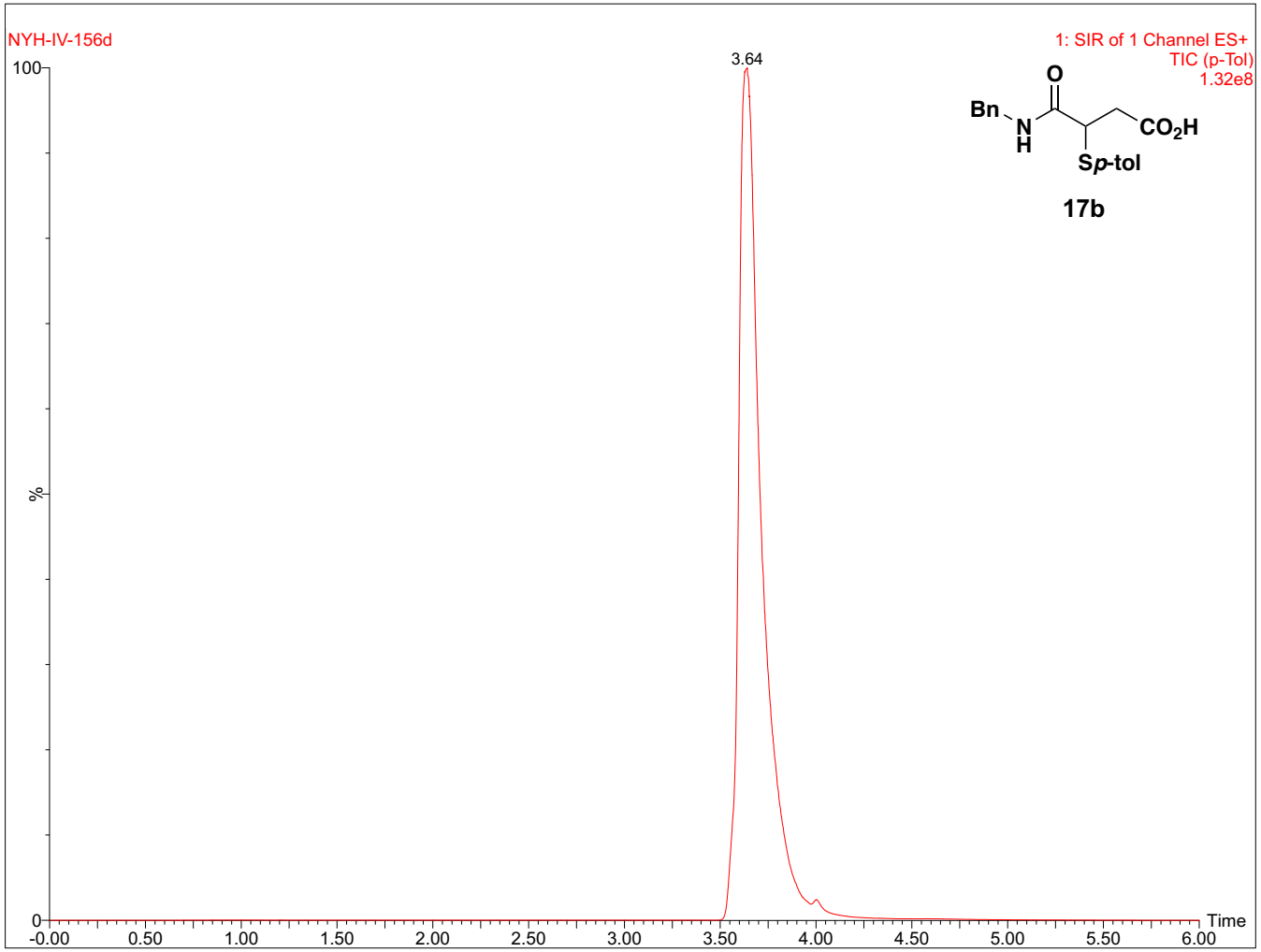
NYH-IV-156d
1: SIR of 1 Channel ES+
TIC (p-Tol)
1.32e8
3.64
100
%
0
Time
-0.00
0.50
1.00
1.50
2.00
2.50
3.00
3.50
4.00
4.50
5.00
5.50
6.00
Bn
N
H
O
CO2H
Sp-tol
17b

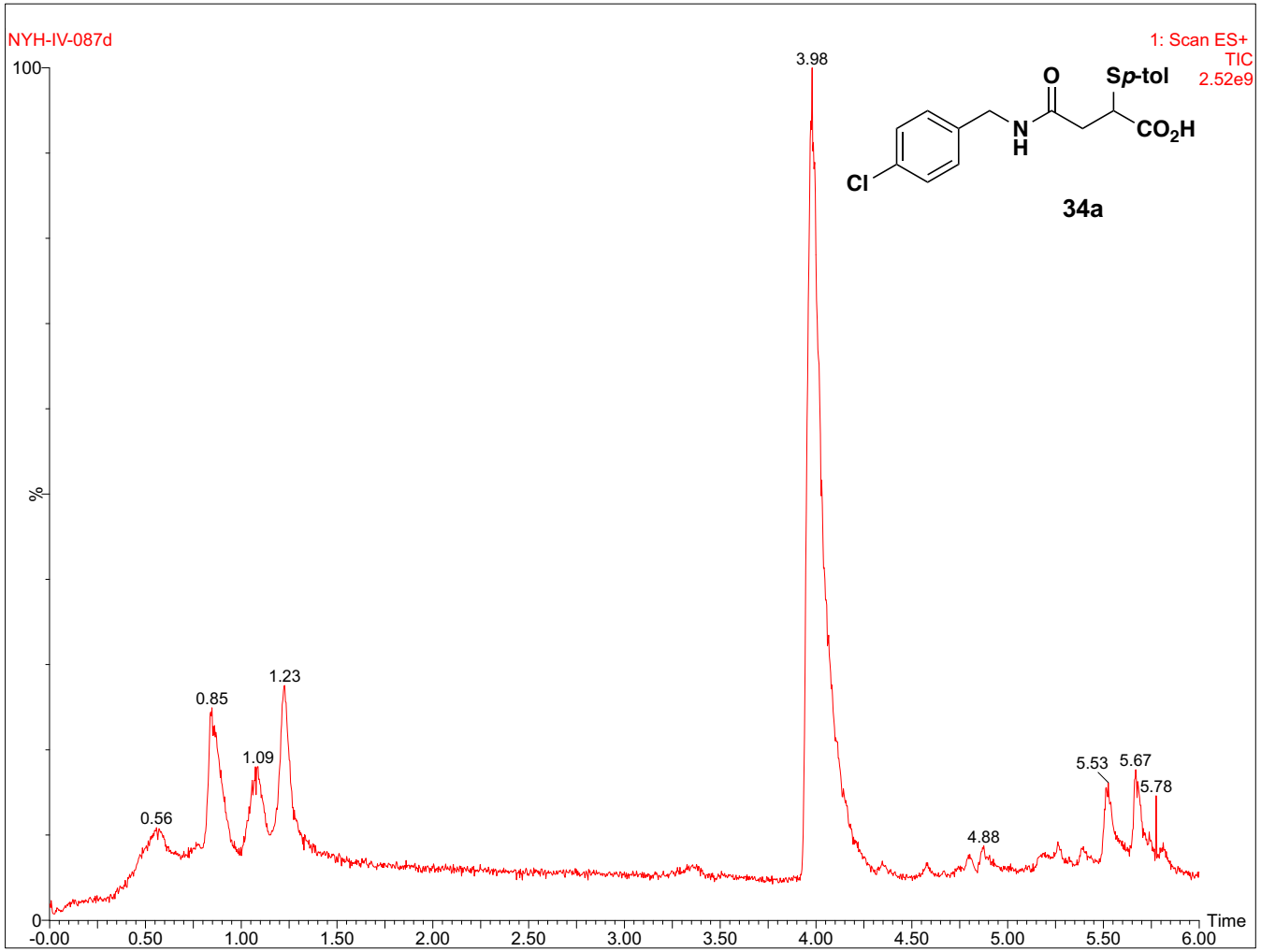
NYH-IV-087d
1: Scan ES+
TIC
2.52e9
100
%
0
3.98
1.23
0.85
1.09
0.56
4.88
5.53
5.67
5.78
Time
-0.00
0.50
1.00
1.50
2.00
2.50
3.00
3.50
4.00
4.50
5.00
5.50
6.00
O
Sp-tol
N
H
CO2H
Cl
34a

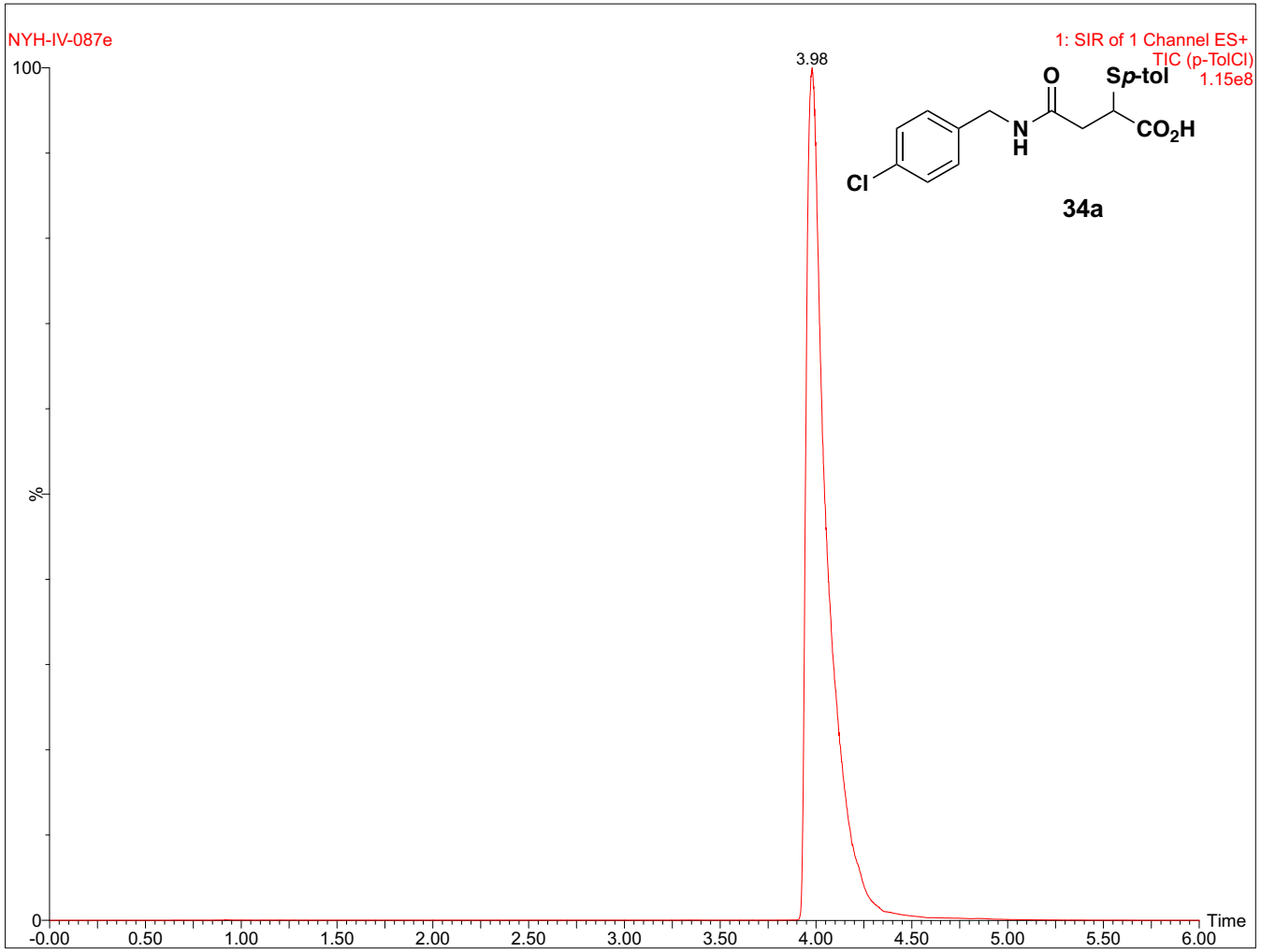
NYH-IV-087e
1: SIR of 1 Channel ES+
TIC (p-TolCl)
1.15e8
3.98
100
%
0
-0.00
0.50
1.00
1.50
2.00
2.50
3.00
3.50
4.00
4.50
5.00
5.50
6.00
Time
O
Sp-tol
N
H
CO2H
Cl
34a

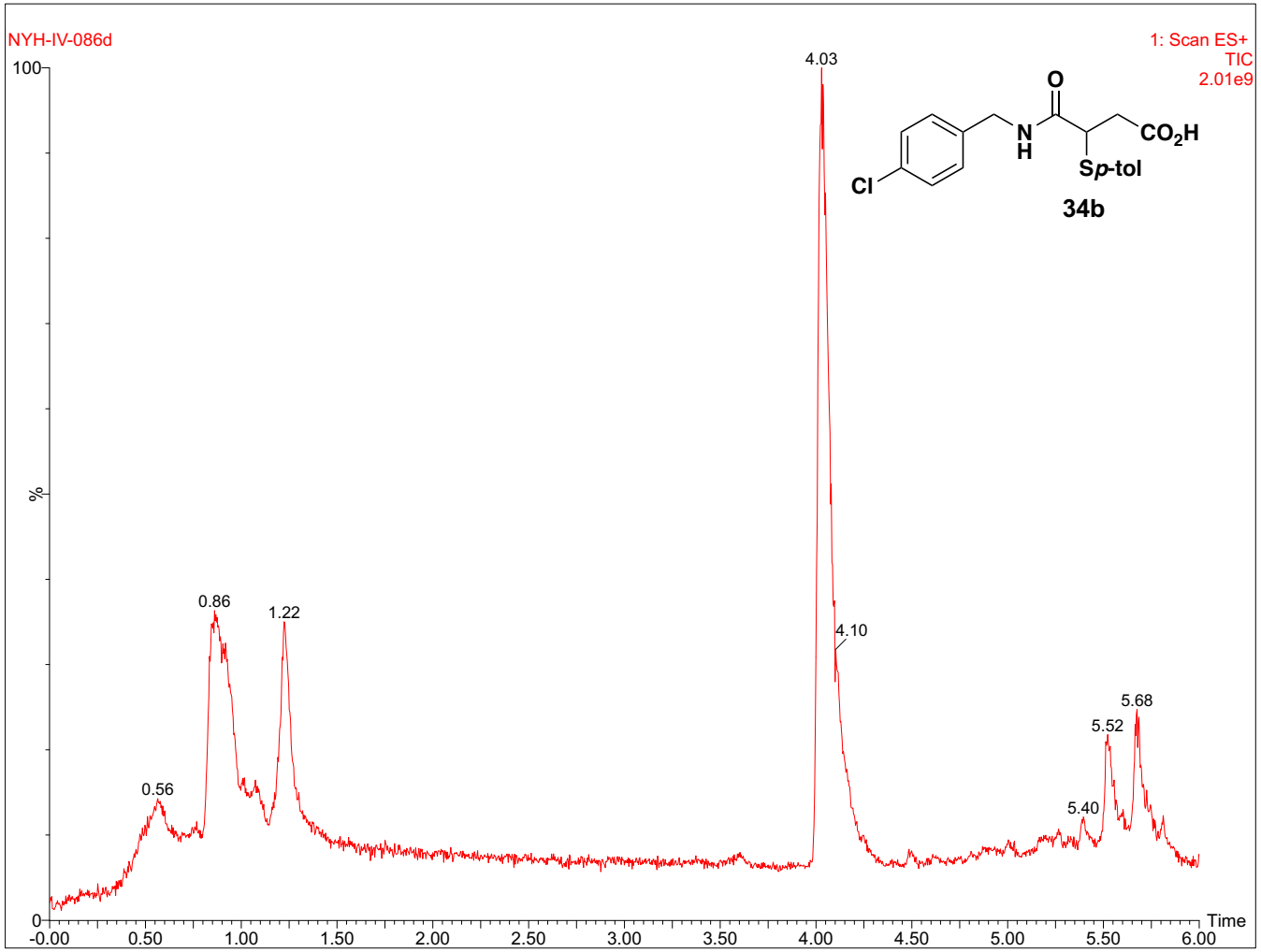
NYH-IV-086d
1: Scan ES+
TIC
2.01e9
100
%
0
4.03
0.86
1.22
0.56
4.10
5.68
5.52
5.40
Time
-0.00
0.50
1.00
1.50
2.00
2.50
3.00
3.50
4.00
4.50
5.00
5.50
6.00
O
N
H
CO2H
Sp-tol
Cl
34b

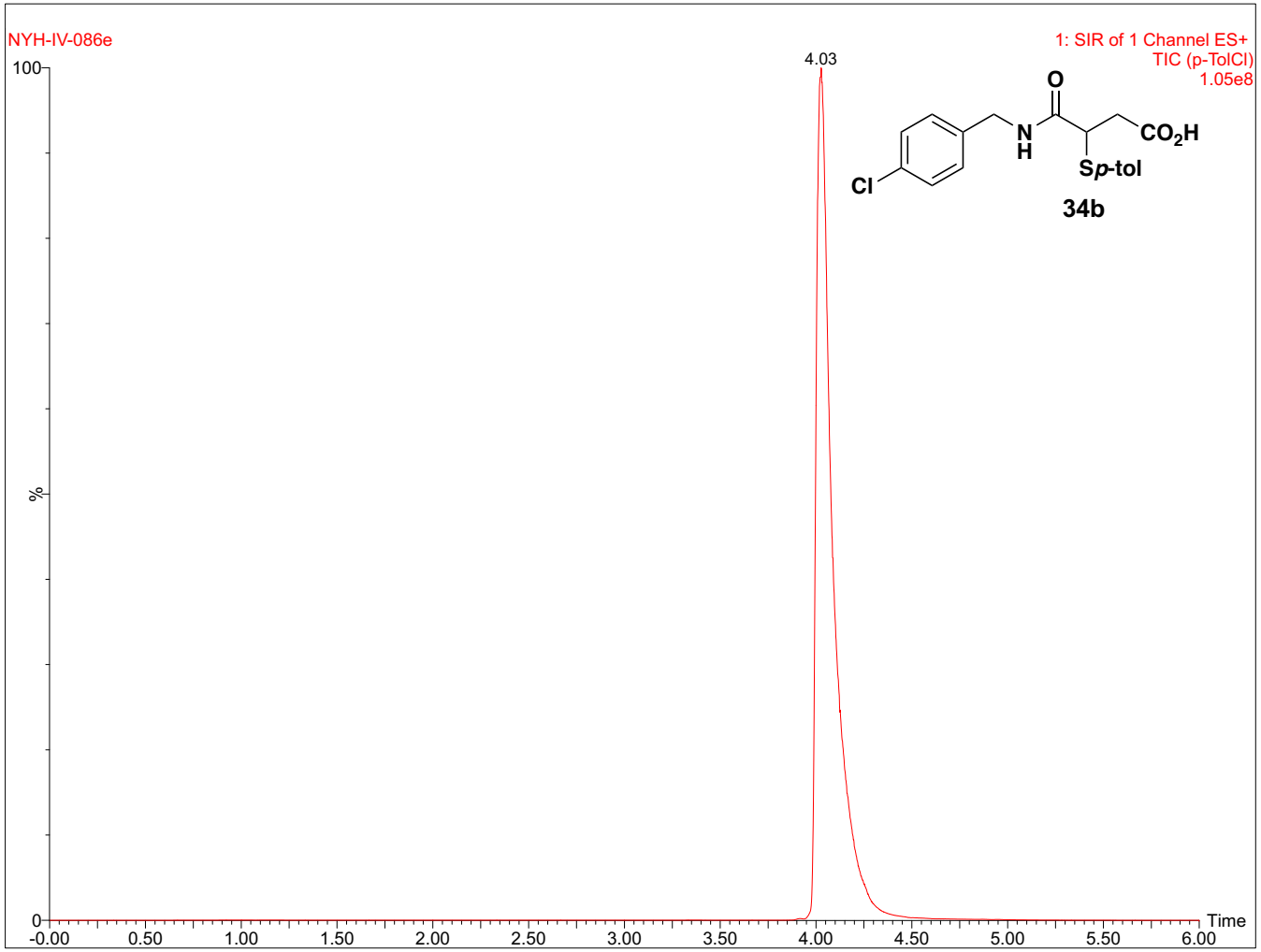
NYH-IV-086e
1: SIR of 1 Channel ES+
TIC (p-TolCl)
1.05e8
4.03
100
%
0
Time
-0.00
0.50
1.00
1.50
2.00
2.50
3.00
3.50
4.00
4.50
5.00
5.50
6.00
O
N
H
CO2H
Sp-tol
Cl
34b

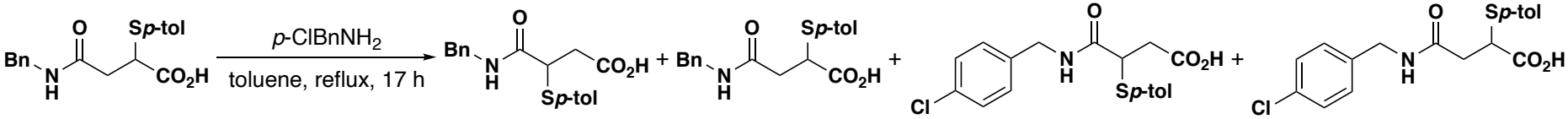
Bn
N
H
O
Sp-tol
CO2H
p-ClBnNH2
toluene, reflux, 17 h
+
Cl

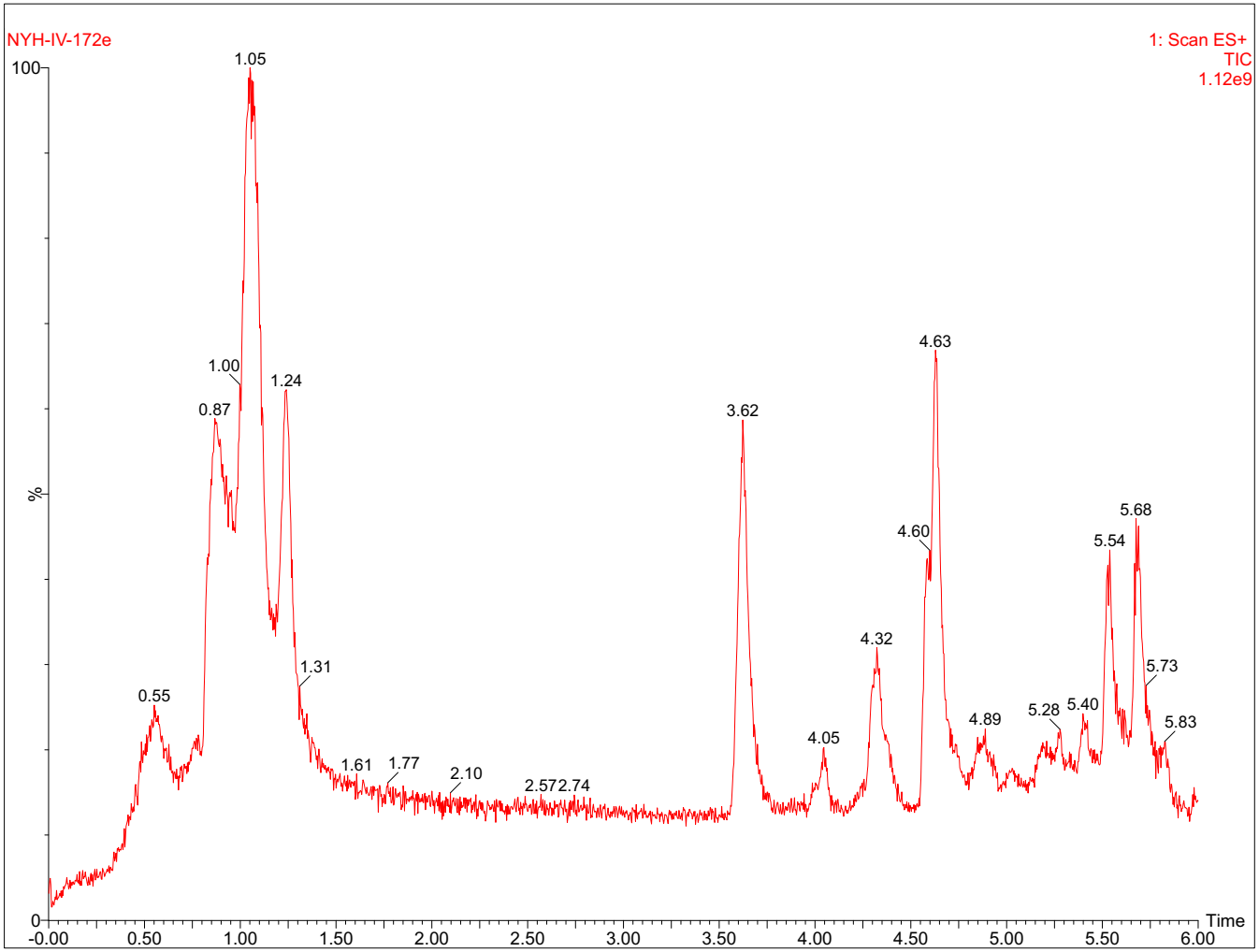
NYH-IV-172e
1: Scan ES+
TIC
1.12e9
100
%
0
1.05
1.00
0.87
1.24
1.31
0.55
1.61
1.77
2.10
2.57
2.74
3.62
4.05
4.32
4.63
4.60
4.89
5.28
5.40
5.54
5.68
5.73
5.83
-0.00
0.50
1.00
1.50
2.00
2.50
3.00
3.50
4.00
4.50
5.00
5.50
6.00
Time

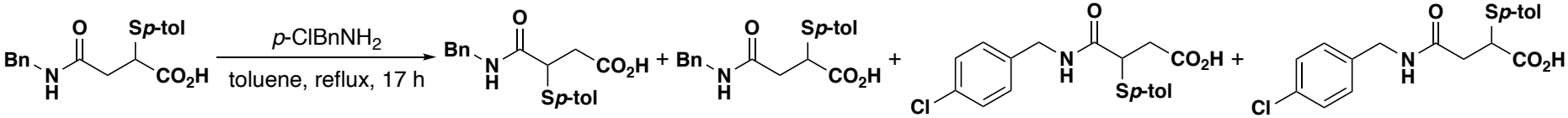

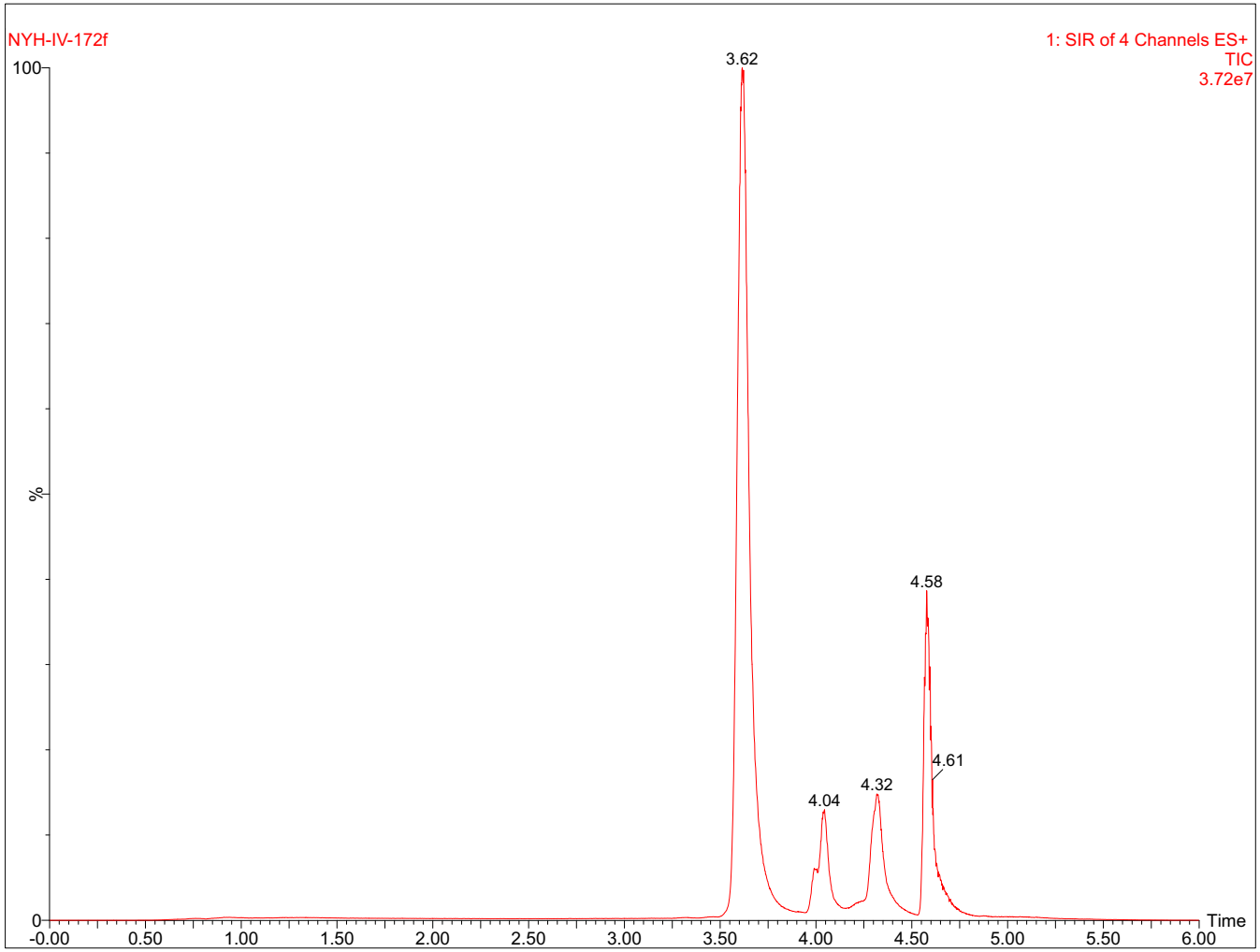

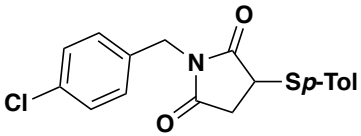

Peak at 4.32 corresponds to mass of *p*-ClBn imide

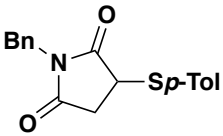

Peak at 4.58 corresponds to mass of Bn imide

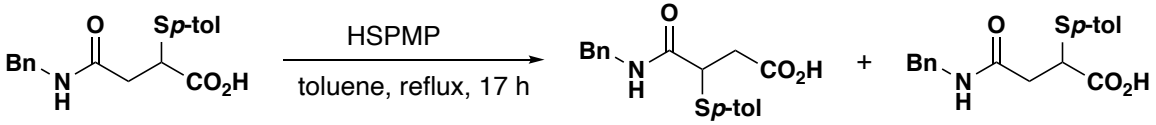
Bn
N
H
O
Sp-tol
CO2H
HSPMP
toluene, reflux, 17 h
+

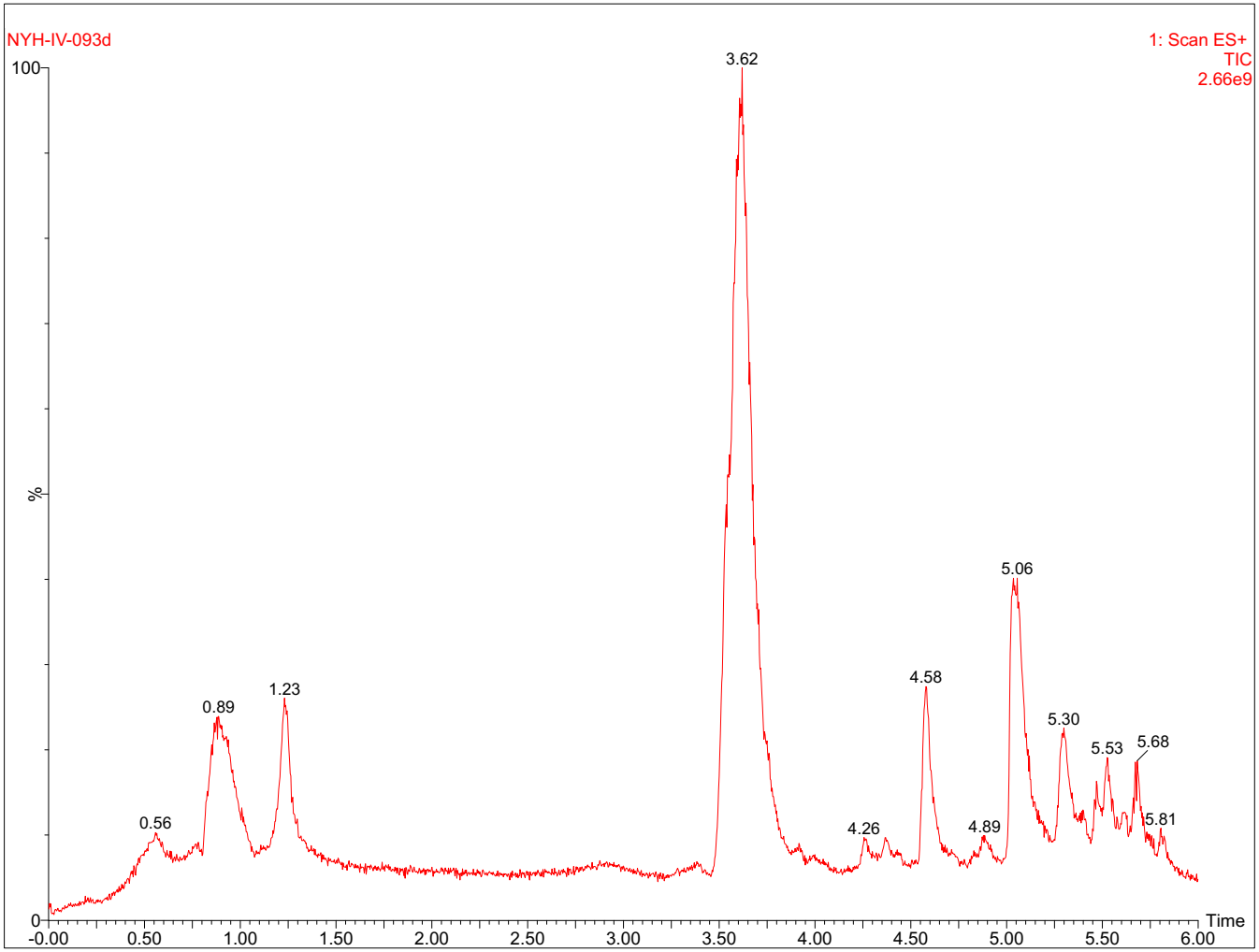
NYH-IV-093d
1: Scan ES+
TIC
2.66e9
100
%
0
3.62
5.06
4.58
1.23
0.89
5.30
5.53
5.68
0.56
4.26
4.89
5.81
Time
-0.00
0.50
1.00
1.50
2.00
2.50
3.00
3.50
4.00
4.50
5.00
5.50
6.00

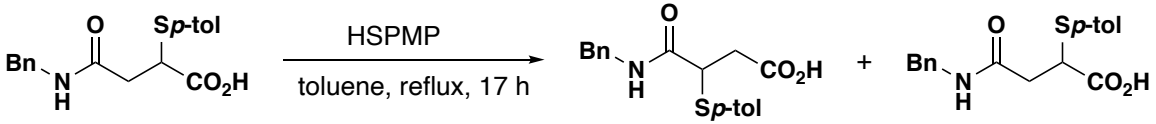
Bn
N
H
O
Sp-tol
CO2H
HSPMP
toluene, reflux, 17 h
+

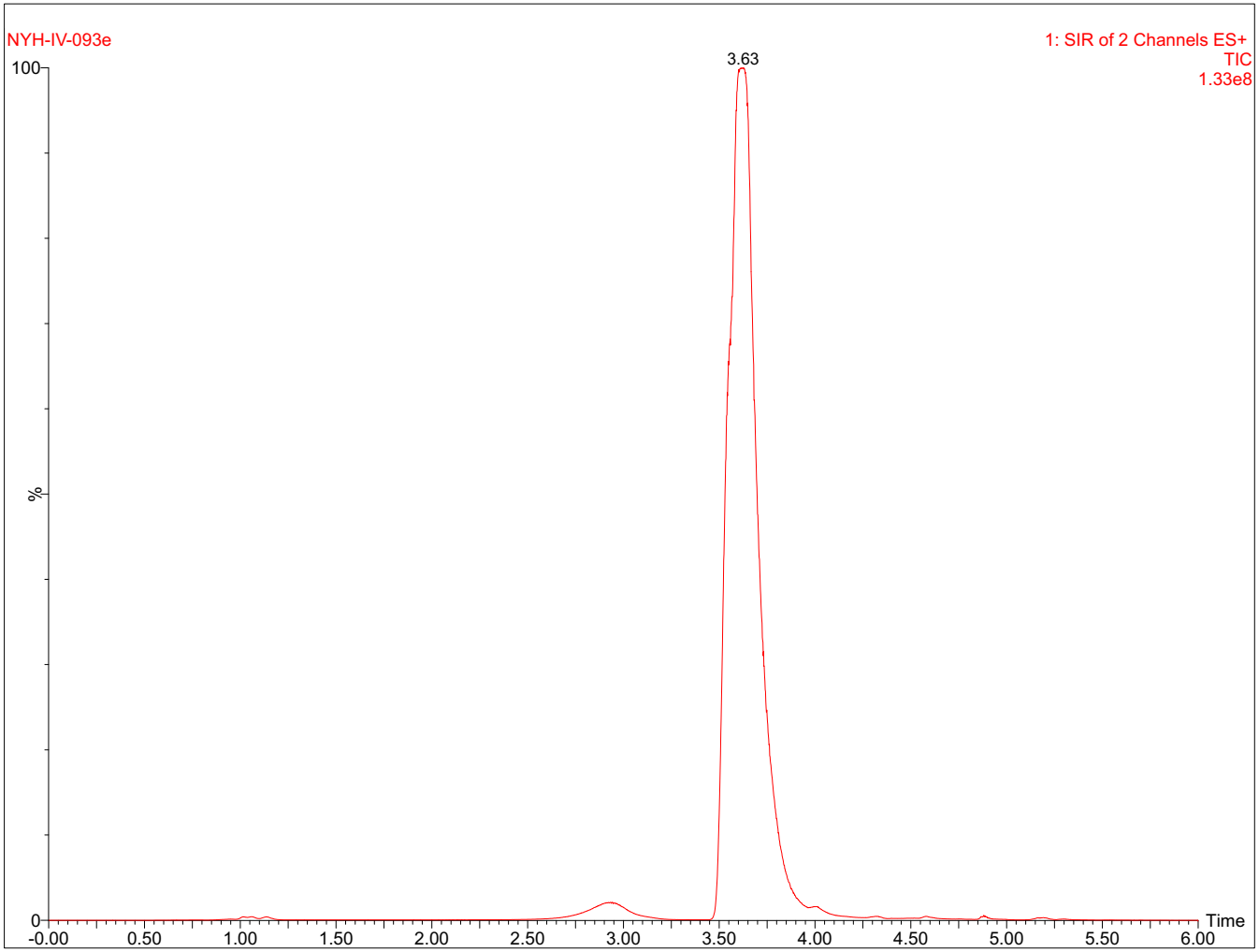
NYH-IV-093e
1: SIR of 2 Channels ES+
TIC
1.33e8
3.63
100
%
0
Time
-0.00
0.50
1.00
1.50
2.00
2.50
3.00
3.50
4.00
4.50
5.00
5.50
6.00

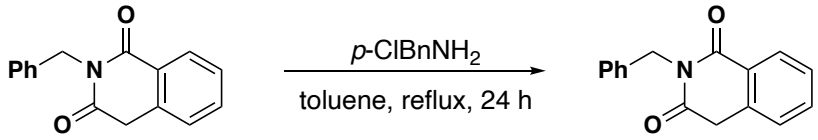
Ph
N
O
O
p-ClBnNH2
toluene, reflux, 24 h
Ph
N
O
O

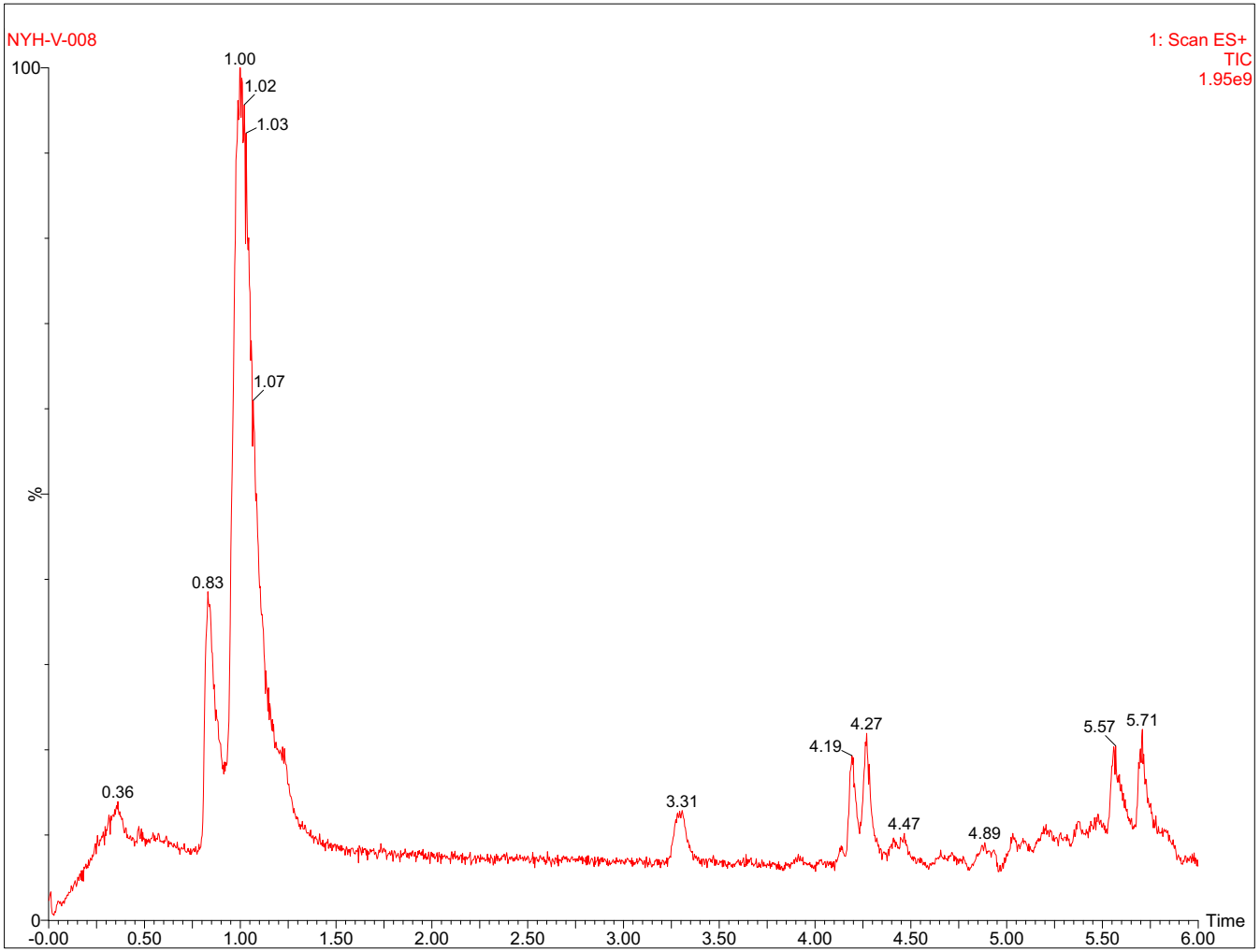
NYH-V-008
1: Scan ES+
TIC
1.95e9
100
%
0
1.00
1.02
1.03
1.07
0.83
0.36
3.31
4.19
4.27
4.47
4.89
5.57
5.71
-0.00
0.50
1.00
1.50
2.00
2.50
3.00
3.50
4.00
4.50
5.00
5.50
6.00
Time

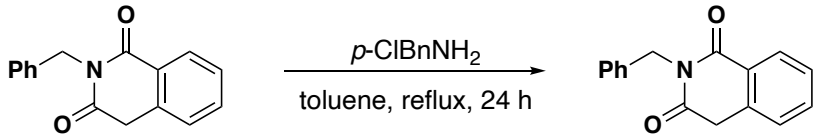
Ph
N
O
O
p-ClBnNH2
toluene, reflux, 24 h
Ph
N
O
O

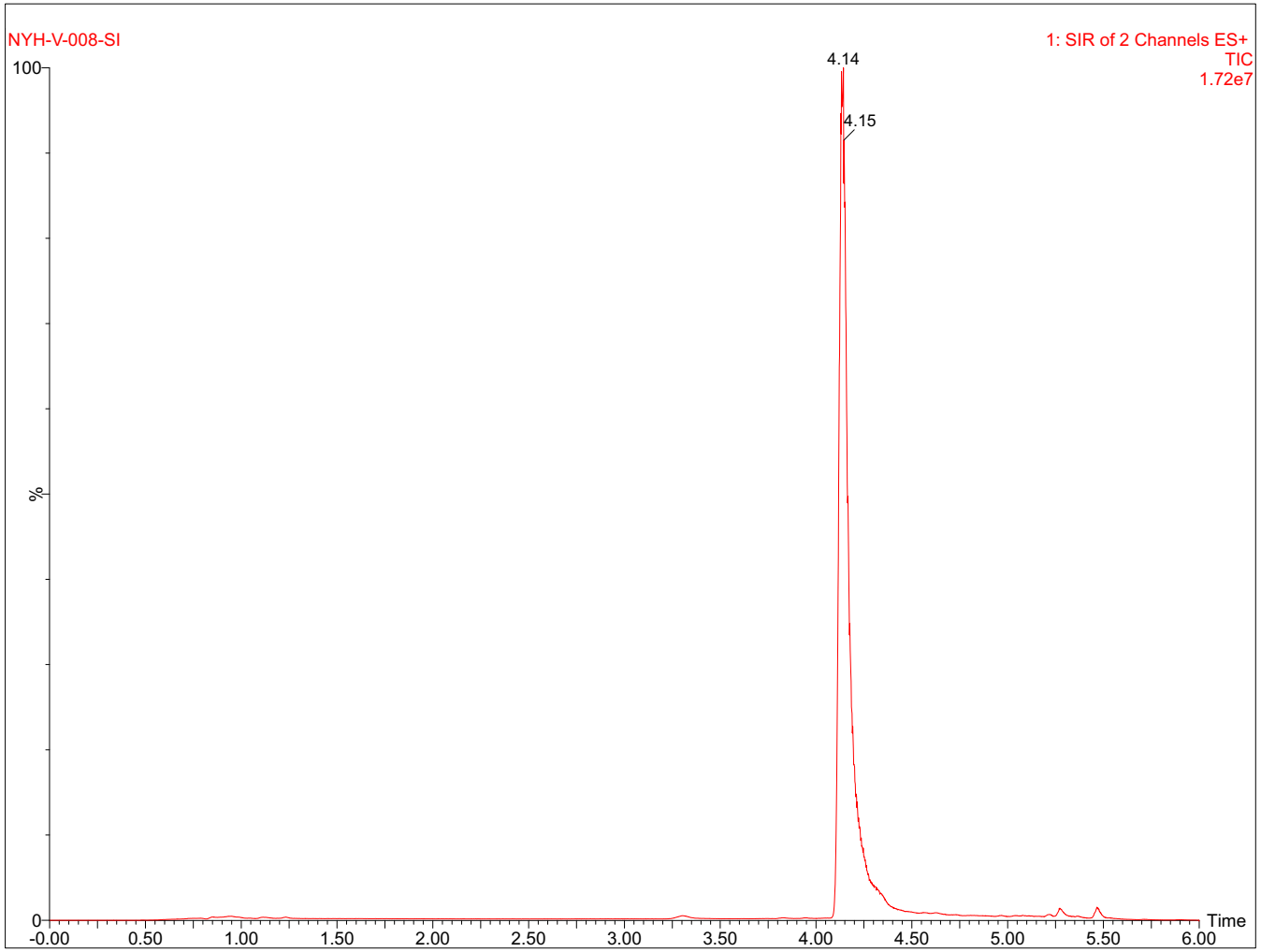
NYH-V-008-SI
1: SIR of 2 Channels ES+
TIC
1.72e7
4.14
4.15
100
%
0
-0.00
0.50
1.00
1.50
2.00
2.50
3.00
3.50
4.00
4.50
5.00
5.50
6.00
Time

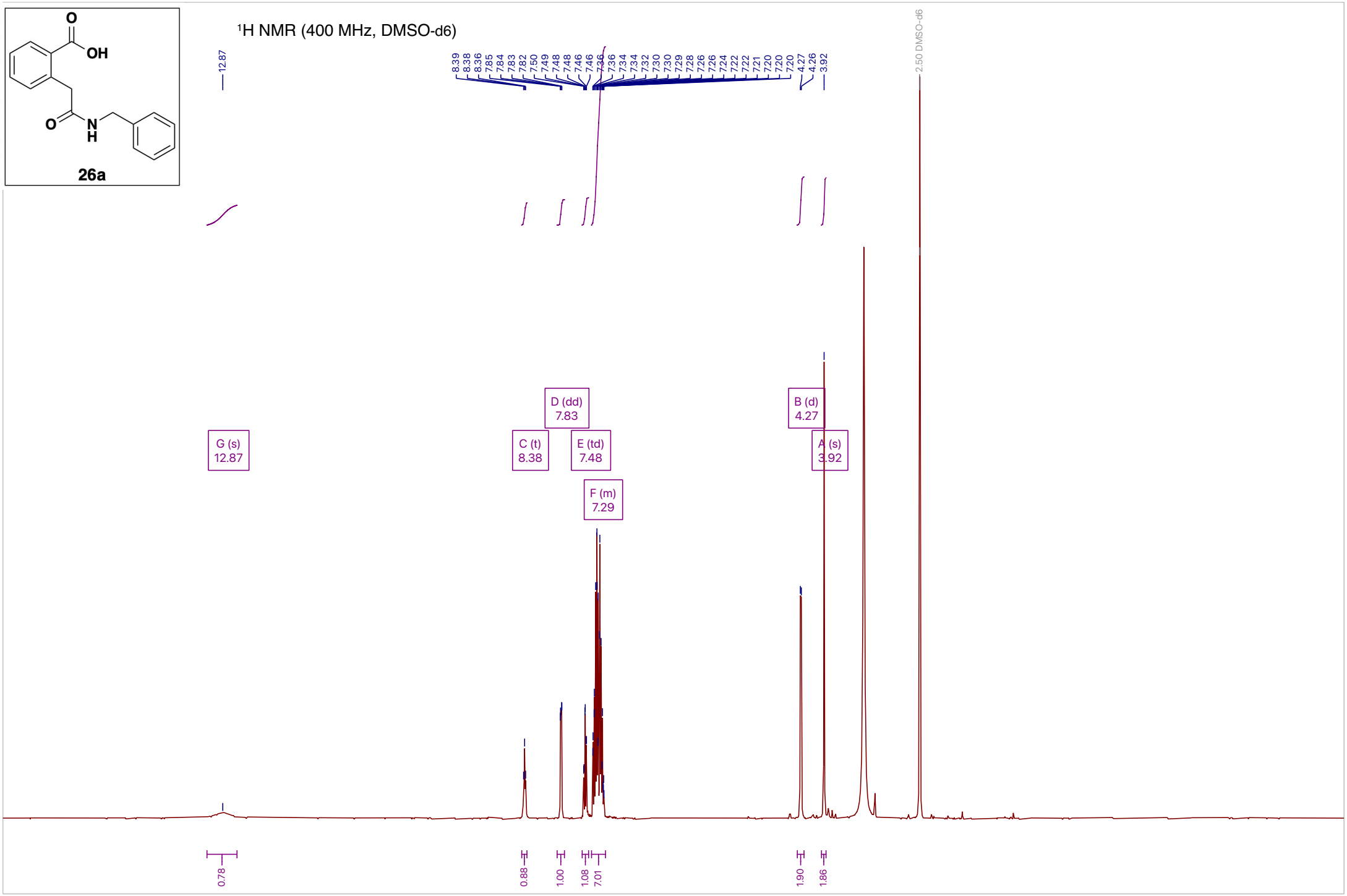
26a
1H NMR (400 MHz, DMSO-d6)
2.50 DMSO-d6
G (s) 12.87
C (t) 8.38
D (dd) 7.83
E (td) 7.48
F (m) 7.29
B (d) 4.27
A (s) 3.92
0.78
0.88
1.00
1.08
7.01
1.90
1.86
f1 (ppm)

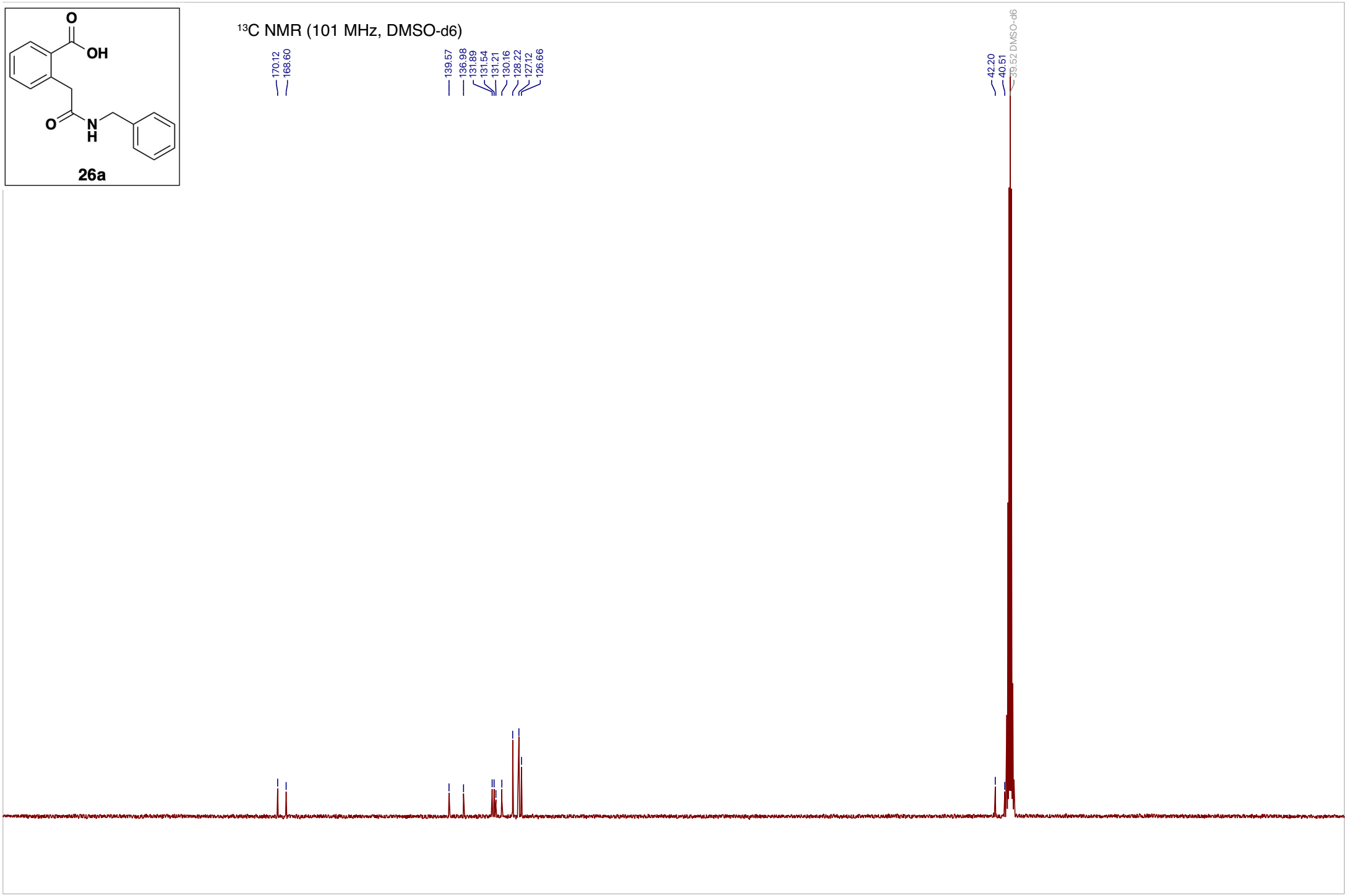
26a
13C NMR (101 MHz, DMSO-d6)
170.12
168.60
139.57
136.98
131.89
131.54
131.21
130.16
128.22
127.12
126.66
42.20
40.51
39.52 DMSO-d6
210 200 190 180 170 160 150 140 130 120 110 100 90 80 70 60 50 40 30 20 10 0 -10 -2
f1 (ppm)

^{1}H NMR (400 MHz, DMSO-d6)

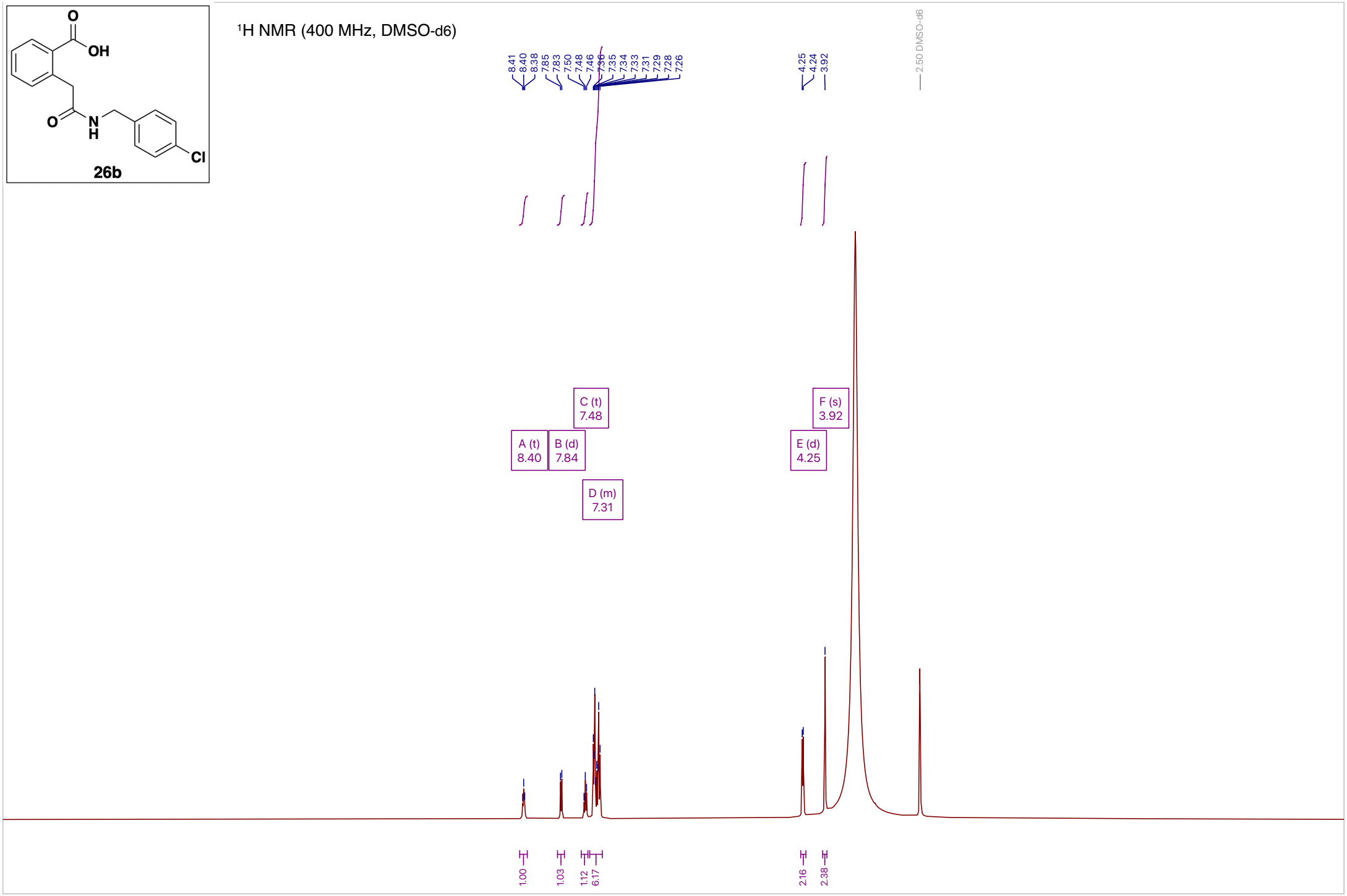

^{13}C NMR (101 MHz, DMSO-d6)

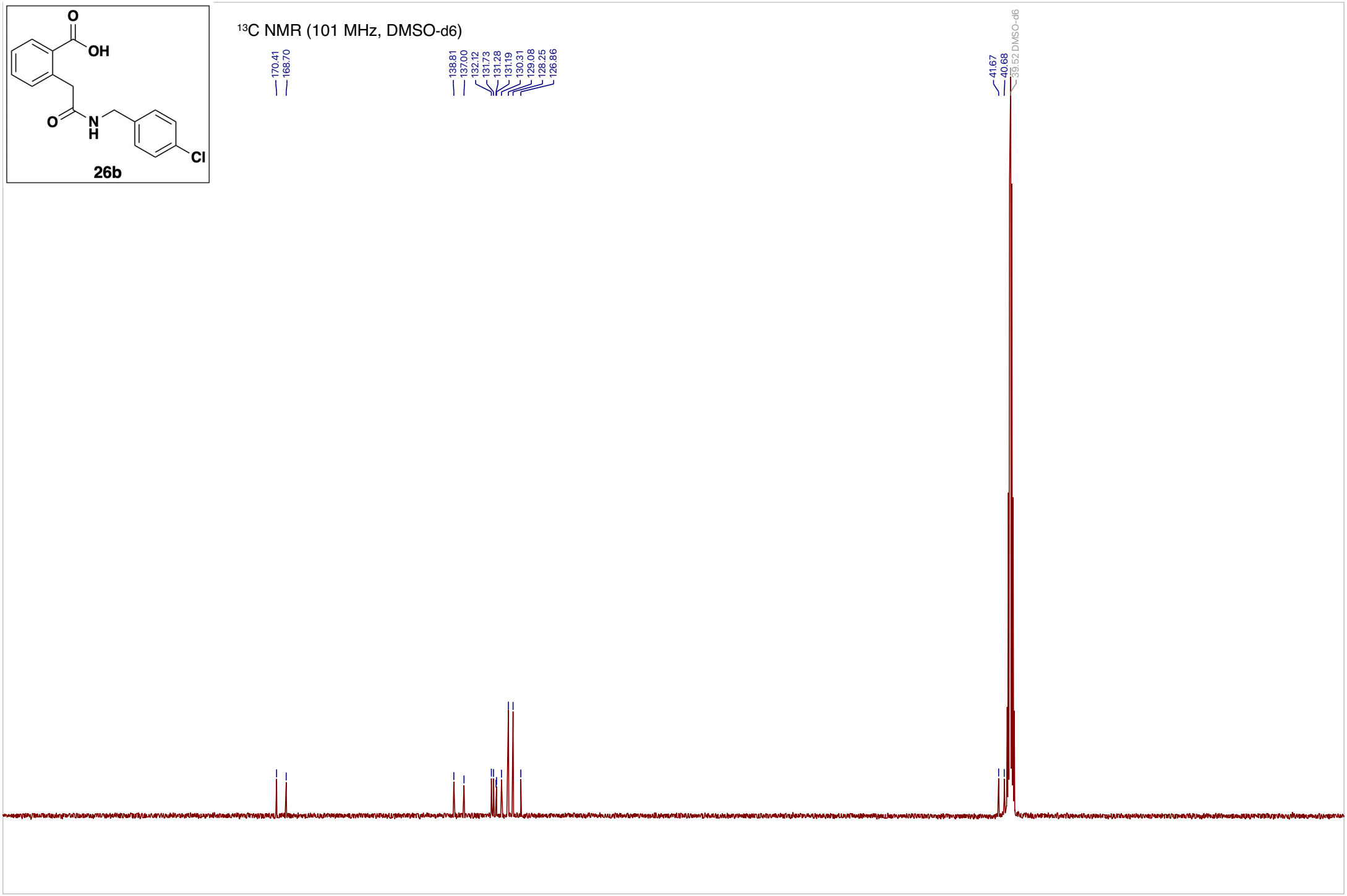

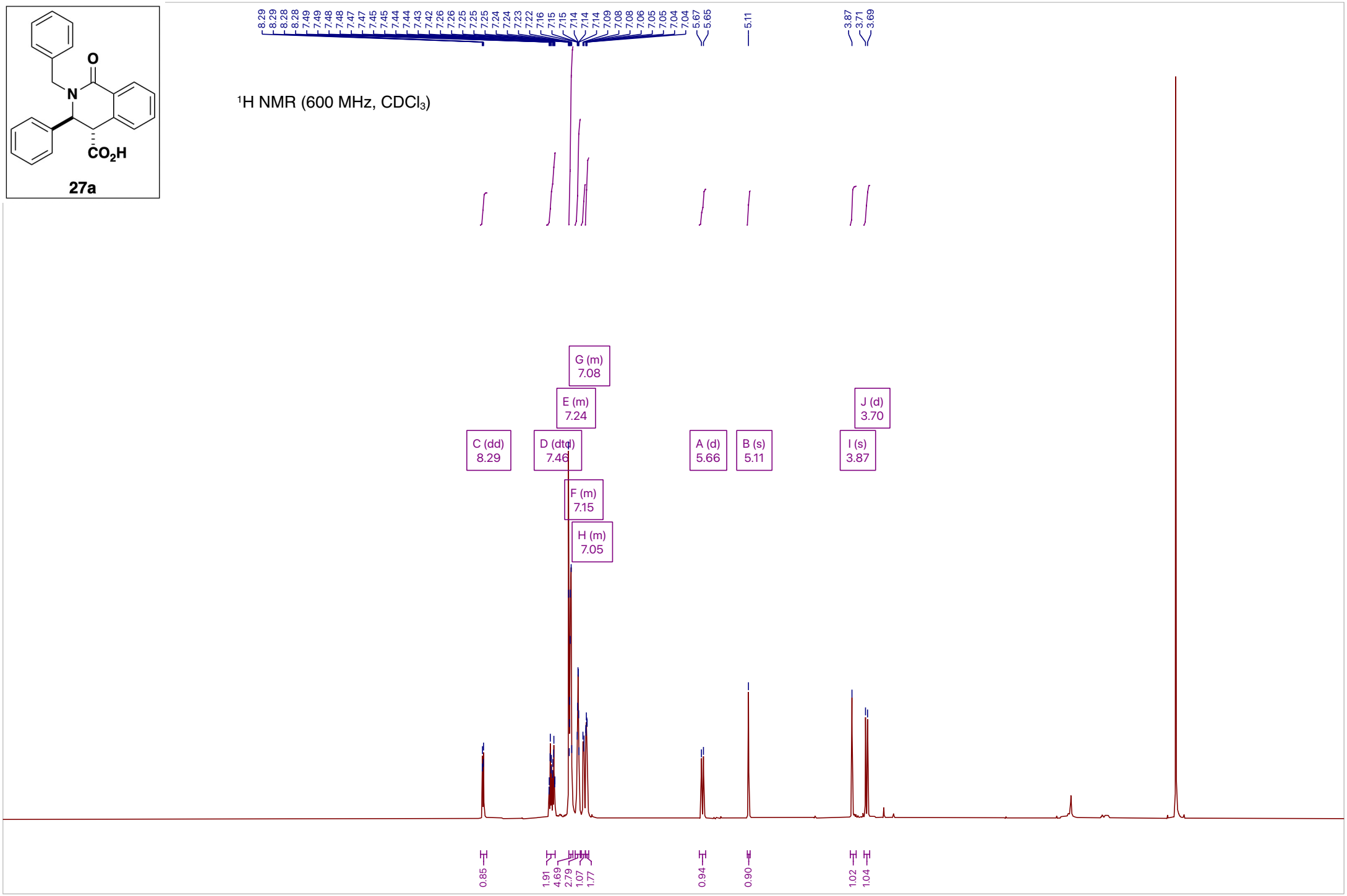
27a
^{1}H NMR (600 MHz, $CDCl_3$)
C (dd) 8.29
D (dtd) 7.46
E (m) 7.24
F (m) 7.15
G (m) 7.08
H (m) 7.05
A (d) 5.66
B (s) 5.11
I (s) 3.87
J (d) 3.70
f1 (ppm)

^{13}C NMR (101 MHz, $CDCl_3$)

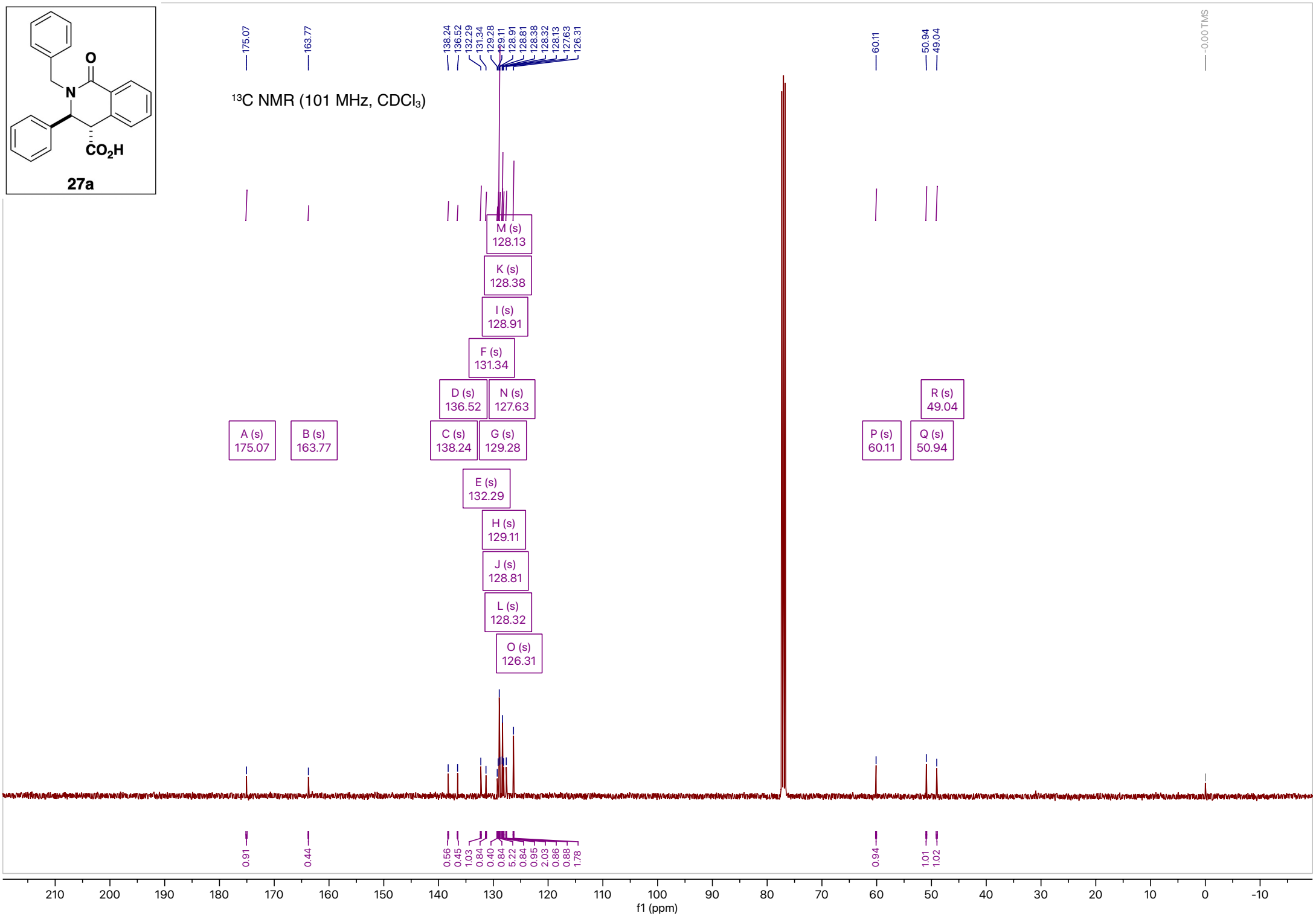

^{1}H NMR (400 MHz, $CDCl_3$)

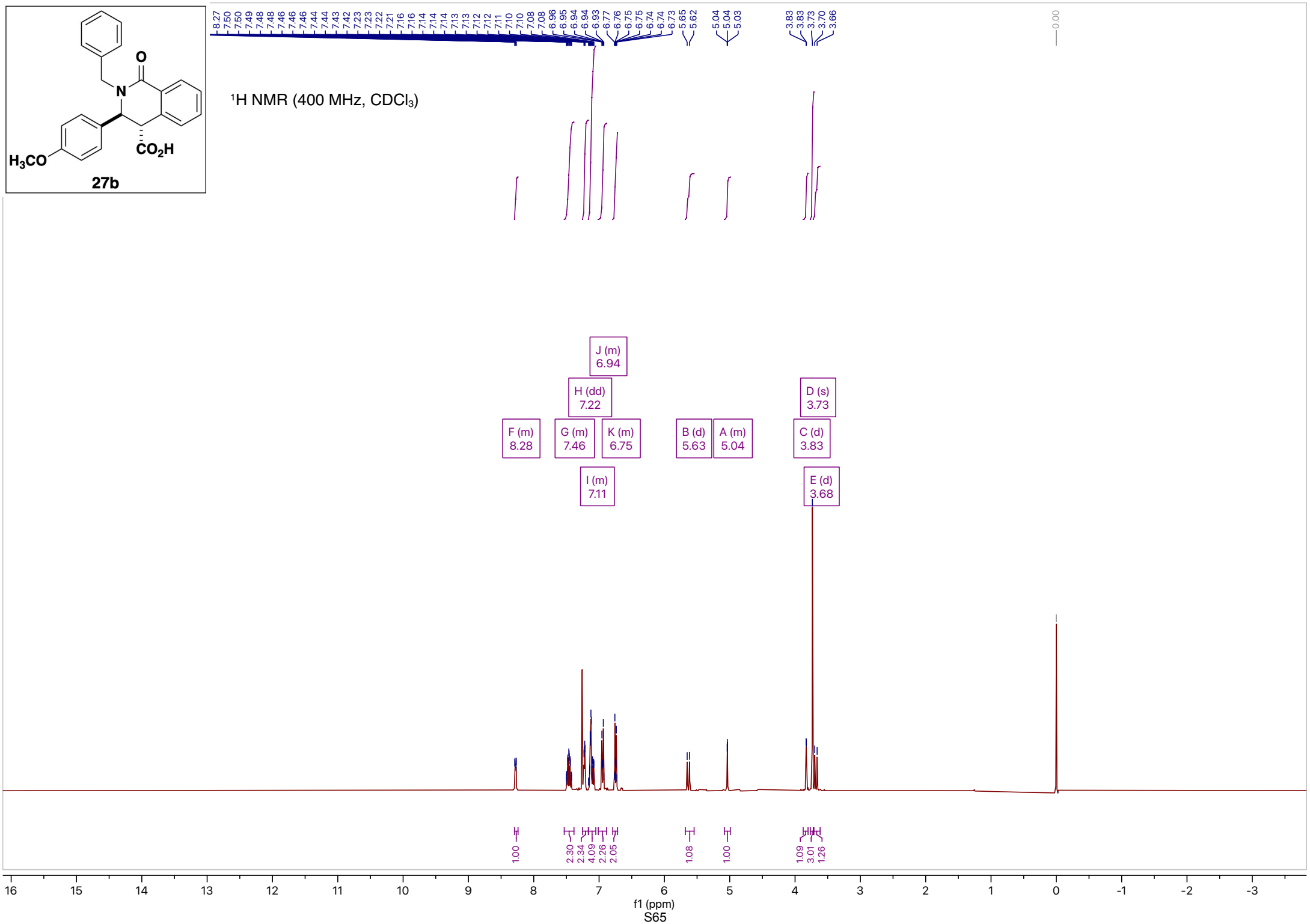

^{13}C NMR (101 MHz, $CDCl_3$)

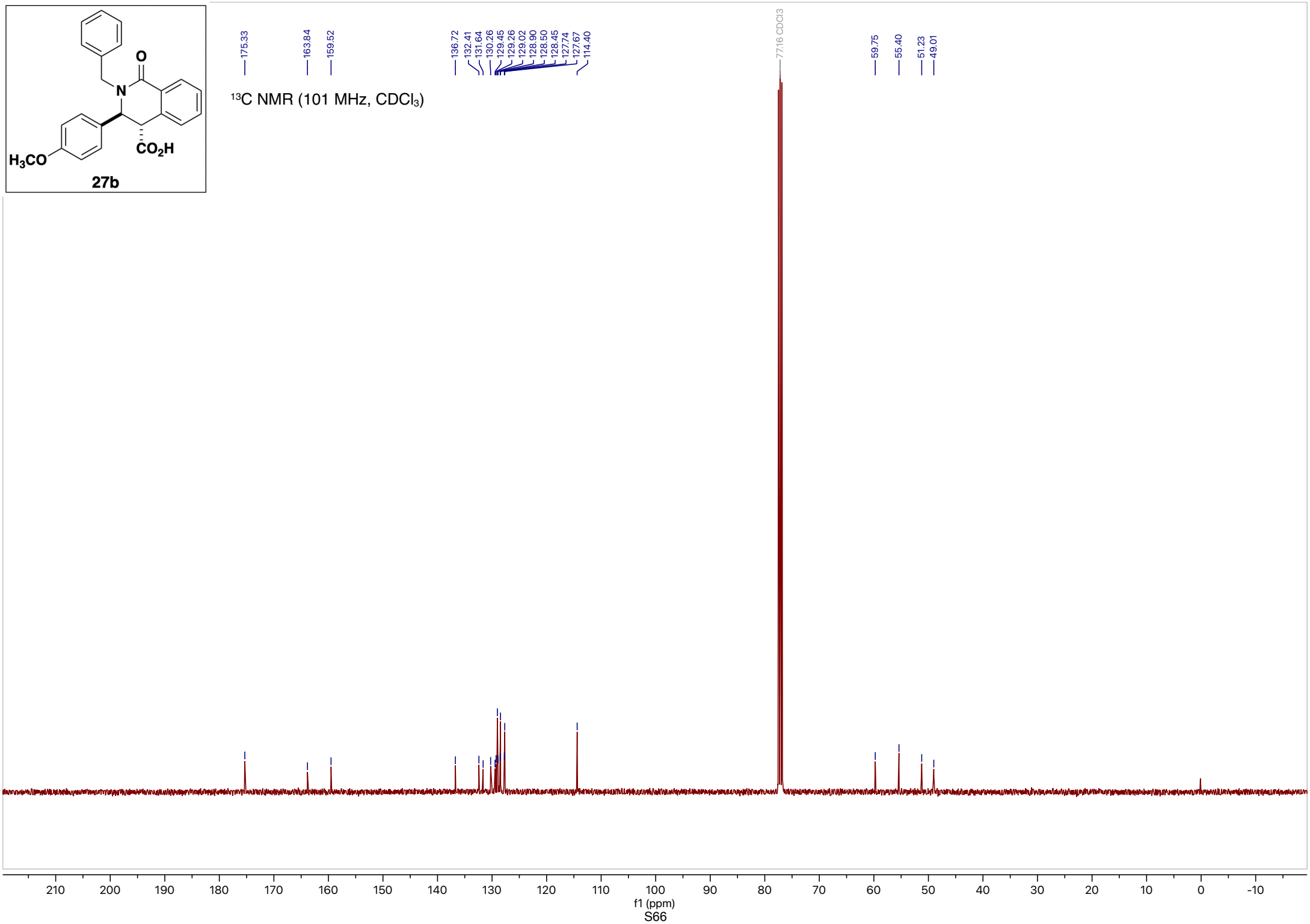

^{1}H NMR (400 MHz, $CDCl_3$)

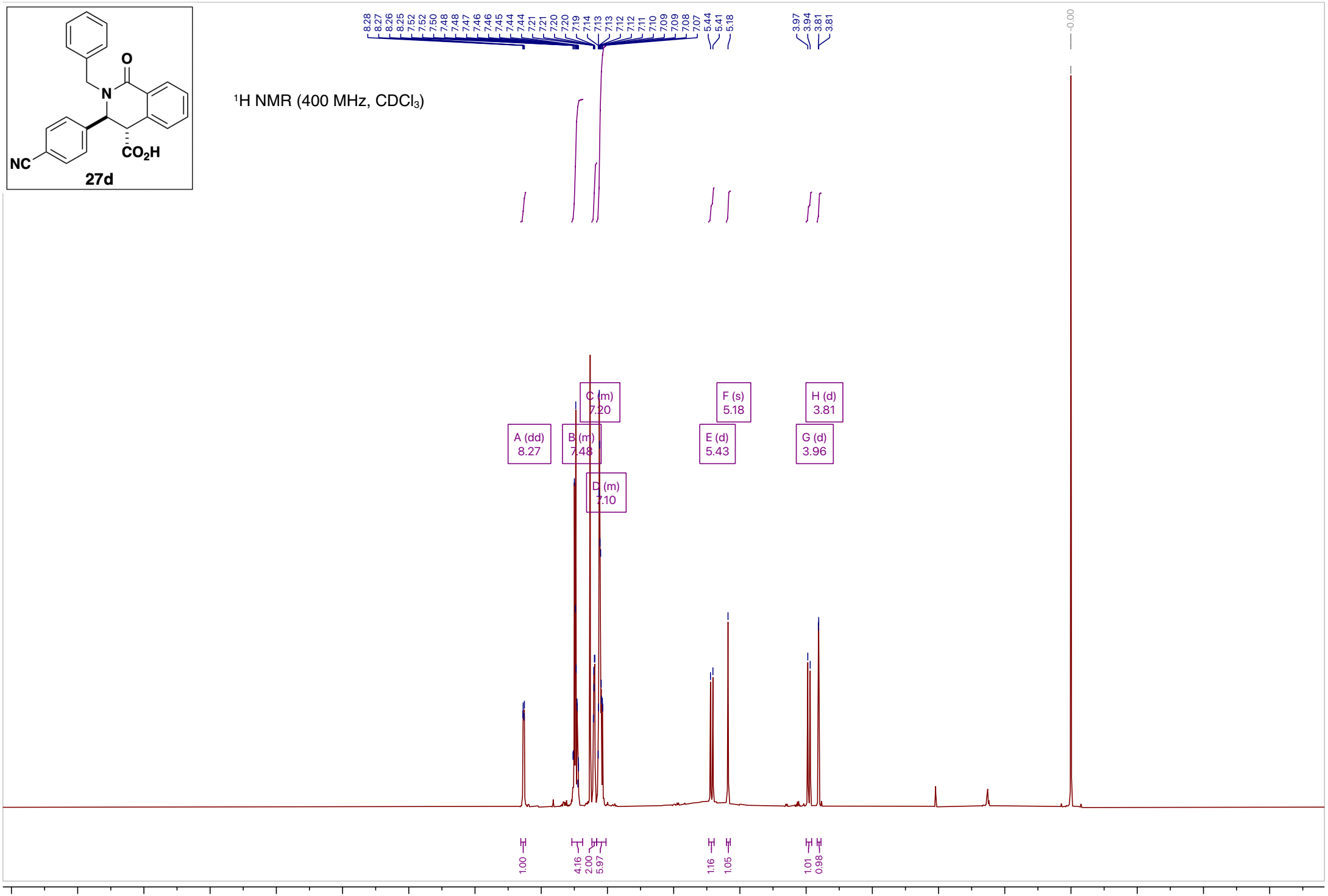

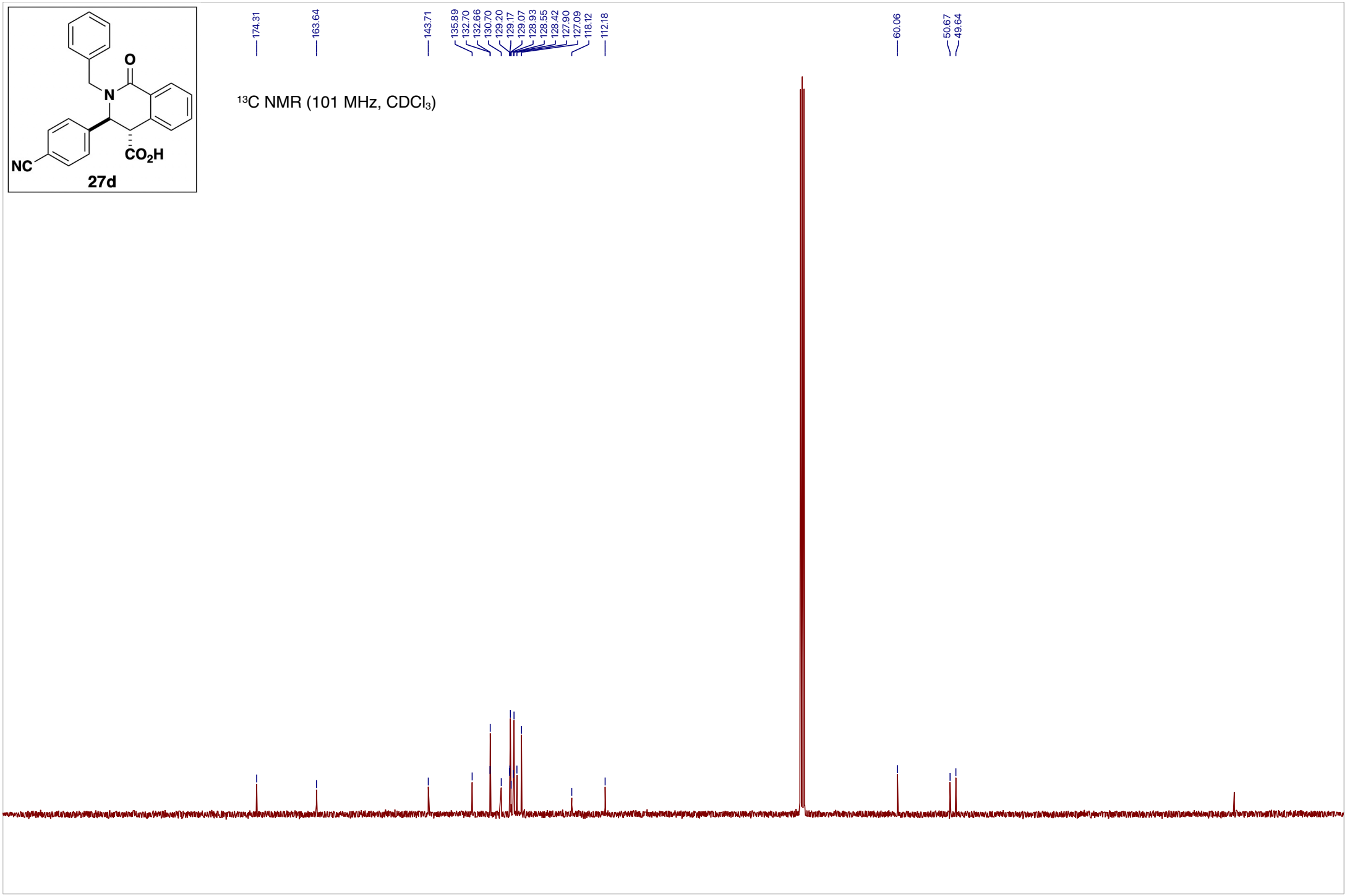
27d
^{13}C NMR (101 MHz, $CDCl_3$)
174.31
163.64
143.71
135.89
132.70
132.66
130.70
129.20
129.17
129.07
128.93
128.55
128.42
127.90
127.09
118.12
112.18
60.06
50.67
49.64
f1 (ppm)

27e

^{1}H NMR (400 MHz, $CDCl_3$)

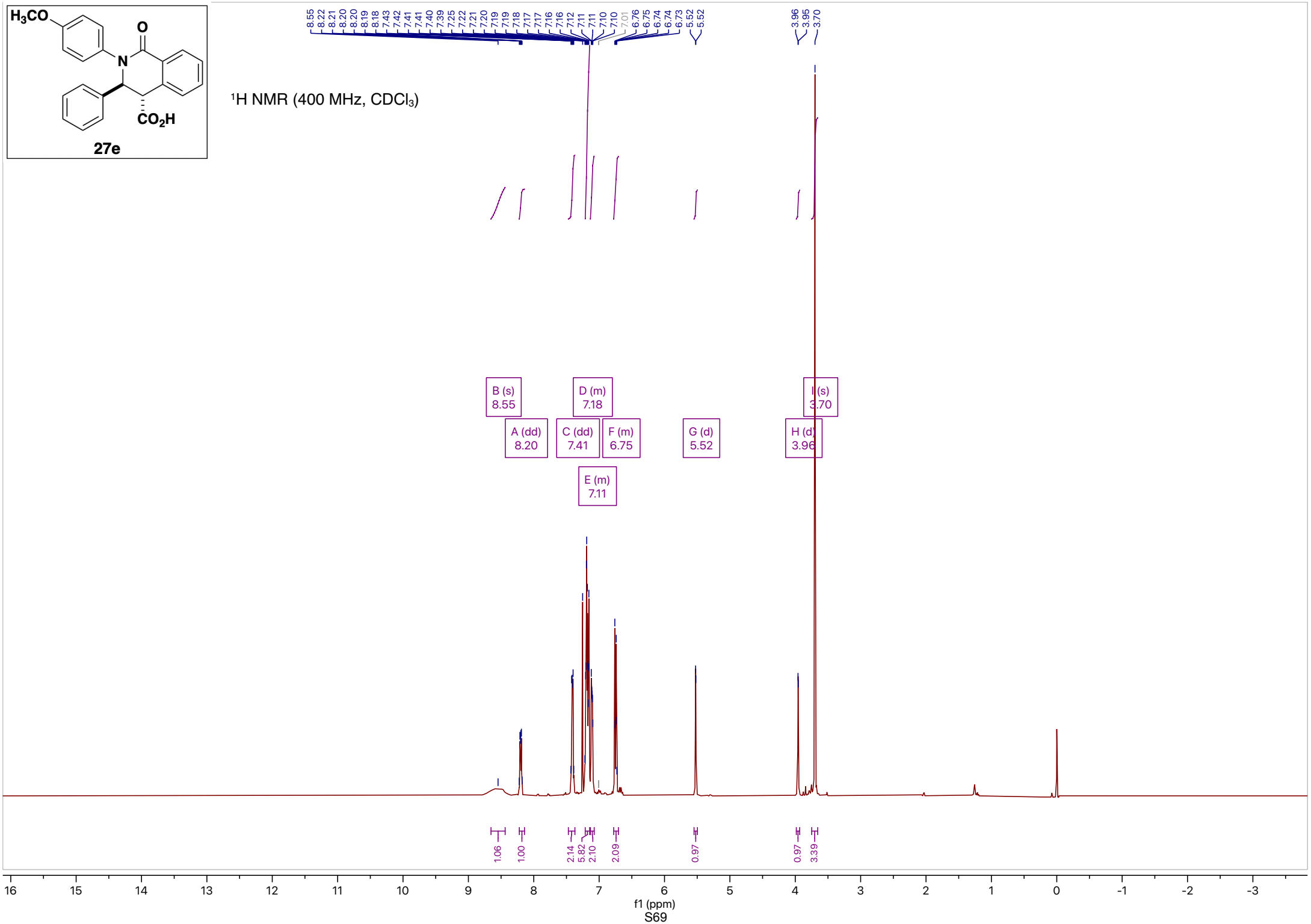

27e

^{13}C NMR (101 MHz, $CDCl_3$)

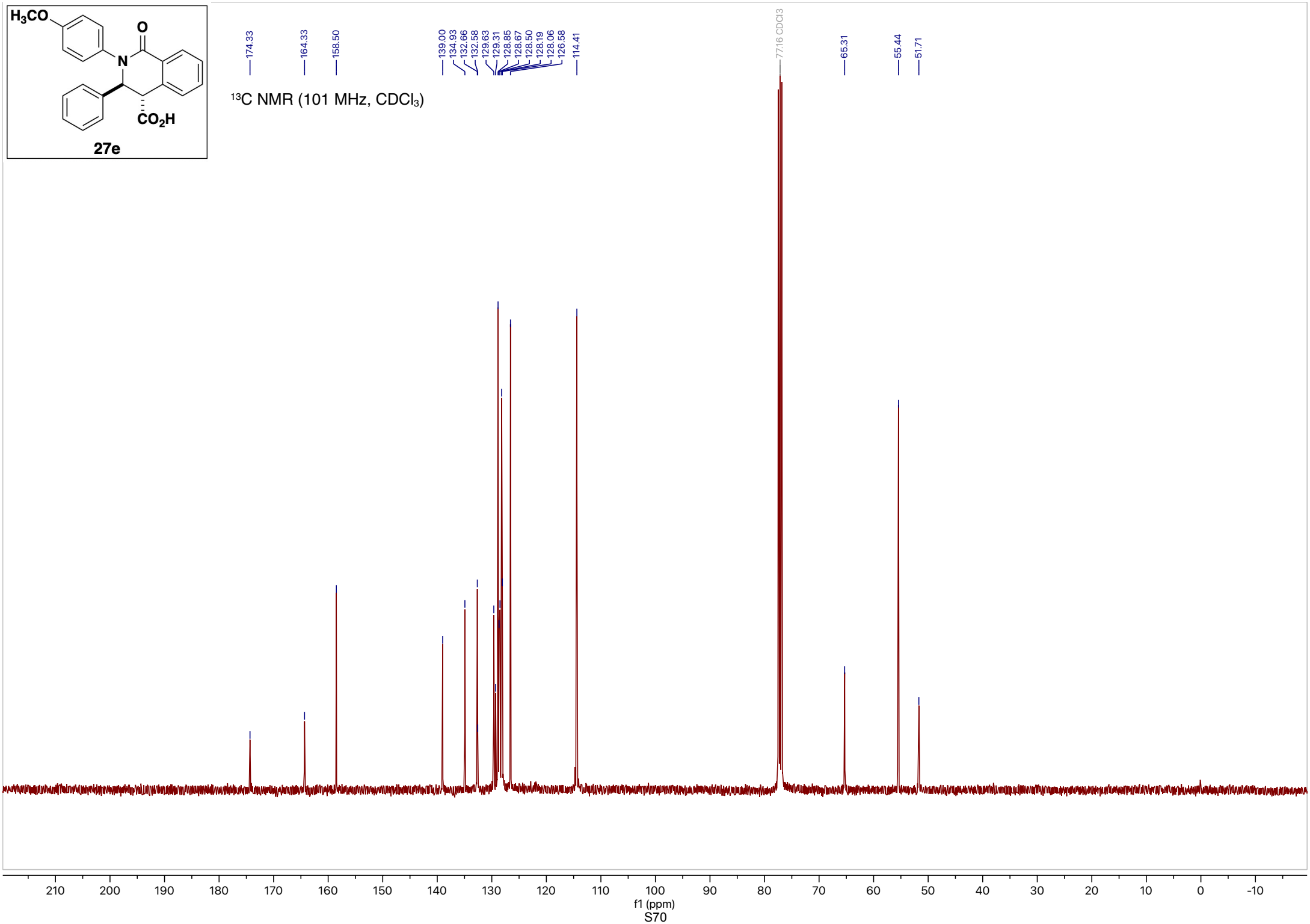

^{1}H NMR (400 MHz, $CDCl_3$)

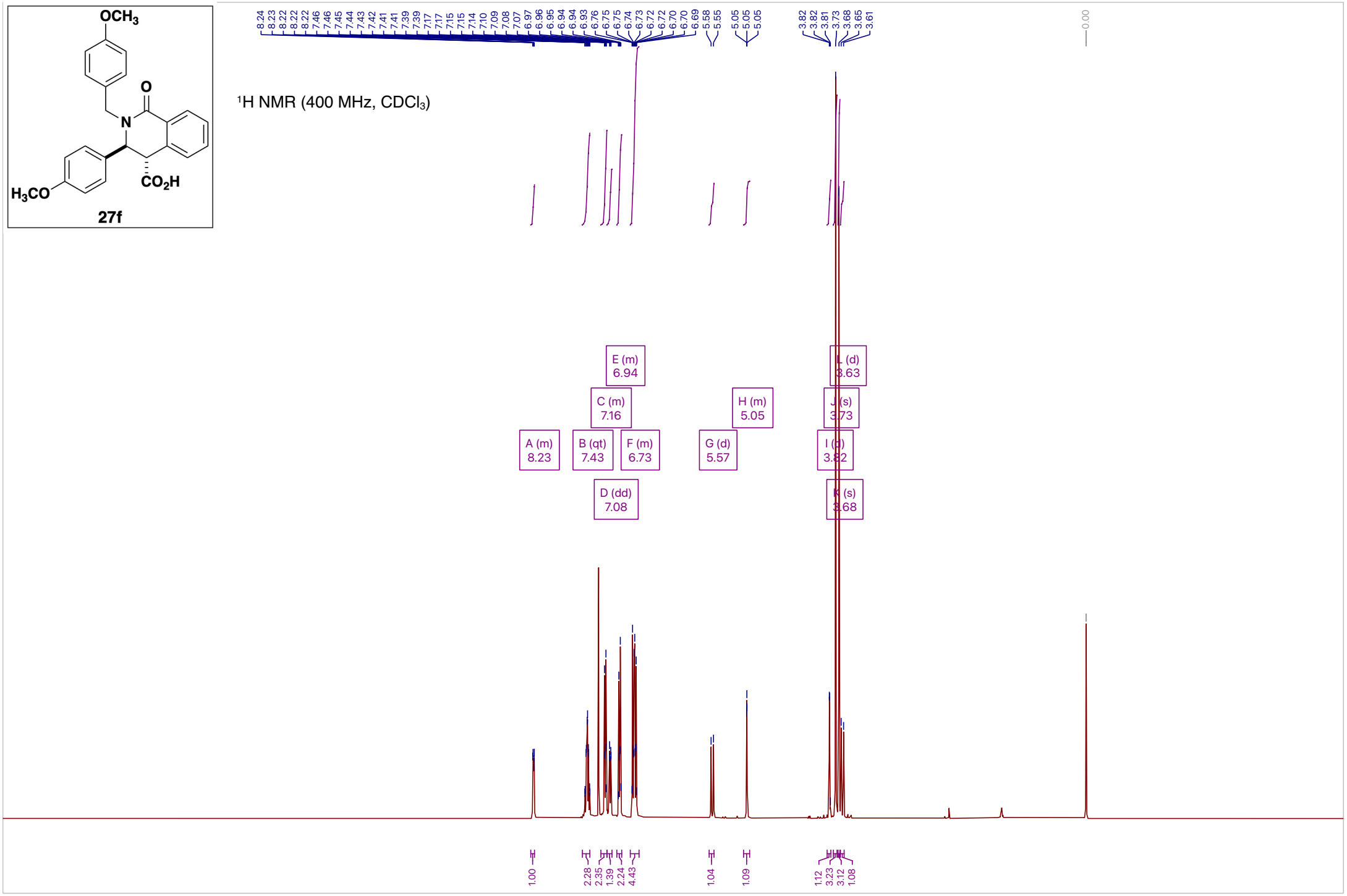

^{13}C NMR (101 MHz, $CDCl_3$)

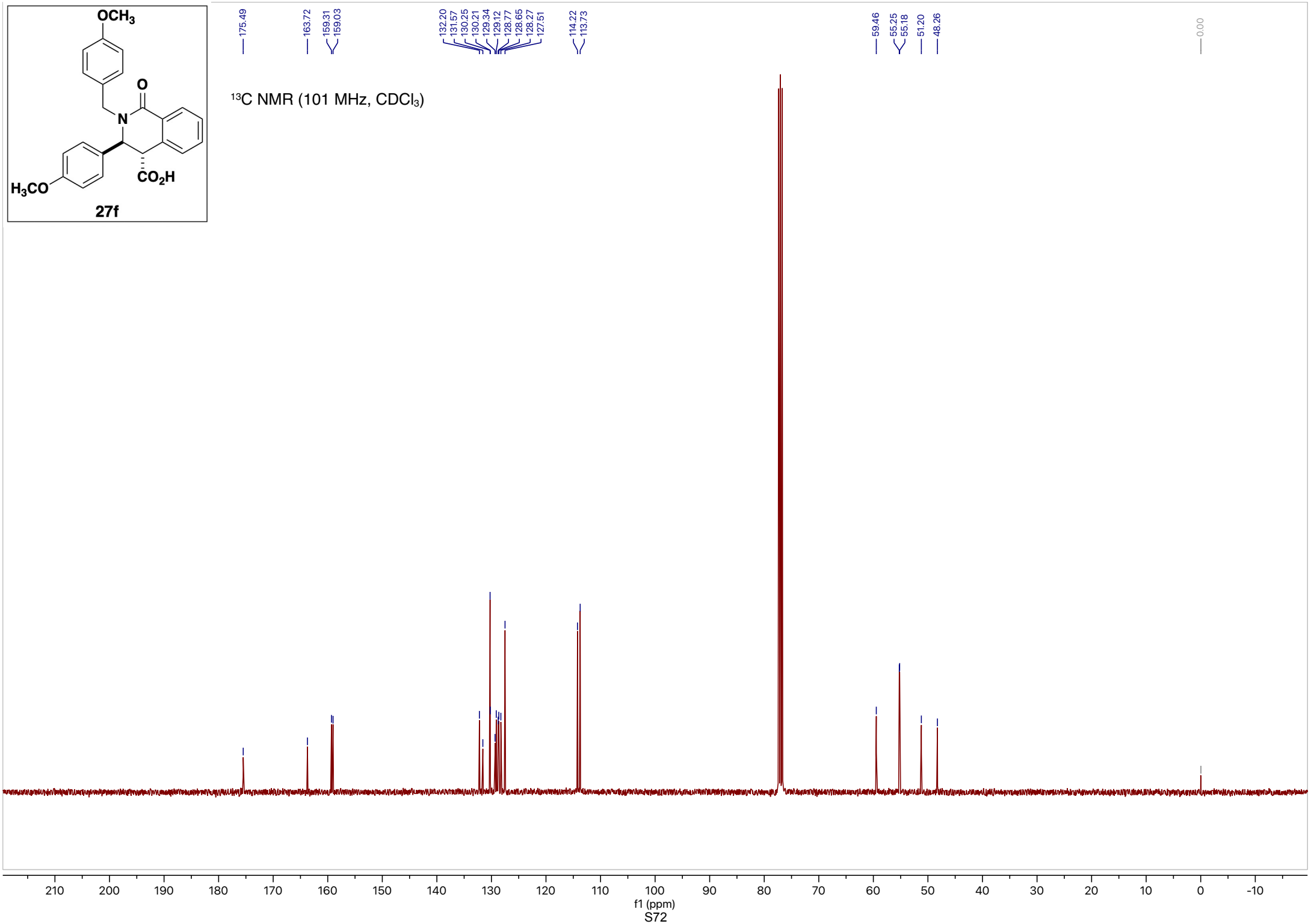

^{1}H NMR (400 MHz, DMSO-d6)

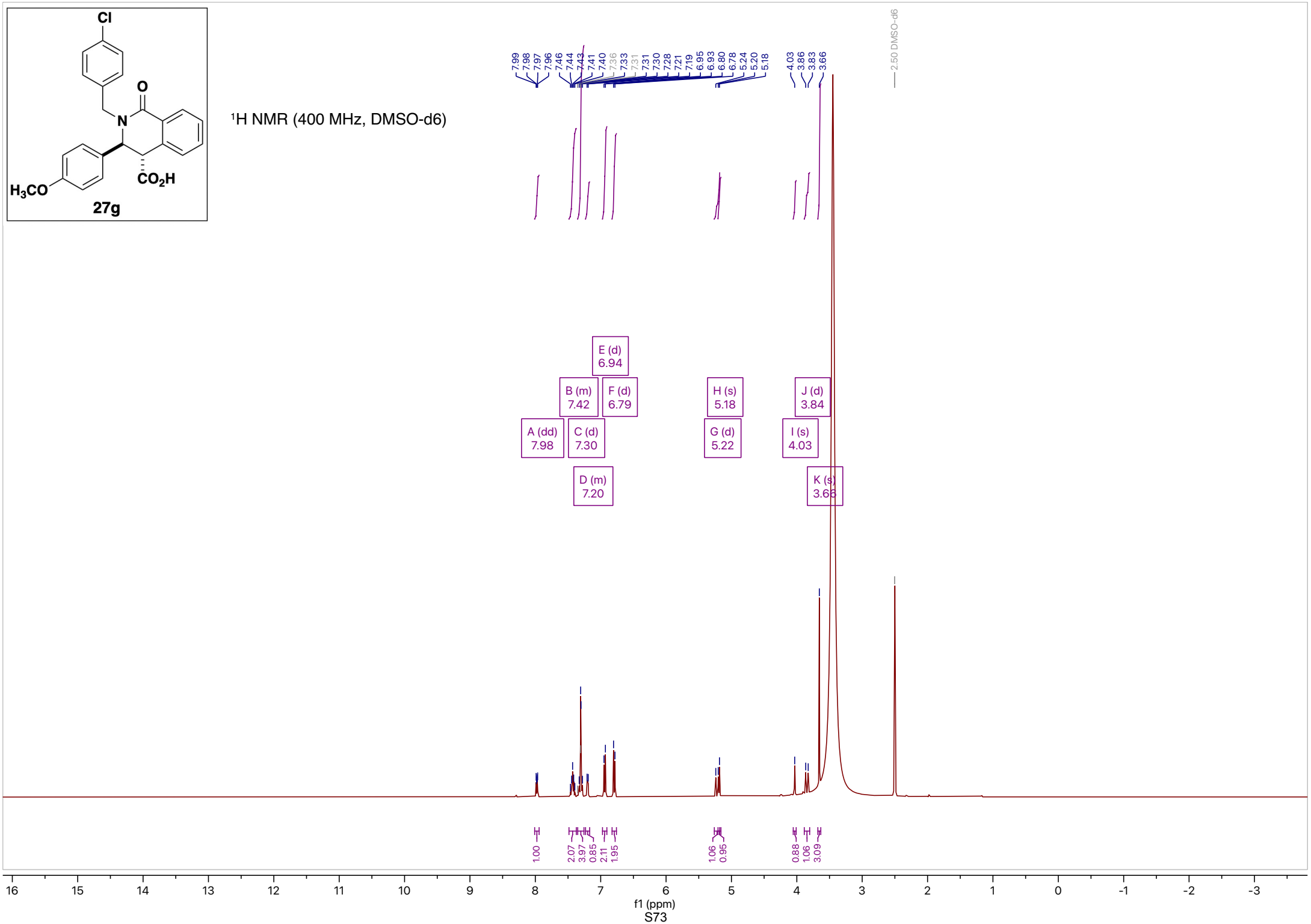

^{13}C NMR (101 MHz, DMSO-d6)

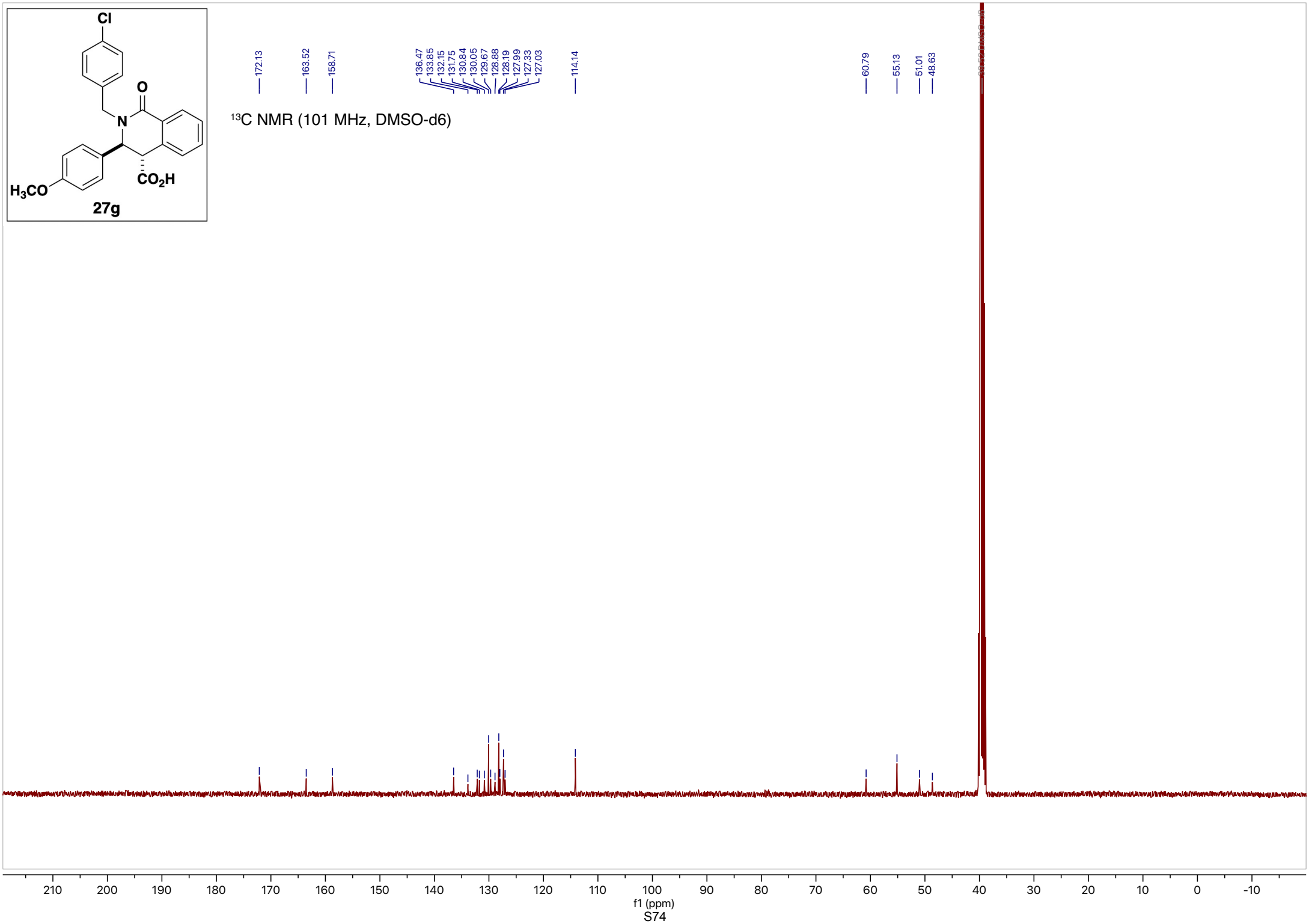

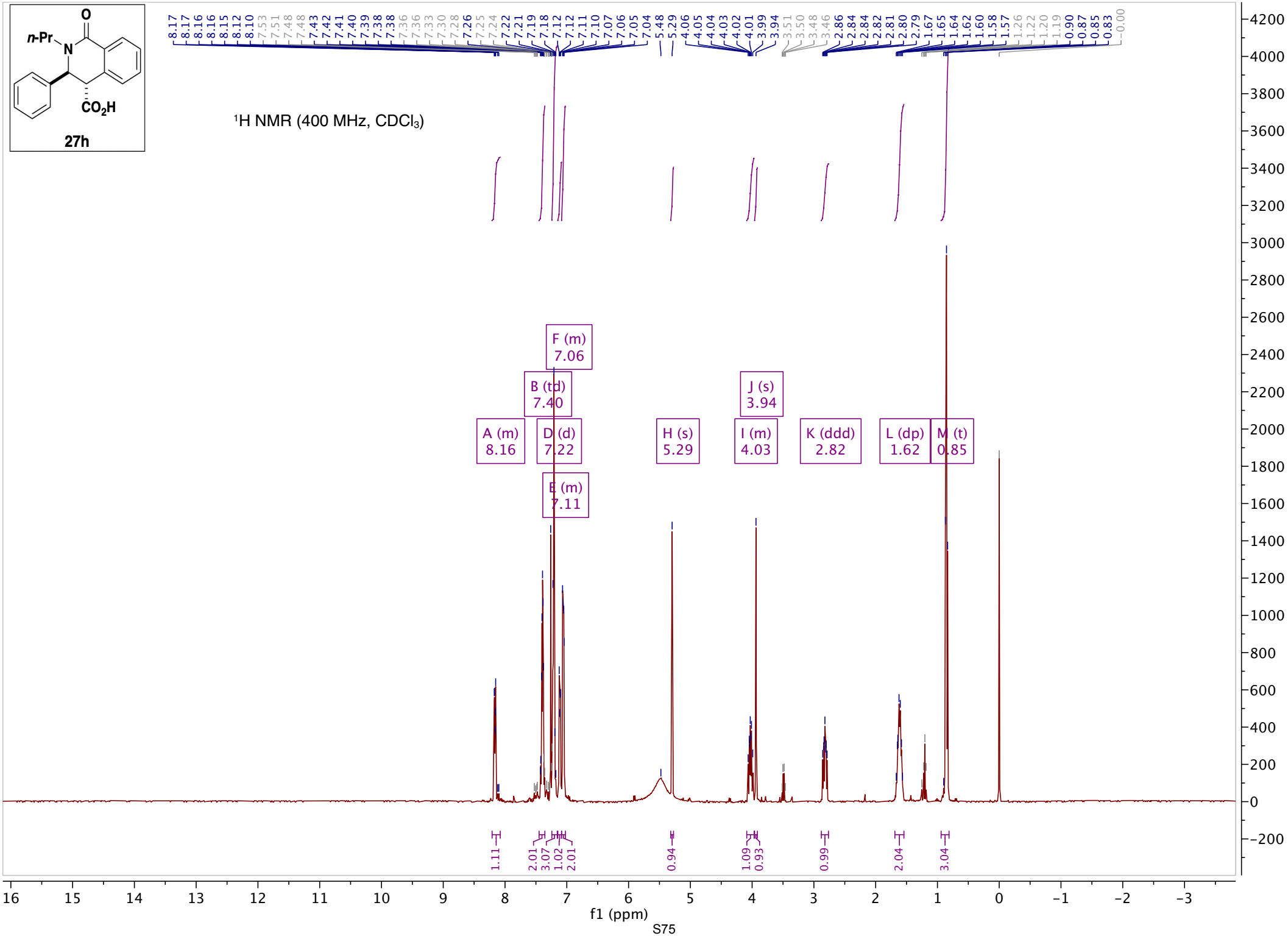
27h
^{1}H NMR (400 MHz, $CDCl_3$)
A (m) 8.16
B (td) 7.40
D (d) 7.22
E (m) 7.11
F (m) 7.06
H (s) 5.29
I (m) 4.03
J (s) 3.94
K (ddd) 2.82
L (dp) 1.62
M (t) 0.85
f1 (ppm)

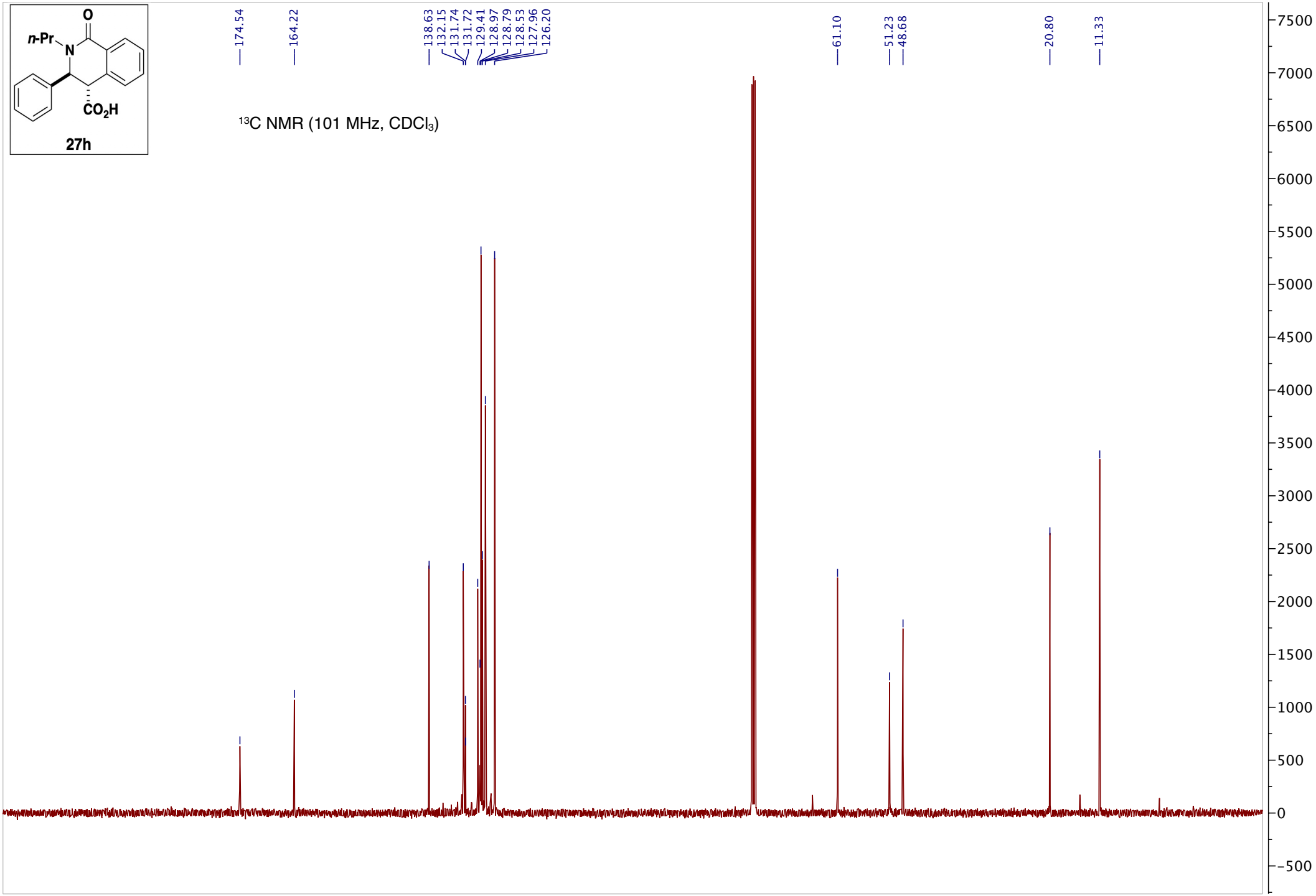
27h
^{13}C NMR (101 MHz, $CDCl_3$)
174.54
164.22
138.63
132.15
131.74
131.72
129.41
128.97
128.79
128.53
127.96
126.20
61.10
51.23
48.68
20.80
11.33
f1 (ppm)

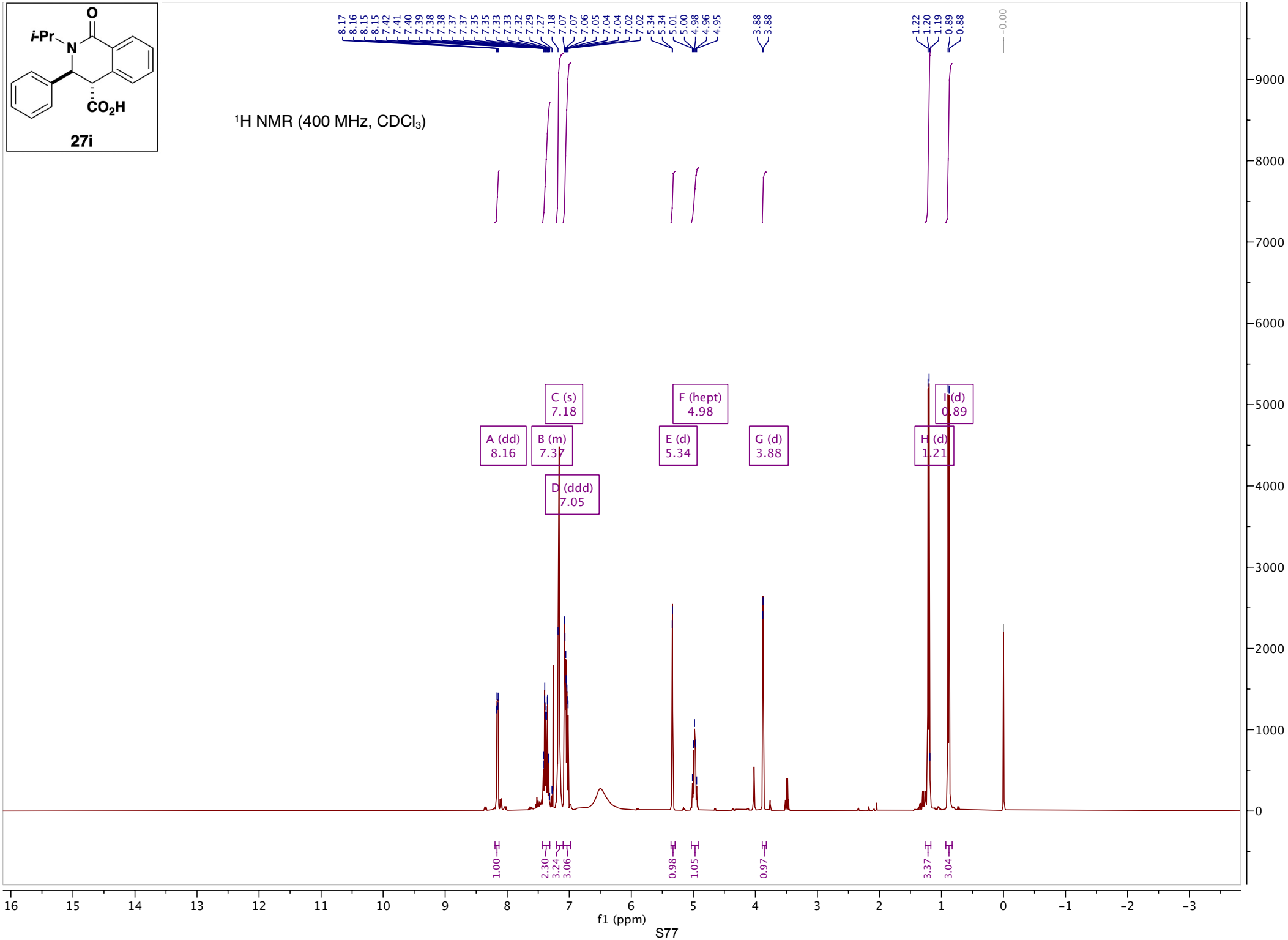
27i
^{1}H NMR (400 MHz, $CDCl_3$)
A (dd) 8.16
B (m) 7.37
C (s) 7.18
D (ddd) 7.05
E (d) 5.34
F (hept) 4.98
G (d) 3.88
H (d) 1.21
I (d) 0.89
f1 (ppm)

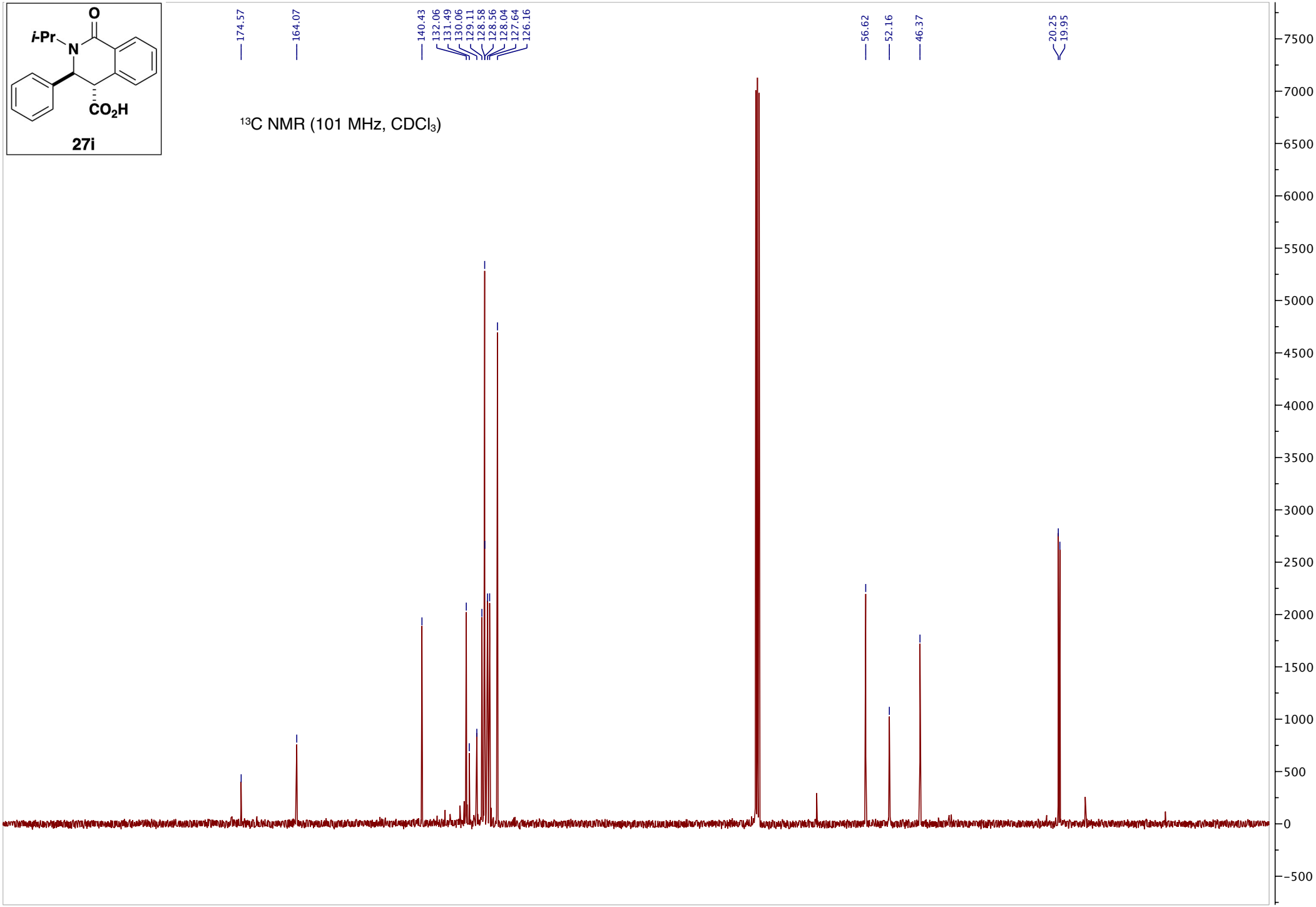
27i
^{13}C NMR (101 MHz, $CDCl_3$)
174.57
164.07
140.43
132.06
131.49
130.06
129.11
128.58
128.56
128.04
127.64
126.16
56.62
52.16
46.37
20.25
19.95
f1 (ppm)

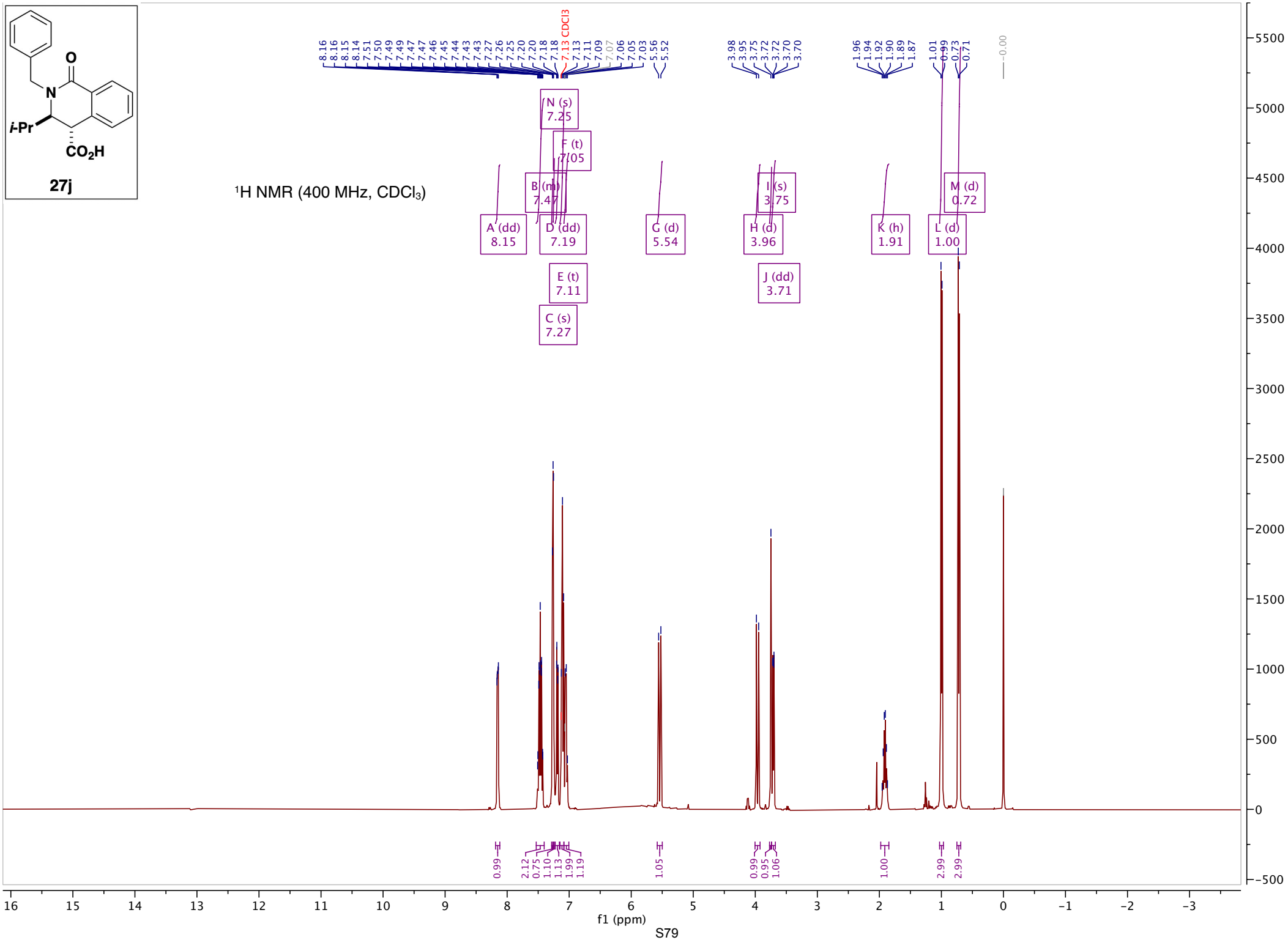
27j
^{1}H NMR (400 MHz, $CDCl_3$)
A (dd) 8.15
B (m) 7.47
C (s) 7.27
D (dd) 7.19
E (t) 7.11
F (t) 7.05
N (s) 7.25
G (d) 5.54
H (d) 3.96
I (s) 3.75
J (dd) 3.71
K (h) 1.91
L (d) 1.00
M (d) 0.72
CDCl3
f1 (ppm)

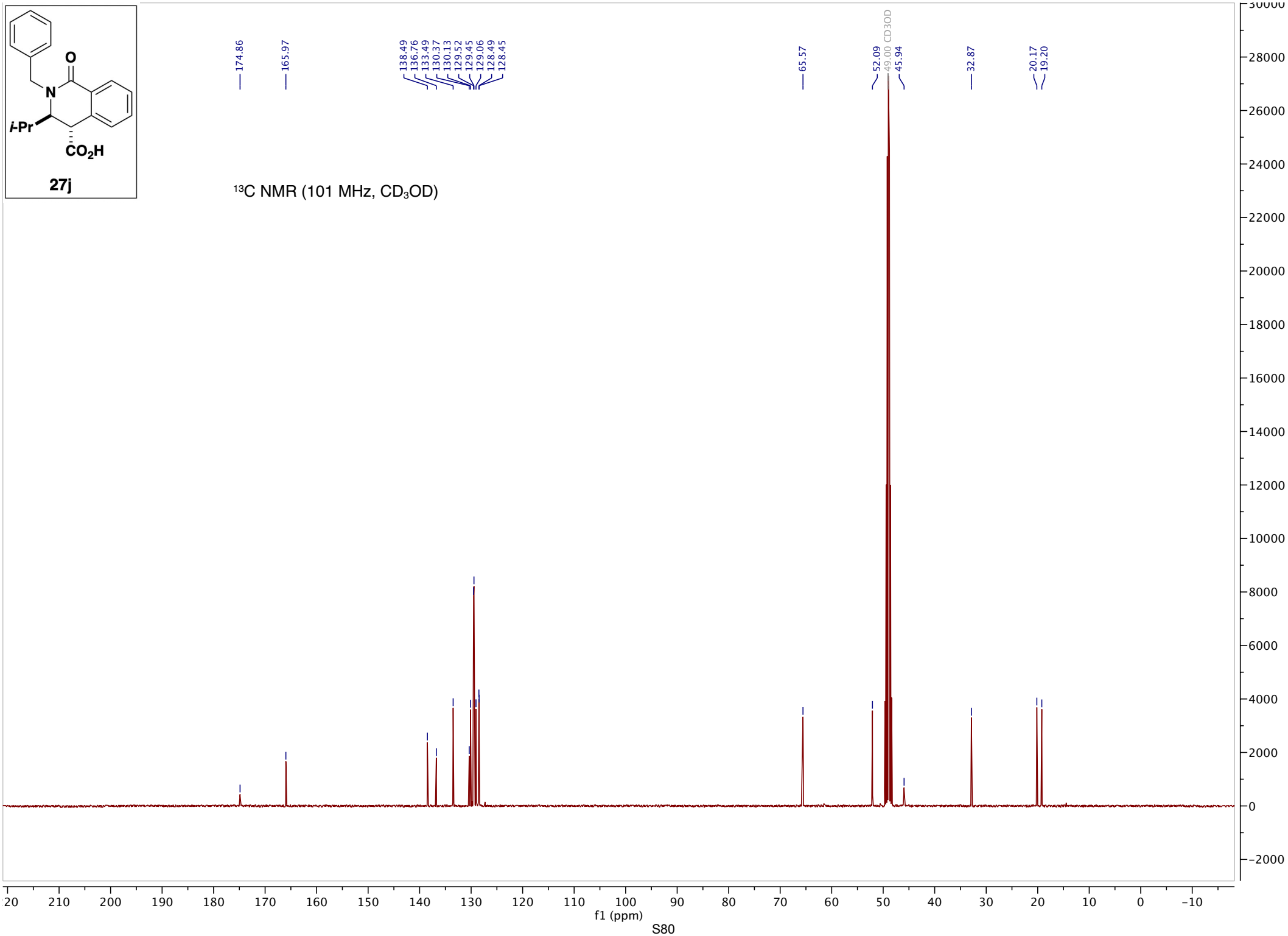
27j
^{13}C NMR (101 MHz, CD_3OD)
174.86
165.97
138.49
136.76
133.49
130.37
130.13
129.52
129.45
129.06
128.49
128.45
65.57
52.09
49.00 CD3OD
45.94
32.87
20.17
19.20
f1 (ppm)

^{1}H NMR (400 MHz, CD_3OD)

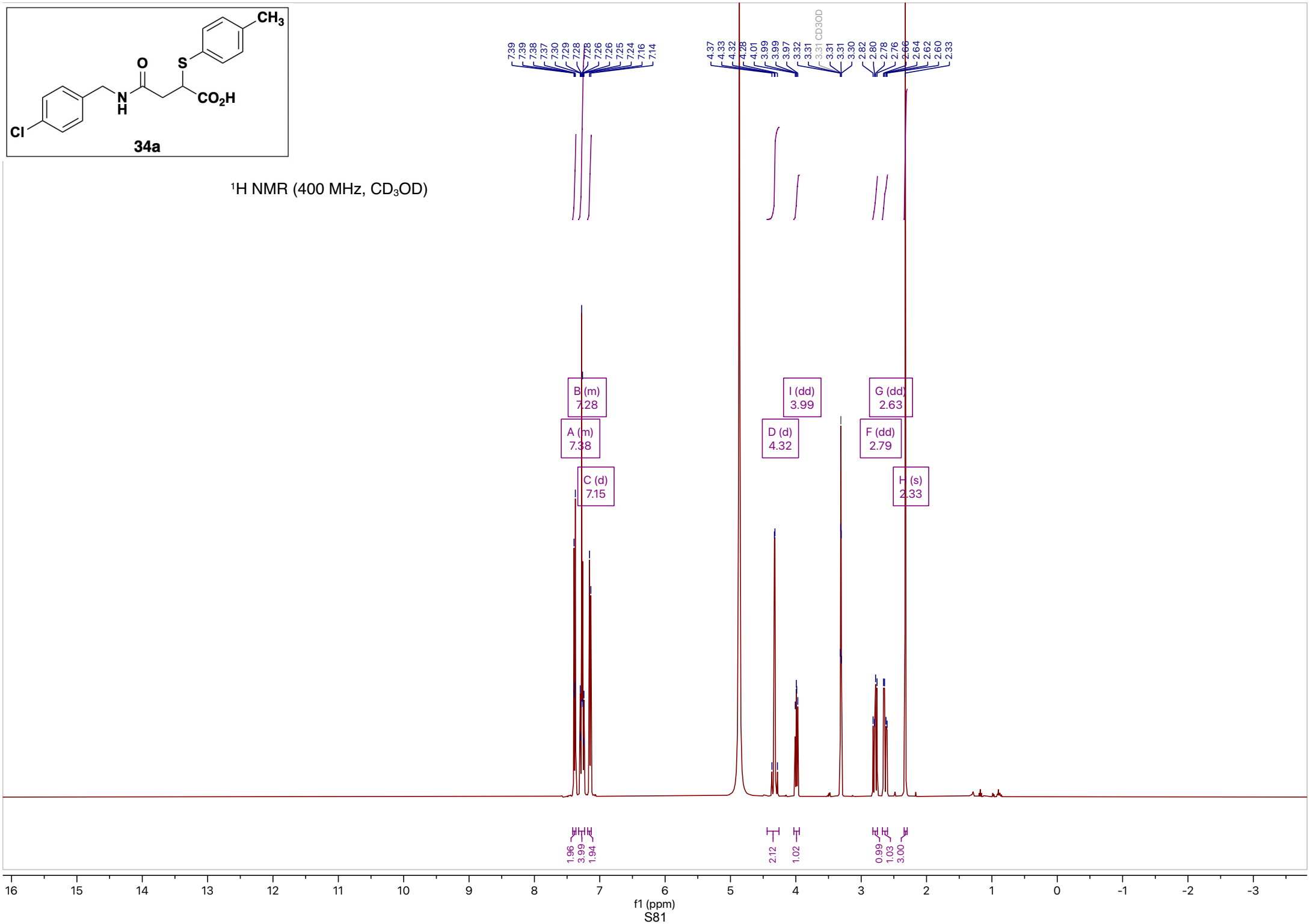

^{13}C NMR (101 MHz, CD_3OD)

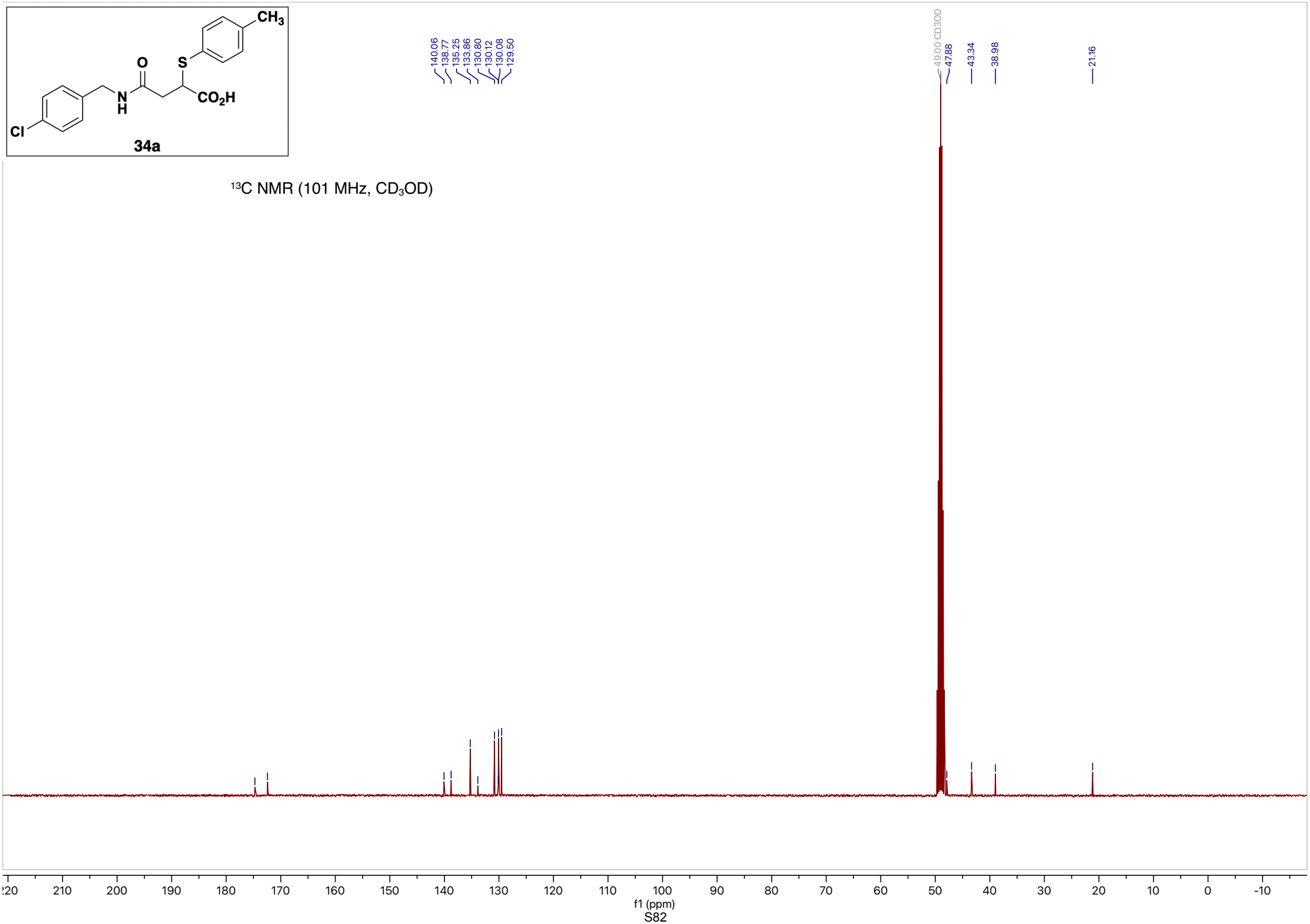

34b

^{1}H NMR (600 MHz, DMSO-d6)

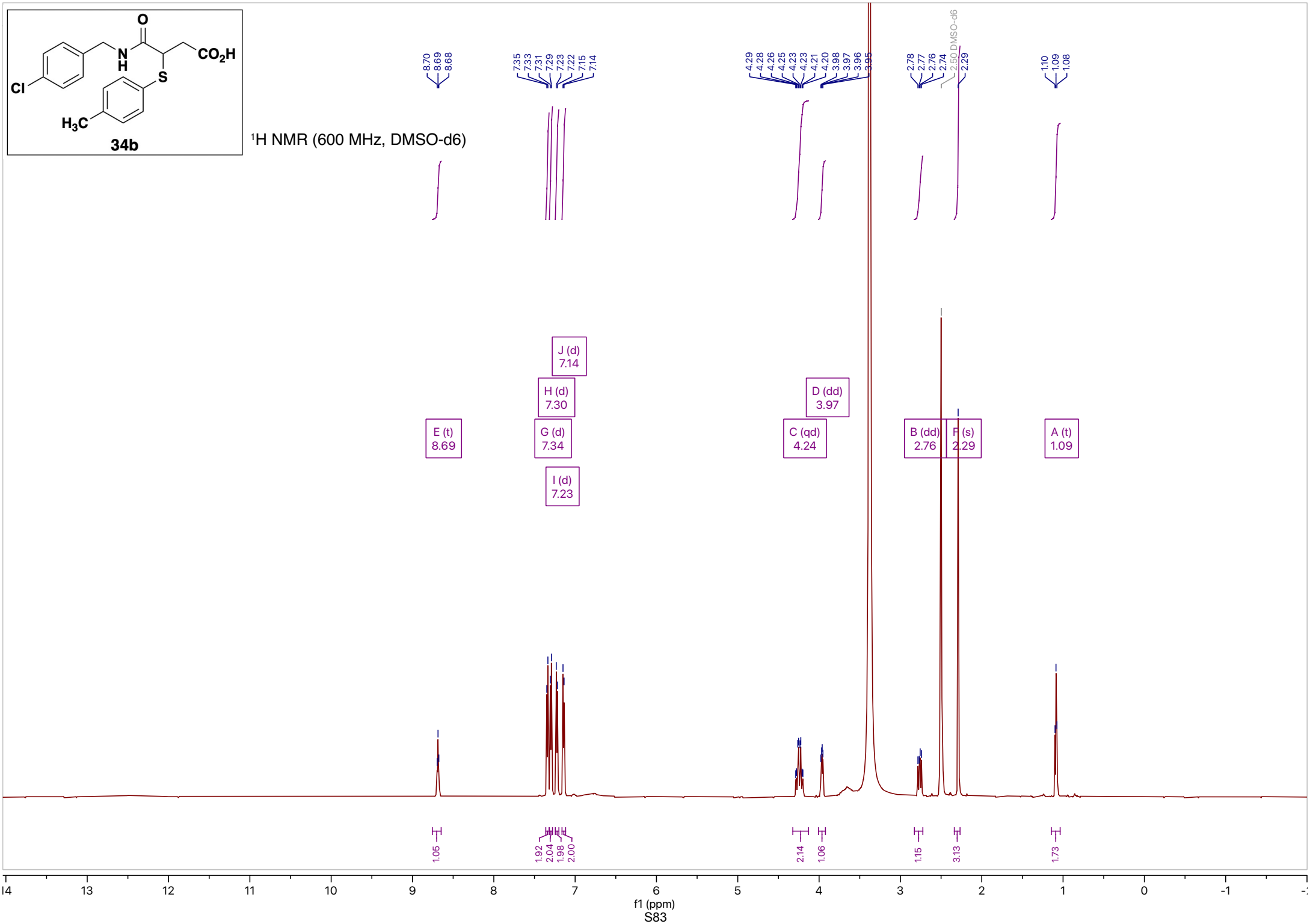

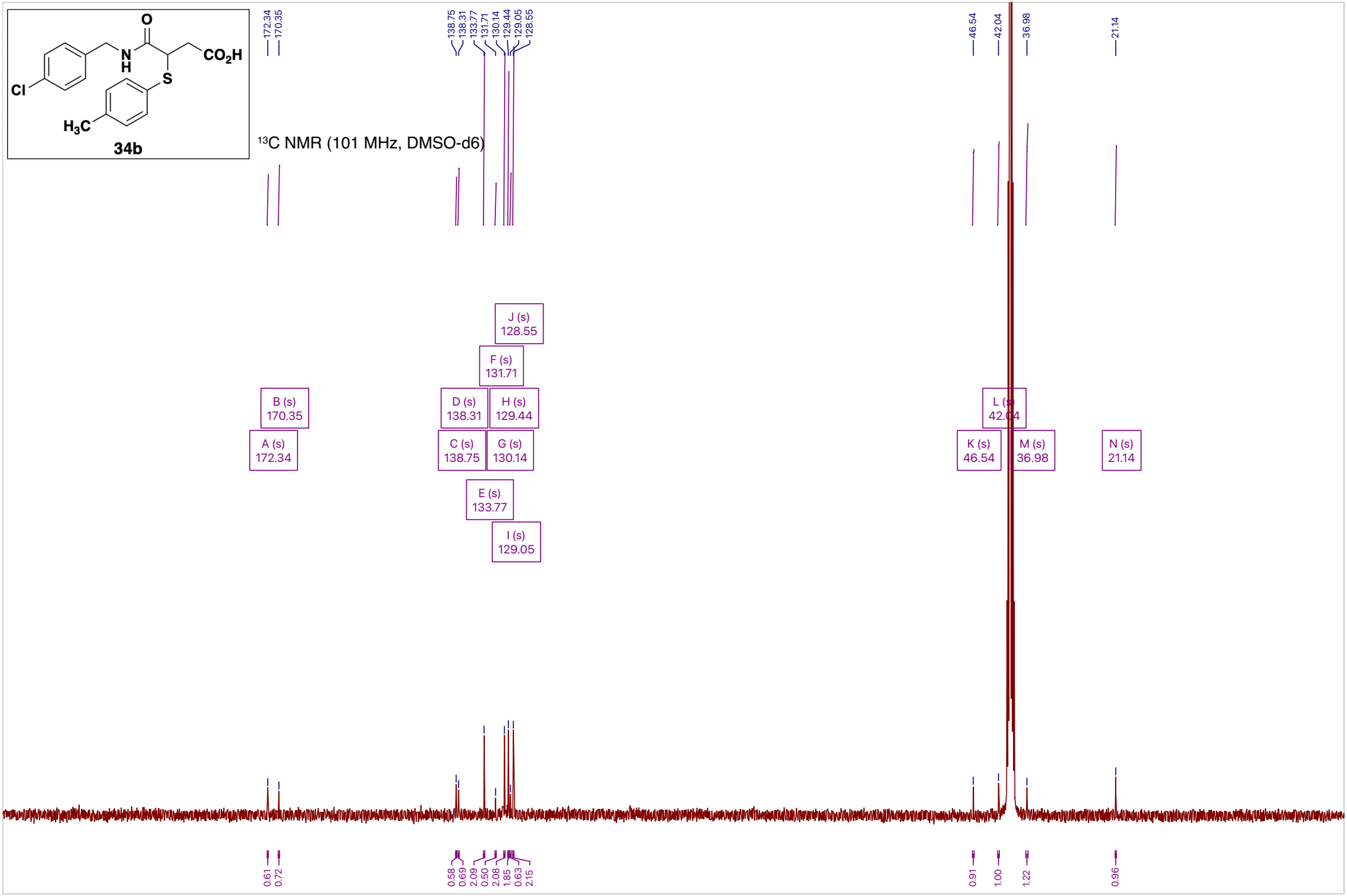
34b
^{13}C NMR (101 MHz, DMSO-d6)
172.34
170.35
138.75
138.31
133.77
131.71
130.14
129.44
129.05
128.55
46.54
42.04
36.98
21.14
A (s) 172.34
B (s) 170.35
C (s) 138.75
D (s) 138.31
E (s) 133.77
F (s) 131.71
G (s) 130.14
H (s) 129.44
I (s) 129.05
J (s) 128.55
K (s) 46.54
L (s) 42.04
M (s) 36.98
N (s) 21.14
0.61
0.72
0.58
0.69
2.09
0.50
2.08
1.85
0.63
2.15
0.91
1.00
1.22
0.96
f1 (ppm)

S1

^{1}H NMR (400 MHz, $CDCl_3$)

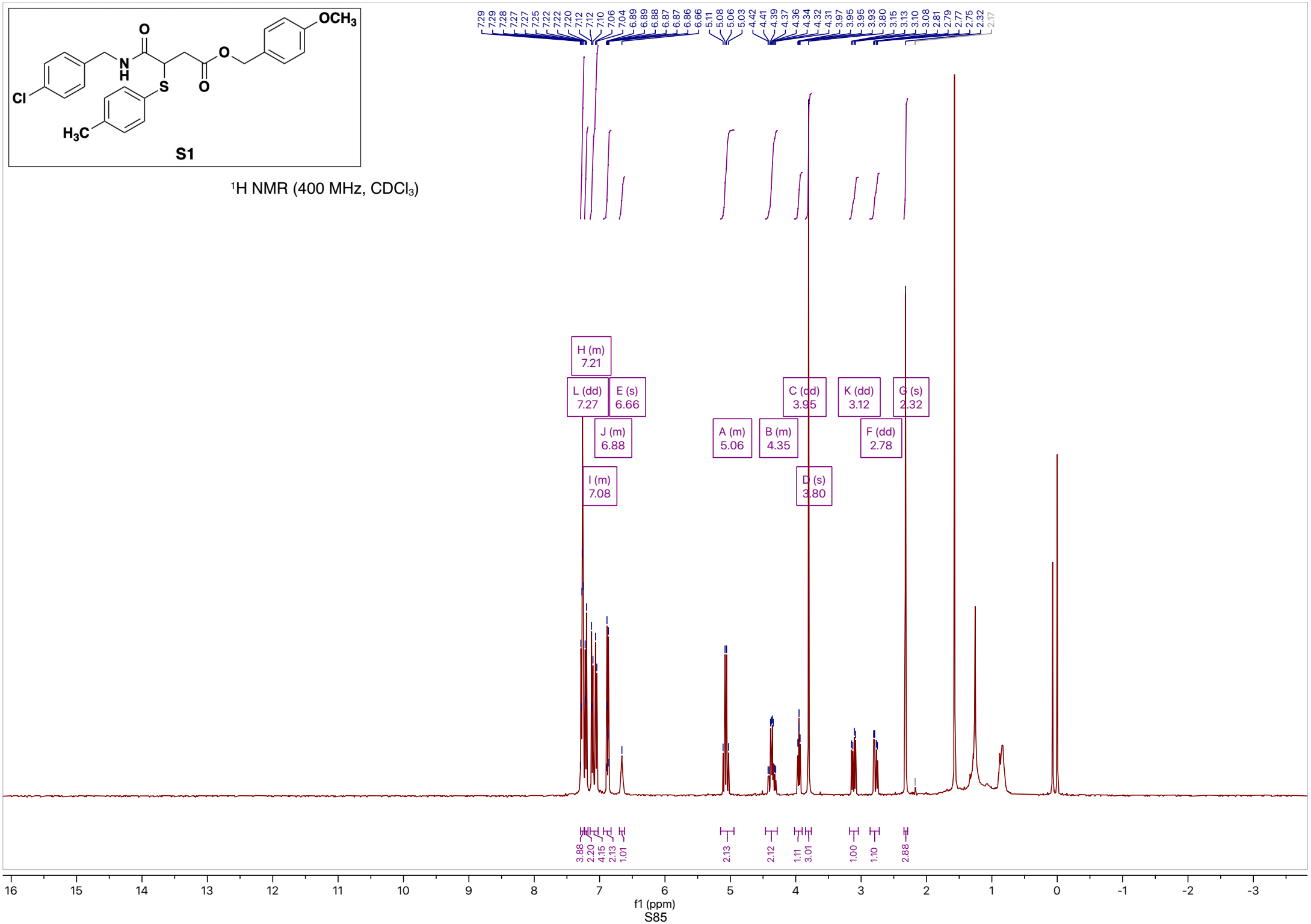

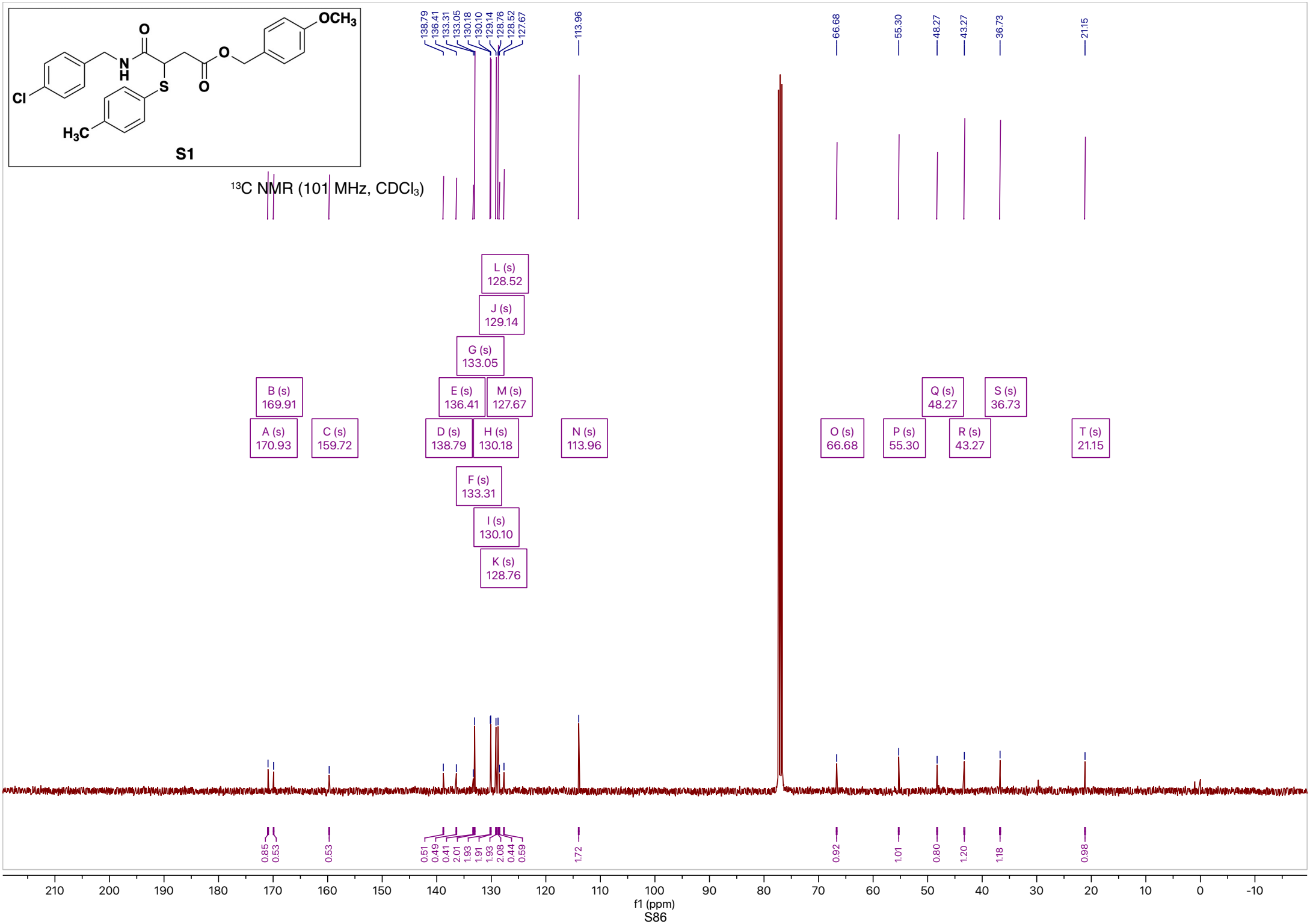
S1
^{13}C NMR (101 MHz, $CDCl_3$)
138.79
136.41
133.31
133.05
130.18
130.10
129.14
128.76
128.52
127.67
113.96
66.68
55.30
48.27
43.27
36.73
21.15
L (s) 128.52
J (s) 129.14
G (s) 133.05
B (s) 169.91
E (s) 136.41
M (s) 127.67
Q (s) 48.27
S (s) 36.73
A (s) 170.93
C (s) 159.72
D (s) 138.79
H (s) 130.18
N (s) 113.96
O (s) 66.68
P (s) 55.30
R (s) 43.27
T (s) 21.15
F (s) 133.31
I (s) 130.10
K (s) 128.76
0.85
0.53
0.53
0.51
0.49
0.41
2.01
1.93
1.91
1.93
2.08
0.44
0.59
1.72
0.92
1.01
0.80
1.20
1.18
0.98
210
200
190
180
170
160
150
140
130
120
110
100
90
80
70
60
50
40
30
20
10
0
-10
f1 (ppm)

S2

^{1}H NMR (400 MHz, $CDCl_3$)

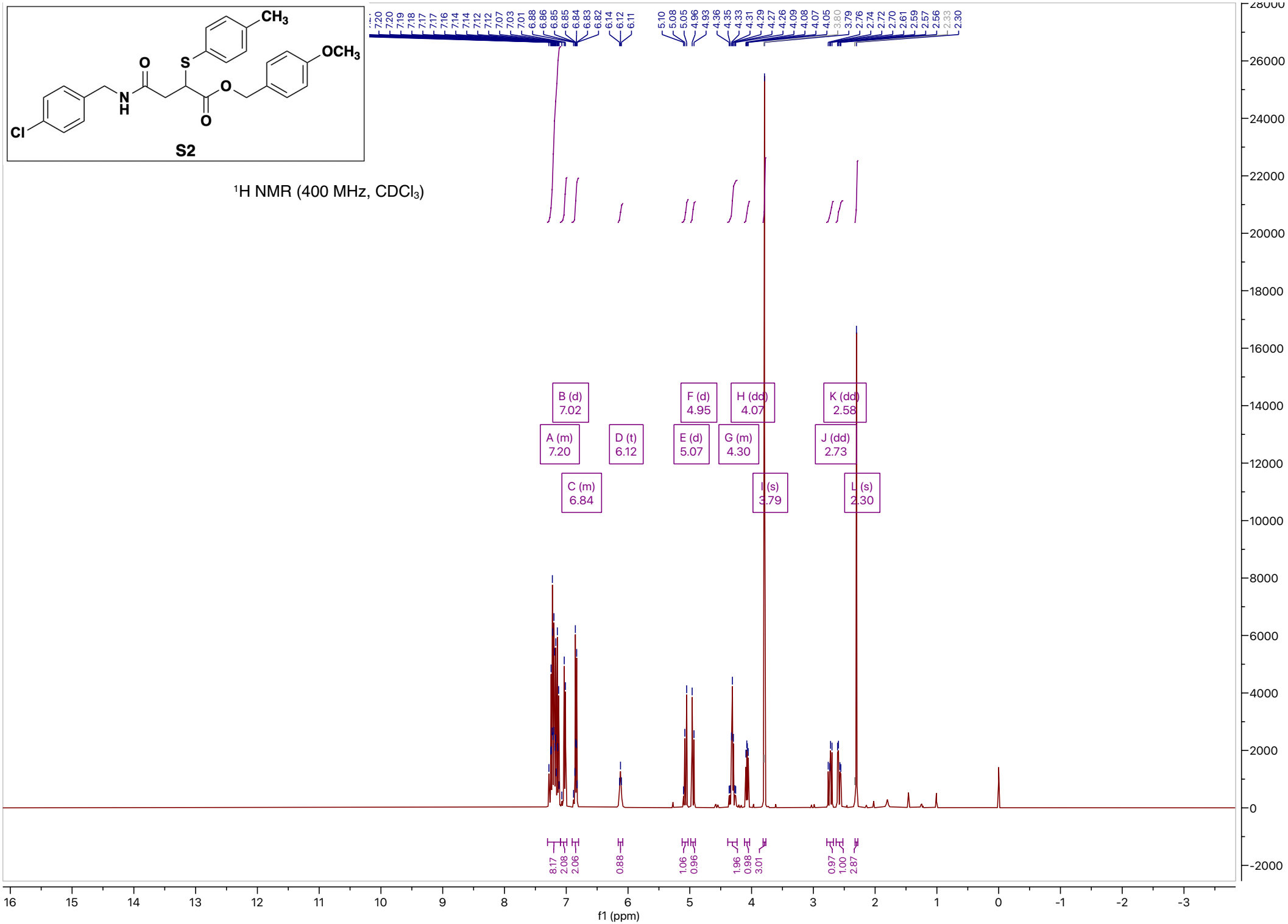

S2

^{13}C NMR (101 MHz, $CDCl_3$)

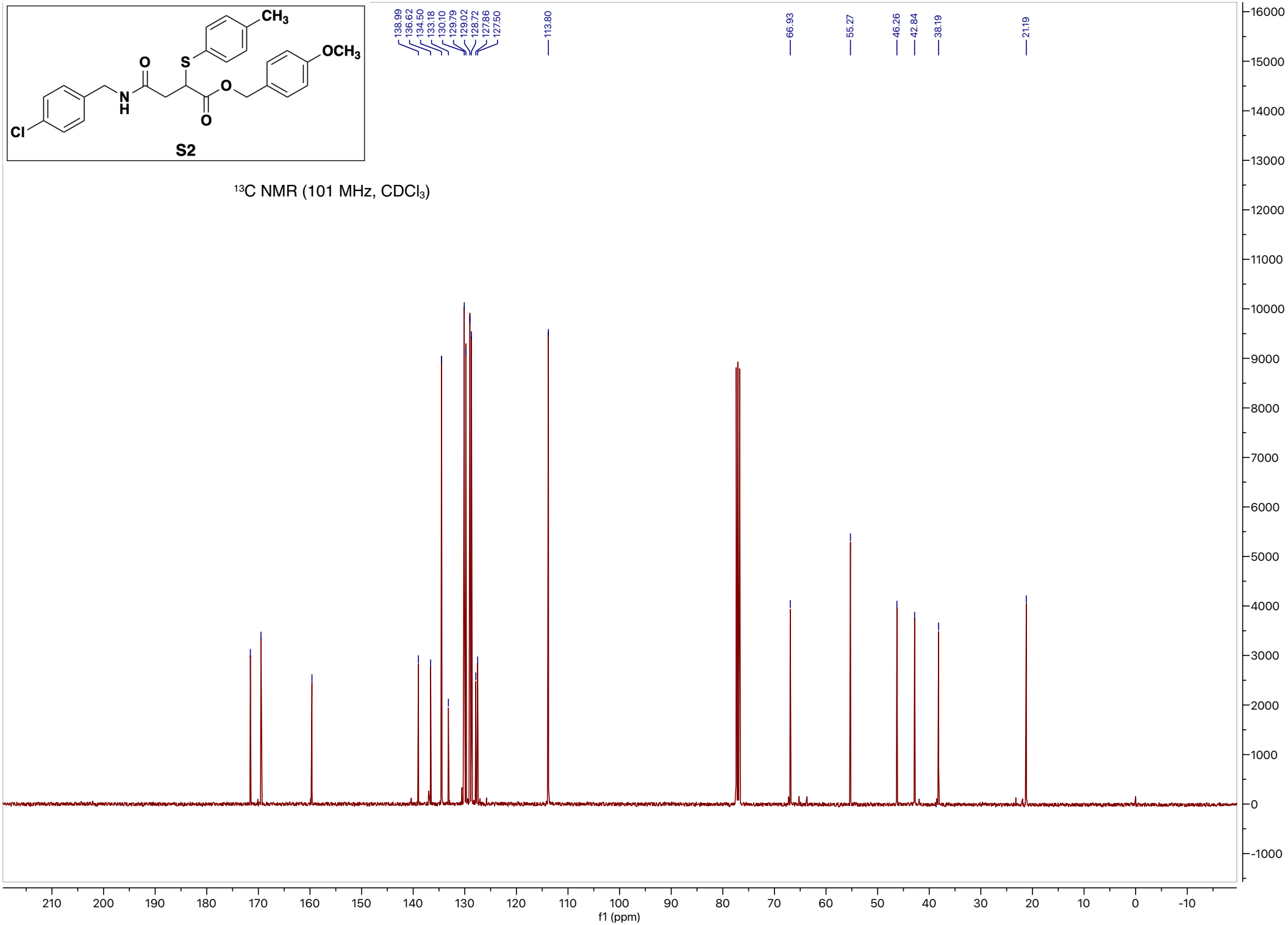

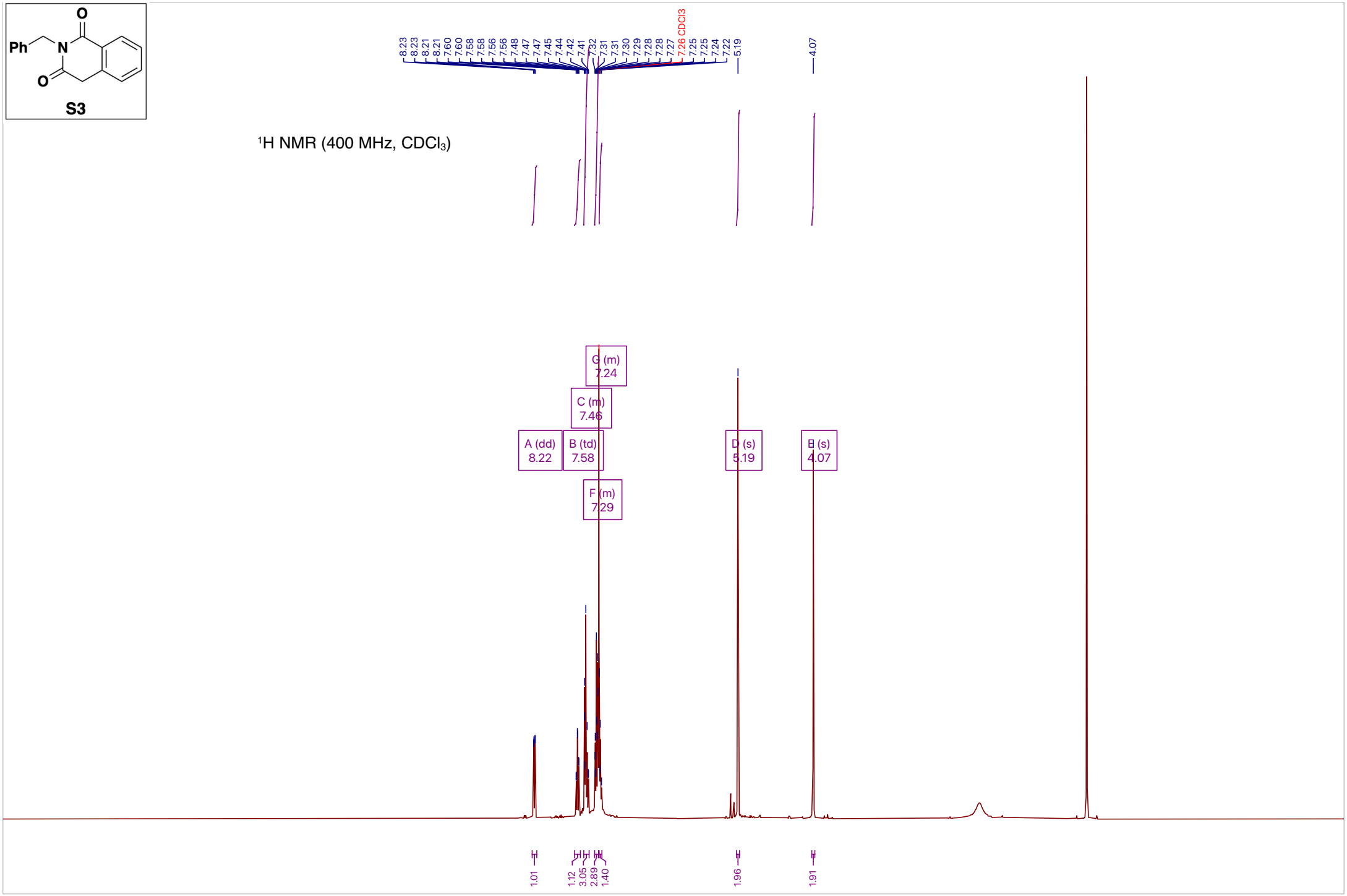
S3
Ph
N
O
O
^{1}H NMR (400 MHz, $CDCl_3$)
8.23
8.23
8.21
8.21
7.60
7.60
7.58
7.58
7.56
7.56
7.48
7.47
7.47
7.45
7.44
7.42
7.41
7.32
7.31
7.31
7.30
7.29
7.28
7.28
7.27
7.26 CDCl3
7.25
7.25
7.24
7.22
5.19
4.07
G (m) 7.24
C (m) 7.46
A (dd) 8.22
B (td) 7.58
F (m) 7.29
D (s) 5.19
E (s) 4.07
1.01
1.12
3.05
2.89
1.40
1.96
1.91
16
15
14
13
12
11
10
9
8
7
6
5
4
3
2
1
0
-1
-2
-3
f1 (ppm)

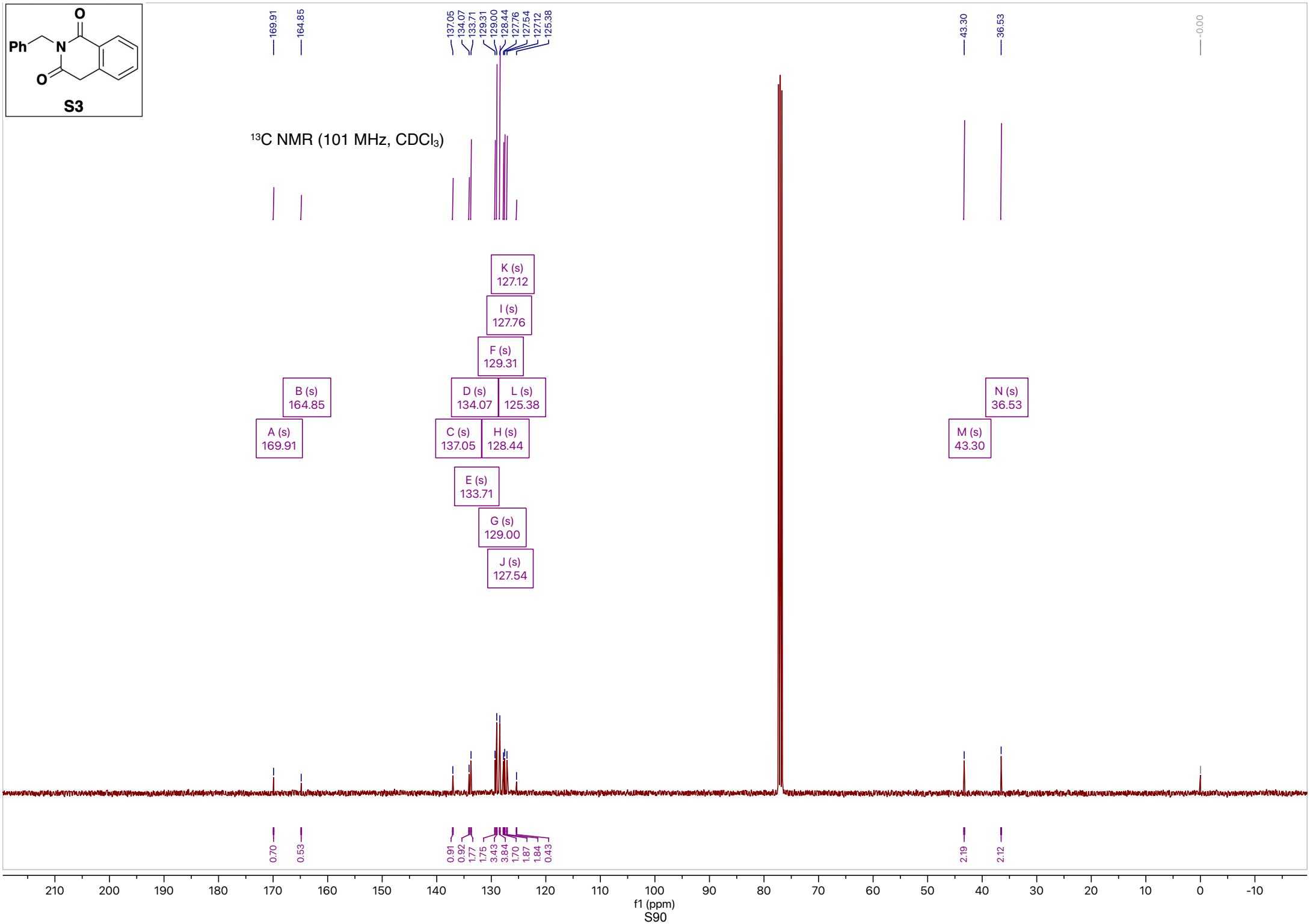
S3
^{13}C NMR (101 MHz, $CDCl_3$)
169.91
164.85
137.05
134.07
133.71
129.31
129.00
128.44
127.76
127.54
127.12
125.38
43.30
36.53
-0.00
K (s) 127.12
I (s) 127.76
F (s) 129.31
B (s) 164.85
D (s) 134.07
L (s) 125.38
N (s) 36.53
A (s) 169.91
C (s) 137.05
H (s) 128.44
M (s) 43.30
E (s) 133.71
G (s) 129.00
J (s) 127.54
0.70
0.53
0.91
0.92
1.77
1.75
3.43
3.84
1.70
1.87
1.84
0.43
2.19
2.12
210 200 190 180 170 160 150 140 130 120 110 100 90 80 70 60 50 40 30 20 10 0 -10
f1 (ppm)